

DETERMINING SERVICE LIFE AND AGEING CHARACTERISTICS OF
COMPOSITE SOLID PROPELLANTS BY THEIR CHEMICAL PROPERTIES

A THESIS SUBMITTED TO
THE GRADUATE SCHOOL OF NATURAL AND APPLIED SCIENCES
OF
MIDDLE EAST TECHNICAL UNIVERSITY

BY

YASEMİN KÖSA

IN PARTIAL FULFILLMENT OF THE REQUIREMENTS
FOR
THE DEGREE OF MASTER OF SCIENCE
IN
CHEMICAL ENGINEERING

FEBRUARY 2022

Approval of the thesis:

**DETERMINING SERVICE LIFE AND AGEING CHARACTERISTICS OF
COMPOSITE SOLID PROPELLANTS BY THEIR CHEMICAL
PROPERTIES**

submitted by **YASEMİN KÖSA** in partial fulfillment of the requirements for the degree of **Master of Science in Chemical Engineering, Middle East Technical University** by,

Prof. Dr. Halil Kalıpçılar
Dean, Graduate School of **Natural and Applied Sciences**

Prof. Dr. Pınar Çalık
Head of the Department, **Chemical Engineering**

Prof. Dr. Deniz Üner
Supervisor, **Chemical Engineering, METU**

Dr. Melis Kesik Mancar
Co-Supervisor, **Roketsan Roket Sanayii ve Ticaret A.S.**

Examining Committee Members:

Prof. Dr. Göknur Bayram
Chemical Engineering, METU

Prof. Dr. Deniz Üner
Chemical Engineering, METU

Prof. Dr. Necati Özkan
Polymer Science and Technology, METU

Asst. Prof. Dr. Cemal Merih Şengönül
Manufacturing Engineering, Atılım University

Asst. Prof. Dr. Necip Berker Üner
Chemical Engineering, METU

Date: 04.02.2022

I hereby declare that all information in this document has been obtained and presented in accordance with academic rules and ethical conduct. I also declare that, as required by these rules and conduct, I have fully cited and referenced all material and results that are not original to this work.

Name Last name : Yasemin Kösa

Signature :

ABSTRACT

DETERMINING SERVICE LIFE AND AGEING CHARACTERISTICS OF COMPOSITE SOLID PROPELLANTS BY THEIR CHEMICAL PROPERTIES

Kösa, Yasemin
Master of Science, Chemical Engineering
Supervisor: Prof. Dr. Deniz Üner
Co-Supervisor: Dr. Melis Kesik Mancar

February 2022, 135 pages

Solid composite propellants are widely used in rocket systems due to their extended manageability and practicality. Service life determination issue of these energetic materials is an extremely important subject as performance and operation safety of rockets may greatly be affected by ageing of propellant. In the literature, service life determination of composite propellants is commonly based on mechanical properties such as stress and strain parameters. In this study, direct monitoring of chemical alterations, such as change in soluble fraction and crosslink density, transpiring within the propellant is also included. Furthermore, building a model for these chemical properties in order to determine ageing characteristics and service life is aimed. Hence, to be able to offer an integral approach, mechanical and physical besides chemical properties of six different hydroxyl-terminated polybutadiene (HTPB) based propellants were observed within the scope of accelerated ageing process. Oxidative crosslinking was the primary ageing mechanism. As a result, stress at break and hardness values increased, whereas strain at break and soluble fraction values decreased during the course of accelerated ageing. Mechanical and

chemical alterations were mathematically modeled using several different approaches. These results provide a basis for studies regarding service life determination of not only propellants, but also energetic and non-energetic polymeric materials.

Keywords: Solid Propellant Rocket Motors, Propellant Ageing, HTPB-based Composite Propellants, Chemical Properties, Mechanical Properties, Modeling

ÖZ

KOMPOZİT KATI YAKITLARIN KİMYASAL ÖZELLİKLERİNİN MODELLENMESİYLE SERVİS ÖMÜRLERİNİN VE YAŞLANMA KARAKTERİSTİĞİNİN BELİRLENMESİ

Kösa, Yasemin
Yüksek Lisans, Kimya Mühendisliği
Tez Yöneticisi: Prof. Dr. Deniz Üner
Ortak Tez Yöneticisi: Dr. Melis Kesik Mancar

Şubat 2022, 135 sayfa

Kompozit katı yakıtlar, kontrol edilebilirliği ve uygulanabilirliği açısından roket sistemlerinde sıkça kullanılan yakıt türlerinden biridir. Yakıtların yaşlanma süreci roketlerin performansını ve çalışma güvenliğini büyük ölçüde etkilediğinden, bu durum yakıtların servis ömürlerinin çalışmasını son derece önemli kılmaktadır. Literatüre bakıldığında, kompozit yakıtların ömür belirleme süreçlerinin çoğunlukla gerilme ve gerinim parametreleri gibi mekanik özelliklerin takibi yapılarak ele alındığı görülmektedir. Bu çalışma kapsamında, çözünen oranı ve çapraz bağ yoğunluğu gibi, yakıtın içerisinde gerçekleşen kimyasal özelliklerindeki değişimlerin gözlemlenmesi ve bu özelliklere ait değişimleri temsil eden, yakıtların servis ömürlerinin ve yaşlanma kinetiğinin belirlenmesinde kullanılacak matematiksel bir model inşası hedeflenmiştir. Bundan ötürü, bütünsel bir yaklaşım oluşturabilmek adına, altı farklı hidroksil-sonlu polibutadien (HTPB) tabanlı yakıtta ait kimyasal özellikler ve bunun yanı sıra mekanik ve fiziksel özellikler hızlı yaşlandırma süresince gözlemlenmiştir. Başlıca yaşlanma mekanizmasının oksidatif çapraz bağlanma olması sebebiyle, hızlı yaşlandırma süreci boyunca takip edilen

kopma gerilmesi ve sertlik deęerlerinde bir artış gözlenirken kopma uzaması ve çözünen oranı deęerlerinin azaldığı görülmüştür. Mekanik ve kimyasal özelliklerde görülen bu deęişikler ise farklı yaklaşımlar kullanılarak matematiksel olarak modellenmiştir. Bu modellemelere ait sonuçlar sadece yakıtların deęil, aynı zamanda enerjik ve enerjik olmayan polimerik malzemelerin servis ömrü belirleme çalışmaları için de temel oluşturmaktadır.

Anahtar Kelimeler: Katı Yakıtlı Roket Motorları, Yakıt Yaşlanması, HTPB Bazlı Kompozit Yakıtlar, Kimyasal Özellikler, Mekanik Özellikler, Modelleme

To the ones who always look up at the stars and lead a life of virtue in this

pale blue dot

ACKNOWLEDGMENTS

First of all, I would like to express my deepest gratitude for my supervisor, Prof. Dr. Deniz Üner, for all her support, perseverance and faith in me finalizing this study.

Besides my supervisor, I would also like to express my warmest gratitude for my co-supervisor and co-worker, Dr. Melis Kesik Mancar, for all her guidance and support.

I am so grateful to have a chance to work with adept in technical team and all my colleagues at ROKETSAN who expended a lot of effort on this study with me during this work.

I would like to thank my parents for their endless support and unrequited love in all my experience. This work would not be possible without them and their everlasting guide.

I would like to thank my superb brother who is always there for me in my most desperate times, picking me up whenever I feel the blues and making this life tolerable by all (yet) unanswered questions related to source of life and existence.

Finally, special thanks to all hail fellows for trusting me in everything I do and tolerating me although my wry humor and groaners. Life would be beyond endurance without them.

TABLE OF CONTENTS

ABSTRACT.....	v
ÖZ.....	vii
ACKNOWLEDGMENTS	x
TABLE OF CONTENTS.....	xi
LIST OF TABLES	xiii
LIST OF FIGURES	xvi
LIST OF ABBREVIATIONS	xviii
LIST OF SYMBOLS	xix
1 INTRODUCTION	1
1.1 Rocket Propellants.....	1
1.2 Service Life Determination of Rocket Propellants	4
2 LITERATURE REVIEW	7
2.1 Methods for Mechanical Property Modeling	9
2.2 Methods for Chemical Property Modeling.....	12
2.3 Scope of the Study.....	14
3 A BRIEF HISTORY OF ROCKET SCIENCE	17
3.1 Classification of Rockets.....	19
4 EXPERIMENTAL SECTION	23
4.1 Propellant Preparation	24
4.2 Ageing Specimen Preparation.....	24

4.3	Propellant Ageing	25
4.4	Tests	27
4.4.1	Uniaxial Tensile Tests	27
4.4.2	Hardness Tests	28
4.4.3	Soluble Fraction Tests	29
5	RESULTS AND DISCUSSION.....	31
5.1	Mechanical Property Change During Ageing.....	31
5.2	Physical Property Change During Ageing.....	39
5.3	Chemical Property Change During Ageing	43
5.4	Comparison of Models.....	48
6	CONCLUSIONS	59
	REFERENCES	61
	APPENDICES	71
A.	Mechanical Test Results	71
B.	Chemical Test Results	119
C.	Physical Test Results	121
D.	Calculation of Activation Energy	123
	Integral Method (Assuming First Order Rate)	123
	Differential Method (Instantaneous Activation Energy).....	124
E.	Severity Index Approach	127
F.	Surface Fit Approach	130
G.	Severity Index Calculation – MATLAB Code Example	133
H.	Fitting a Polynomial Surface – MATLAB Code Example.....	134

LIST OF TABLES

TABLES

Table 1. Polymers being used in the structure of studied propellants.	23
Table 2. Ageing periods and durations of the propellants.	26
Table 3. First order equation rate parameters for strain values and corresponding sum of squared errors (SSE).	48
Table 4. First order equation rate parameters for soluble fraction values and corresponding sum of squared errors (SSE).	49
Table 5. Activation energies obtained by integral method.	49
Table 6. Activation energies calculated for strain values obtained by integral and differential methods* for comparison.	52
Table 7. Activation energies calculated for soluble fraction values by integral and differential methods** for comparison.	52
Table 8. Severity factor equation parameters for strain values and corresponding SSE.....	53
Table 9. Severity factor equation parameters for strain values and corresponding SSE.....	53
Table 10. Surface fit equation parameters for strain values of propellants A, B and C, and corresponding SSEs.	54
Table 11. Surface fit equation parameters for strain values of propellants D, E and F, and corresponding SSEs.	54
Table 12. Surface fit equation parameters for soluble fraction values of propellants A, B and C, and corresponding SSEs.	55
Table 13. Surface fit equation parameters for soluble fraction values of propellants D, E and F, and corresponding SSEs.	55
Table 14. Total SSE of the models.	55
Table 15. 90°C Mechanical test results for propellant A.	71

Table 16. 90°C Mechanical test results for propellant A, cont'd.	72
Table 17. 80°C Mechanical test results for propellant A.	73
Table 18. 80°C Mechanical test results for propellant A, cont'd.	74
Table 19. 70°C Mechanical test results for propellant A.	75
Table 20. 70°C Mechanical test results for propellant A, cont'd.	76
Table 21. 60°C Mechanical test results for propellant A.	77
Table 22. 60°C Mechanical test results for propellant A, cont'd.	78
Table 23. 90°C Mechanical test results for propellant B.....	79
Table 24. 90°C Mechanical test results for propellant B, cont'd.	80
Table 25. 80°C Mechanical test results for propellant B.....	81
Table 26. 80°C Mechanical test results for propellant B, cont'd.	82
Table 27. 70°C Mechanical test results for propellant B.....	83
Table 28. 70°C Mechanical test results for propellant B, cont'd.	84
Table 29. 60°C Mechanical test results for propellant B.....	85
Table 30. 60°C Mechanical test results for propellant B, cont'd.	86
Table 31. 90°C Mechanical test results for propellant C.....	87
Table 32. 90°C Mechanical test results for propellant C, cont'd.	88
Table 33. 80°C Mechanical test results for propellant C.....	89
Table 34. 80°C Mechanical test results for propellant C, cont'd.	90
Table 35. 70°C Mechanical test results for propellant C.....	91
Table 36. 70°C Mechanical test results for propellant C, cont'd.	92
Table 37. 60°C Mechanical test results for propellant C.....	93
Table 38. 60°C Mechanical test results for propellant C, cont'd.	94
Table 39. 90°C Mechanical test results for propellant D.	95
Table 40. 90°C Mechanical test results for propellant D, cont'd.	96
Table 41. 80°C Mechanical test results for propellant D.	97
Table 42. 80°C Mechanical test results for propellant D, cont'd.	98
Table 43. 70°C Mechanical test results for propellant D.	99
Table 44. 70°C Mechanical test results for propellant D, cont'd.	100
Table 45. 60°C Mechanical test results for propellant D.	101

Table 46. 60°C Mechanical test results for propellant D, cont'd.....	102
Table 47. 90°C Mechanical test results for propellant E.	103
Table 48. 90°C Mechanical test results for propellant E, cont'd.	104
Table 49. 80°C Mechanical test results for propellant E.	105
Table 50. 80°C Mechanical test results for propellant E, cont'd.	106
Table 51. 70°C Mechanical test results for propellant E.	107
Table 52. 70°C Mechanical test results for propellant E, cont'd.	108
Table 53. 60°C Mechanical test results for propellant E.	109
Table 54. 60°C Mechanical test results for propellant E, cont'd.	110
Table 55. 90°C Mechanical test results for propellant F.	111
Table 56. 90°C Mechanical test results for propellant F, cont'd.	112
Table 57. 80°C Mechanical test results for propellant F.	113
Table 58. 80°C Mechanical test results for propellant F, cont'd.	114
Table 59. 70°C Mechanical test results for propellant F.	115
Table 60. 70°C Mechanical test results for propellant F, cont'd.	116
Table 61. 60°C Mechanical test results for propellant F.	117
Table 62. 60°C Mechanical test results for propellant F, cont'd.	118
Table 63. Chemical test results of propellants A, B and C, respectively.....	119
Table 64. Chemical test results of propellants D, E and F, respectively.	120
Table 65. Physical test results of propellants A, B and C, respectively.....	121
Table 66. Physical test results of propellants D, E and F, respectively.	122
Table 67. Strain at break values of Propellant A aged at 90°C.....	123
Table 68. Evaluating reaction rate by altering sum of normalized error.	124
Table 69. Strain at break values of Propellant A.	125
Table 70. Change in strain at break values for the first three ageing periods of Propellant A.	126
Table 71. Calculation of $-\ln(1-a)$ named as <i>alfa</i> for strain values of Propellant A.	128
Table 72. Conversion results for strain values of Propellant A.	131

LIST OF FIGURES

FIGURES

Figure 1-1. Life cycle of a rocket system.	4
Figure 2-1. Chemical structure of hydroxyl-terminated polybutadiene (Khan, Dey, Athar, & Sikder, 2014).	7
Figure 2-2. Aziridine group.	10
Figure 3-1. Main parts of a solid rocket motor (Açık, 2010).	20
Figure 3-2. Schematic flow diagram of a liquid propellant rocket engine with a gas pressure feed system (Sutton & Biblarz, 2001).	21
Figure 3-3. Schematic flow diagram of a liquid propellant rocket engine with turbopump feed system (Sutton & Biblarz, 2001).	21
Figure 4-1. IBK Industriebedarf GmbH Oven and Vötsch Explosion-Proof Heating and Drying Oven VFT 60/90, respectively (IBK Industriebedarf GmbH Vacuum Drying Ovens); (Weiss Technik Explosion-Proof Drying oven, VFT with ATEX type examination).	25
Figure 4-2. A photo of dog-bone shaped samples after uniaxial tests were completed.	28
Figure 4-3. 5900 Series Universal Testing Systems (Instron Testing Systems).	28
Figure 4-4. Hand-held analog durometer type A.	29
Figure 4-5. Foss Soxtec 2055 extractor (FOSS Analytical, 2007).	29
Figure 4-6. A photo of soluble fraction test samples before extraction.	30
Figure 5-1. Stress at break values of propellants aged at 90°C.	32
Figure 5-2. Stress at break values of propellants aged at 80°C.	32
Figure 5-3. Stress at break values of propellants aged at 70°C.	33
Figure 5-4. Stress at break values of propellants aged at 60°C.	33
Figure 5-5. Strain at break values of propellants aged at 90°C.	34
Figure 5-6. Strain at break values of propellants aged at 80°C.	34
Figure 5-7. Strain at break values of propellants aged at 70°C.	35
Figure 5-8. Strain at break values of propellants aged at 60°C.	35

Figure 5-9. Stress at break values for a single propellant type. (A) Stress at break values for Propellant A aged at different temperatures, (B) Stress at break values for Propellant A corresponding real-life ageing duration at ambient conditions....	37
Figure 5-10. Strain at break values for a single propellant type. (A) Strain at break values for Propellant A aged at different temperatures, (B) Strain at break values for Propellant A corresponding real-life ageing duration at ambient conditions....	38
Figure 5-11. Hardness values of propellants aged at 90°C.....	39
Figure 5-12. Hardness values of propellants aged at 80°C.....	40
Figure 5-13. Hardness values of propellants aged at 70°C.....	40
Figure 5-14. Hardness values of propellants aged at 60°C.....	41
Figure 5-15. Hardness values for a single propellant type. (A) Hardness values for Propellant A aged at different temperatures, (B) Hardness values for Propellant A corresponding real-life ageing duration at ambient conditions.....	42
Figure 5-16. Soluble fraction values of propellants aged at 90°C.	44
Figure 5-17. Soluble fraction values of propellants aged at 80°C.	44
Figure 5-18. Soluble fraction values of propellants aged at 70°C.	45
Figure 5-19. Soluble fraction values of propellants aged at 60°C.	45
Figure 5-20. Soluble fraction values for a single propellant type. (A) Soluble fraction values for Propellant A aged at different temperatures, (B) Soluble fraction values for Propellant A corresponding real-life ageing duration at ambient conditions.	47
Figure 6-1. $\ln(\Delta S)$ versus $1/T$	126
Figure 6-2. Iteration result of β , γ and ω values for strain values of Propellant A.	129
Figure 6-3. MATLAB output regarding conversion versus time and temperature (Propellant A).....	129
Figure 6-4. Surface fit equation and resulting coefficients for strain values of Propellant A.	132
Figure 6-5. Surface fit graph for strain values of Propellant A.	132

LIST OF ABBREVIATIONS

AN	Ammonium Nitrate
AP	Ammonium Perchlorate
BRM	Burning Rate Modifier
DB	Double-Base
DOA	Dioctyl Adipate
DOS	Dioctyl Sebacate
GAP	Glycidyl Azide Polymer
HTPB	Hydroxyl-terminated Polybutadiene
HTPE	Hydroxyl-terminated Polyether
HDI/HMDI	Hexamethylene Diisocyanate
IPDI	Isophorone Diisocyanate
LSM	Least Squares Method
MAPO	Tris-1-(2-methylaziridinyl) Phosphine Oxide
MDI	Methylene Diphenyl Diisocyanate
SD	Standard Deviation
SRM	Solid Rocket Motor
SRP	Solid Rocket Propellant
SSE	Sum of Squared Errors
TDI	Toluene Diisocyanate

LIST OF SYMBOLS

E_A	Activation energy parameter in Arrhenius equation
α	Conversion of the specified property
β	Dimensionless reaction rate constant
γ	Correction factor for equation to be applicable for high conversion levels
ω	Characteristic parameter of propellant altering for each propellant

CHAPTER 1

INTRODUCTION

Composite solid propellants harbor reams of materials reacting with one another, generating a 3D network to be cured enough for operations of rocket and missile systems. Lifespan of a rocket system commences with the last step of the production and comes to an end where the rocket will not be able to perform the desired specifications (Zibdeh & Heller, 1989). Ageing can be defined as the process of becoming older due to variety of changes or reaching the end of useful life for a product (Simpson, Weiner, & Oxford University Press, 1989). It is a critical concern not for only propellants, but also for epoxy resins (Cook, Mehrabi, & Edward, 1999), tires (Stoček, Kratina, Ghosh, Maláč, & Mukhopadhyay, 2017) and electronic components (Johlitz, 2012). As ageing takes place irreversibly, to study possible failure modes and their affects thoroughly in design stage of a rocket system becomes more of an issue as performance and operation safety of rockets may greatly be affected by ageing. In order to have a grasp of propellant ageing mechanism, it is better to cut along with definition and types of rocket propellants.

1.1 Rocket Propellants

Rocket propellants are energetic materials present in missiles providing thrust and impulse (Mason & Roland, 2019); (Davenas, 1992). Solid propellants are mostly preferred due to their simplicity on the production and ease of handling. There are mainly two types of solid propellants: single/double/triple-base propellants termed as homogeneous and composite propellants as heterogeneous. Double-base (DB), being the most common type of homogeneous propellants, generally contains nitrocellulose or nitroglycerine and produced through extrusion method in order to be shaped (Chaturvedi & Dave, 2019). Most of SRMs contain polymer-based

composite propellants if there is not a specific motive for using cartridge, thy name is DB propellant. Composite propellants are fundamentally polymeric binder matrices consisting of energetic ingredients such as fuel or oxidizing agent.

Composite propellants are polymeric matrices embodying different kinds of substances in charge of distinctive responsibilities. Constituents inside of a typical composite propellant and related tasks of them are as follows:

Binder: Polymeric material that contains every other energetic and non-energetic element within itself embedded, providing dimensional stability and mechanical endurance after curing of the propellant (Davenas, 1992). Besides, it acts as fuel when oxidized (Chaturvedi & Dave, 2019). One of the main examples is hydroxyl-terminated polybutadiene abbreviated as HTPB. It is widely being used due to its low glass transition temperature, low viscosity, high combustion heat and promising mechanical properties after being cured (Davenas, 1992).

Oxidizer: Substance that principally provides thrust by creating a considerable amount of combustion heat and consequently vast amount of energy dissemination (Chaturvedi & Dave, 2019). One of the most frequently used oxidizers is ammonium perchlorate (AP), an inorganic salt, due to its high energy releasing efficiency, thermal stability and combustion performance leading to shorter ignition delay time and higher burning rate of its habitat (Deng, Wang, Yang, Ren, & Jiao, 2020).

Fuel: Material that contributes heat release and density of the propellant thereupon enhancing thrust (Chaturvedi & Dave, 2019). The most preferred fuel type is Aluminum by virtue of its availability and extenuation of combustion instability (Price, Sigmani, Sambamurthi, & Park, 1982); (Vorozhtsov, et al., 2020).

Plasticizer: Liquid substance added to the propellant in order to adjust viscosity and improve processability besides lowering the glass transition temperature of the composite (Davenas, 1992). The most frequently used plasticizers are dioctyl adipate (DOA) and dioctyl sebacate (DOS) (Jr. Lutz & Grossman, 2001); (Hoffman, Hawkins, Lindsay, Wardle, & Manser, 1994).

Burning Rate Modifier: Introduced in favor of fine-tuning burning rate of the propellant. It might have accelerating or moderating effect to the composite (Chaturvedi & Dave, 2019). State of the matter can be either liquid or solid depending on the requirements of the energetic material. Iron (III) oxide is one of the commonly used solid burning rate modifier (BRM) on the grounds of procuring homogeneous burning rate resulting in a more stable combustion profile (Kohga & Togo, 2020).

Curative / Curing Agent: Liquid material forming bonds with the binder thus constituting long chains, in this way servicing for completion of curing after mixing of the propellant (Chaturvedi & Dave, 2019). Curative selection substantially depends on the requirements of the processability and production since it has an effect upon duration composite casting, termed as “pot life” (Lee, Choi, Hong, & Lee, 2015). Commonly used curatives could be named as isophorone diisocyanate (IPDI), hexamethylene diisocyanate (HMDI) and toluene diisocyanate (TDI).

Antioxidant: Introduced in order to prevent severe degradation of the propellant that may take place mechanically or chemically (Davenas, 1992); (Villar, Silva, Diniz, Takahashi, & Rezende, 2010). This process is called as “ageing” and it has direct impact on the polymeric network. Essential examples of antioxidants would be 2,6-di(tert-butyl)hydroxytoluene (BHT) (Celina, Elliott, Winters, Assink, &

Minier, 2006) and 2,2-methylene-bis-(4-methyl-6-tert-butylphenol) (BKF) known with the trading name AO2246 (Lokander & Stenberg, 1998).

1.2 Service Life Determination of Rocket Propellants

During storage or plying between operations, rockets are prone to many compelling circumstances and they can result in failures or even catastrophic outcomes, especially when remarkable amount of time passes after the production as it can be seen representatively in Figure 1-1. This entire process called as “ageing” of the propellant is attention-grabbing over the recent years (Muhammad, Lu, & Ren, 2006). Being pupillary of the rocket and missile systems, energetic materials’ cost reduction and prolonged service life issues are urged by civil and military customers (Farhadian, et al., 2015).

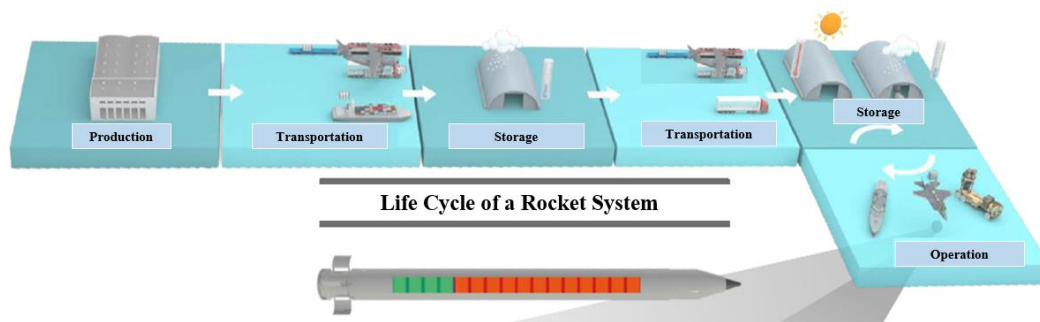


Figure 1-1. Life cycle of a rocket system.

Due to loadings of thermal, vibrational or gravitational forces, properties of solid propellants deteriorate eventually leading to structural integrity casualty of the grain. These failure modes may originate from different types of ageing forms such as chemical (oxidation, moistening, thermal reactions, temperature variations), mechanical (vibrational and thermally induced stresses) and physical (migration of liquid components) (Keizers, Brouwer, Weijl, & Weterings, 2002). Surely, these

forms of ageing may have additive or subtractive effect depending on the load that propellant grain encounters (Adel & Liang, 2019). Among these, chemical ageing is a major complication as oxidative crosslinking may result in hardening, ultimately bringing forth cracking, which is a critical mechanism for composite solid rocket propellants (Bunyan, Cunliffe, Davis, & Kirby, 1993).

In order to track ageing, service life determination studies are being conducted. In general, lifespan of a propellant would change in between 10 (Naseem, Yerra, Murthy, & Ramakrishna, 2021); (Singh, 2005) to 35 (Genov, Nedelchev, Mihovski, & Mirchev, 2019) years. Observing propellant properties directly during its lifetime may not be a facile way to appoint degradation mechanism as it would take aeon. Instead, “accelerated ageing” method is preferred to predict surveyed property of the propellant donating much shorter times (Biggs, 2009). Since chemical reactions speed up at higher temperatures, ageing in real life at ambient temperatures could be simulated by carrying out tests with energetic materials placed and held at elevated temperatures for predetermined periods of time (Cerri, Bohn, Menke, & Galfetti, 2009). Sometimes, accelerated ageing process is also named as “artificial ageing” since during ageing phase, temperatures higher than ambient temperature - that will not be encountered during service life of a rocket motor - are chosen in order to trigger ageing in terms of chemical reactions within much shorter periods of time: in the order of months instead of years. Thereafter, service life prediction is provided by integrating test results into proper mathematical models (Connors, 1990).

CHAPTER 2

LITERATURE REVIEW

Being a very important aspect of rocket science, service life prediction of propellants depends on modeling of property change during ageing process as elaborated in the previous chapter. Due to its advantages aforementioned, hydroxyl-terminated polybutadiene based propellants take the lead on the subject of composite propellants. Along these lines, this study will be more focused on the ageing of HTPB-based polymers. In more detailed scheme of things, accentuated oxidative crosslinking occurs due to HTPB with a structure of double bonds, see Figure 2-1, being susceptible to oxygen attacks.

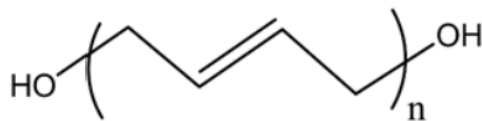


Figure 2-1. Chemical structure of hydroxyl-terminated polybutadiene (Khan, Dey, Athar, & Sikder, 2014).

In order to reduce HTPB's sensibility due to its unsaturated character, propellants are stabilized with antioxidants that have restraining effect on oxidation mechanism (NC, 1993). By the time of progress, antioxidant depletion or deactivation arises both during curing and long term ageing processes. Once the protective effect of antioxidants ramps down, thermo-oxidative ageing embarks upon dominating and degradation of polymer progresses rapidly, abandoning polymer to its fate: ultimate lifetime (Celina, Elliott, Winters, Assink, & Minier, 2006).

Ageing of a HTPB-based composite solid propellant could be monitored by several techniques. Measurement of mechanical properties such as modulus, tensile strength

or tensile strain is the most used method in the relevant area. However, chemical properties such as soluble fraction described as the section of the polymeric matrix that has not been oxidatively crosslinked (yet) and hereby, crosslink density described as the section of the polymeric matrix that has been already oxidatively crosslinked could be tracked and regarded as ageing assessment parameter by way of macromolecular properties like mechanical properties. Extent of crosslinking can be represented and evaluated by first analyzing soluble fraction inside of a propellant, then proceeding with Charlesby-Pinner equation, where S represents the soluble fraction which is attained by extraction from propellant samples (Military Agency for Standardization, 2006):

$$\textit{Crosslinking Density} = \frac{(1 - S) * [2 - (S + \sqrt{S})]}{(S + \sqrt{S})} \quad \text{Equation 1}$$

In the literature, ageing is mostly modeled through mechanical properties. However, mechanical tests require much more labor and operational cost in practical terms when they are compared to chemical tests. Furthermore, since rocket motors have a cylindrical shape, it is thorny to withdraw mechanical test samples from the propellant bulk inside of the motor as these samples have both round and cornered parts. An example of a dog-bone shaped uniaxial tensile test sample, having dimensions of 12.5 mm x 25.5 mm x 125.5 mm, can be seen in Figure 4-2. For chemical tests on the other hand, tiny amounts, equivalent nearly to 3 grams sliced with dimensions of roughly 1 mm x 2 mm x 2 mm demonstrated in Figure 4-6, propellant are adequate (Military Agency for Standardization, 2006).

This ageing phenomena resulting in completion life of a propellant has been described through several mathematical models. These models can be summarized in two main headings here below.

2.1 Methods for Mechanical Property Modeling

One kinetic approach is based on classical Arrhenius approach predicting how acceleration or deceleration of a reaction rate occurs with temperature. First proposed by Jacobus Hendricus van't Hoff in 1884 as an empirical expression and then physically justified and interpreted by Svante Arrhenius in 1889 (McKeen, 2017), Arrhenius Equation is considered as one of the best models describing kinetic data regarding processes including chemical reaction and mass transfer.

$$k = A * \exp\left(\frac{-E_A}{R * T}\right) \quad \text{Equation 2}$$

Where k is reaction rate, A is pre-exponential factor, E_A is the activation energy of the reaction, R is universal gas constant and T is the absolute temperature. This equation is widely being used in pharmaceutical (Yoon, 2014), food (Corradini & Peleg, 2006) and rocket industries (Judge, 2003) in order to have an insight on shelf life of the related product for warranty and safe life cycle issues.

There are two possible ways to apply Arrhenius equation to data set to be able to have an approach regarding ageing. First option is to obtain activation energy without presuming any reaction order (Judge, 2003), by incorporating property change data within time intervals directly into the model. Another option is first attaining reaction rates for each ageing temperature test data and then proceeding with known reaction rates to build Arrhenius equation. In order to calculate reaction rates, test results should be represented by a decent model that fits the experimental data with a good fit. There are several studies enumerating the usage of Arrhenius equation while determining service life of energetic materials by applying different types of reaction equations.

Layton's model proposing both gel (crosslinked portion) fraction and mechanical properties of a propellant are linear functions of logarithmic ageing time (Layton, 1975):

$$P(t) = P_0 + k * \ln\left(\frac{t}{t_0}\right) \quad \text{Equation 3}$$

Where P(t) is property such as stress at break, strain at break or modulus; being observed while changing with increasing age time, P₀ is the initial value of that property after completion of curing before artificial ageing begins, t is ageing time, t₀ is the time after curing completes before artificial ageing begins and k is the ageing rate constant in this case. The sign in front of k depends on the property being observed.

Layton suggested that during ageing period, amount of gel continues to increase and the rate of this increment becomes greater with increasing temperature. According to Layton, observing just mechanical properties of propellant during artificial ageing is not enough to model them properly. Especially for long ageing durations, when measured data is obliged to be extrapolated, predicted values should be in good agreement with the built model. Hence, chemical and physical properties should also be monitored and correlated with the change in mechanical properties.

Another kinetic approach is first order kinetic equation, see Equation 4, taking initial softening behavior into account when aziridinyl compounds (compound consisting aziridine group as can be seen in Figure 2-2) are present inside of the propellant used as curing or bonding agent (Adel & Liang, 2019).

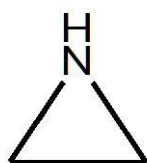


Figure 2-2. Aziridine group.

$$\ln(P(t)) = \ln(P_0) + k * t \quad \text{Equation 4}$$

The sign in front of k depends on the property being observed. When change in conversion rather than property change is integrated into Equation 5, another version of this equation is obtained:

$$-\ln(1 - \alpha) = k * t \quad \text{Equation 5}$$

Where α stands for the conversion of the studied property:

$$\alpha = \frac{P_0 - P(t)}{P_0} \quad \text{Equation 6}$$

Although first order kinetic equation is a simple differential equation representing mostly single-step reactions, it is also favorable for complex and multi-step functions when investigating these steps one by one could be tedious. As mentioned earlier, propellant consists of several compounds reacting each other in a manner that is nontrivial to elucidate the reaction steps thoroughly. Thus, considering oxidative ageing from the point of mass transfer aspect in total, first order rate equation stands as a prospective method to account for the change in properties.

Arrhenius equation is based on random collision processes through Boltzmann statistics. If the chemical conversion involves more than one step between the initial and final states, one has to carefully consider the whole path, and then develop a mathematical model with sufficient complexity to take everything into consideration such that a relationship accurate enough between temperatures and/or time and the rate of the process can be elucidated. Hence, priory to obtaining reaction rate, mathematical model representing property-time relationship should be decided on discreetly. Since Arrhenius approach consists of a two-step calculation, in order not to lose the solidity of the model, each step is needed to be well-defined. Having regard to the fact that although Arrhenius equation is a world widely accepted and easy to handle model, carrying also the mentioned drawbacks, it would not be incorrect to say that *with great power comes great responsibility* as Uncle Ben told Peter Parker in movie: Spider-Man (Lee & Ditko, 2002).

Although most of the models described in this section are widely used for modeling mechanical properties of a propellant, whether they are employable for chemical properties or not is a topic that is worth-stressing. Thus and so, not only chemical property modeling, but also mechanical property modeling is discussed over the course of the study.

2.2 Methods for Chemical Property Modeling

Some of the models already being used for modeling mechanical properties through ageing are also capable of modeling chemical properties. Notwithstanding, since modeling of chemical properties is a less considered issue historically in terms of propellant ageing, method variety is much narrower when compared to that of mechanical properties. For instance, Layton's approach displayed by Equation 4 is employable for both mechanical and chemical properties (Layton, 1975) as it is mentioned in the previous chapter.

Another approach anticipated to be apt for modeling chemical properties is, as shown in Equation 7, zeroth order rate equation (Bohn & Cerri, 2010) where the sign in front of k depends on the property being observed. Bohn and Cerri observe an increase in crosslink density indispensably while soluble fraction is decreasing and hence, it is implied that oxidative crosslinking is more pronounced than chain scission during artificial ageing process.

$$P(t) = P_0 + k * t \quad \text{Equation 7}$$

Yet another approach put forward is to integrate chemical property test data collected during prolonged storage, 21 months, at elevated temperatures of 38, 43 and 60°C into Arrhenius equation (see Equation 3) without presuming any reaction order (Judge, 2003), as also precluded in the previous chapter. To be only expected, rate of degradation of propellant increases with increasing temperature, having evidential value that accelerated ageing is a coherent way to form an opinion about lifetime of an AP/HTPB based solid rocket propellant. Judge also states that choosing close

temperatures for accelerated ageing process might not be reasonable for calculations as the property change within specific time interval would be very close to each other for these temperatures due to test variations and data scatter inherent in the testing processes. Thus, modeling is held by reckoning two distinctive temperatures into calculation of activation energies and obtained as 71.0 kJ/mol and 74.3 kJ/mol, respectively for mechanical and chemical properties.

Yet another kinetic equation to model propellant properties with artificial ageing is the usage of *reaction severity index* (Dubois & Perreault, 2002). Considerations regarding Arrhenius approach lead some authors to a more general shelf life predicting tool. Integrating dimensionless time-temperature variables into mathematical models have been performed in several studies involving different reactions in regards to kinetics of complex systems such as biological applications including lignocellulosics fractionation (Abatzoglou, Chornet, Belkacemi, & Overend, 1992), thermolysis of glycol lignin (Thring & Chornet, 1993) or petrochemical applications of heavy-oil cracking (Shu & Ross, 1982). Within severity concept, ageing time and ageing temperature variables are expressed in dimensionless form in the kinetic models used to depict degradation of polymeric binder. Since polymeric binder degradation process follows a first order kinetics with a slightly changed version of Equation 5 on the score of dimensionless severity factor, R , the reaction rate can be described as follows:

$$-\ln(1 - \alpha) = \beta * R \quad \text{Equation 8}$$

$$R_w = \int_0^t \exp\left(\frac{|T_r - T_b|}{\omega}\right) dt \quad \text{Equation 9}$$

Where T_r is reaction temperature, T_b is base temperature where no degradation occurs, t is ageing duration, β is reaction rate constant in dimensionless form and ω is characteristic parameter which is propellant-specific, containing activation energy parameter (E_A) within itself (Garrote, Dominguez, & Parajo, 2002).

To be able to eliminate low resolution of the equation at high conversion values, severity dependent rate constant (γ) is integrated into the equation forming a new relation:

$$-\ln(1 - \alpha) = \frac{\beta}{\gamma} * R^\gamma \quad \text{Equation 10}$$

Herewith, constants can be evaluated by accommodating experimental data into this nonlinear differential equation using procedures like nonlinear least squares minimization.

2.3 Scope of the Study

Being au fait with the information that main degradation mechanism over time is oxidative crosslinking of the polymeric binder during ageing, course of this study is built to represent this phenomenon in terms of chemical property test results to be used for both service life determination and extension of propellants. Service life determination is held whether in the design phase of a rocket motor or when necessary, appointing properties of subsystems of a rocket motor at any time. Service life extension is an operation where worn out elements of rocket system are replaced with renewed ones if performance and reliability criteria of the subcomponents are not met after the examination via destructive and/or non-destructive tests. Since constituents of rockets are very expensive in aspects of development and production, service life extension is more preferable both for producer and end user.

To be able to exemplify the real situation, first of all, propellant samples are designed to be aged in a confined way as propellants are ordinarily contained in a sealed rocket motor. In order to eliminate loss or migration of liquid substances as much as possible, samples are confined using aluminum foil. Sealing of a rocket motor is indubitably much sheltering since most of bonnets are steely products. Thus, on this level of sampling, model to be used will be conservative to a degree as it represents a worse case than the real situation in terms of chemical ageing.

When it comes to mathematical modeling, there are plenty of approaches already being used and made an impression in the literature. Nonetheless, not all models seem to fulfill the need for the deficit in the related area. Oxidative crosslinking can be regarded as a classical mass transfer problem. That being the case, zero order rate equation might not be a reasonable choice due to the nature of the reaction as there is a limited number of double bonds that is available to form crosslinks. The very same explanation applies to Layton's model as well: this model includes time parameter in exponential form, which is not quite sensible on sober reflection.

In order to forge a mathematical model utilizable for most of rocket propellants, modeling of mechanical properties is carried out by taking strain values into consideration since strain is driven practically by polymeric network, whereas stress and modulus are functions of both binder stiffness and binder/filler interactions (Davis, 2001). As oxidative crosslinking concept is exclusively related with the polymeric network itself, strain values are thought-out to be a better representation to analogize with chemical properties. Additionally, while modeling, soluble fraction test results are taken under review as they are direct results of chemical tests, rather than putting crosslink density calculation into perspective in order to eliminate extra steps of computations.

CHAPTER 3

A BRIEF HISTORY OF ROCKET SCIENCE

Since the first employment of a “rocket”, simply a tube containing gunpowder lidded at one end and attached to a long baton, in 13th Century dating back to a battle between Chinese and Mongols, rocket science seeds had been planted (Brief History of Rockets, n.d.). After the first ignition of this idea (and the rocket, of course), rocket science had been developed swiftly through the years and recently became apple of investors’ eye (Bryce Space and Technology, 2017). This field had become a focus of interest as rocket motors have been used in missile systems for both military and space exploration products.

Rationale of rocket science is at the heart of Newton’s Third Law of Motion (Rocket Fundamentals, 2012). According to this law, every action has an equal and opposite reaction, that is, if an object is pushed towards one direction, the object pushes back with the same amount of force. In rocketry, a rocket system is being pushed by the products (exhaust gas) of burning fuel providing thrust giving rise rocket to blast off and move in the opposite direction due to conservation of momentum.

Although first implementation of rockets was in 13th Century, dawn of modern rocketry is dated back in early 1900’s (The History of Spaceflight, 2011). Konstantin Tsiolkovsky, Russian schoolteacher, stated the “rocket equation” expressing the relation between the velocity changes that rocket lives through due to burning fuel with decreasing mass by reason of expelled exhaust gas:

$$\Delta v = u * \ln\left(\frac{m_i}{m}\right) \quad \text{Equation 11}$$

Where v is rocket velocity, u is velocity of gas being ejected by engine motors, m is instantaneous rocket mass: summation of mass of rocket itself and mass of fuel at that specific time, m_i is total initial mass (Rocket Fundamentals, 2012).

Robert Goddard, American physicist, proposed that rockets can achieve higher altitudes with liquid fuel due to its lower density and became the first person to build a successful liquid propellant rocket in 1920's (Bilis, 2016). He, holding over 200 patents regarding rocket technology, is merited as the "father of rocketry" by authorities (Clark University Robert H. Goddard Library, 2021). Hermann Oberth gazed upon space and became the pioneer of modern rocket technology and spaceflight as he played a key role regarding practical applications of rocket propulsion (Howell, 2018).

Subsequent to World War II, space race has begun between Soviet Union and United States as a show of strength in the international community (Siddiqi A. A., 2000). World's first artificial satellite, Sputnik I, was launched into the space in 1957. In 1961, Yuri Gagarin became the first person ever present in space with Vostok-K rocket while Alan Shepard made suborbital spaceflight with Redstone rocket in the following weeks (Launius, 2004). The first crewed Moon landing was accomplished in 1969 with renowned Apollo 11 program, using Saturn V rocket (Clegg, 2020). In the process of time, space race became more civilian as more countries got involved. Today; due to high levels of funding, interest of common people and technological developments, space has become more international (Siddiqi A. , 2008).

Although these accomplishments are thrilling for history of rocket flight, of course, failures alongside took place as well. In 1944, RAF Fauld ammunition depot in England detonated while being stored (Fauld explosion 70th anniversary: New memorial unveiled, 2014). This incident is passed as one of the most devastating non-nuclear explosions in the world since 4000 tons of explosives and 500 millions of bullets created a pit, known as the Hanbury Crater: 30 meters in depth with a diameter of 300 meters. 70 people were found dead besides numerous vanished animals and buildings (Hardy, 2015). Space Shuttle Challenger disaster occurred because of an o-ring failure causing a catastrophic explosion which ended up loss of lives of seven astronauts, in 1986 (Boin, 2008). In 2003, shed insulation foam of the external propellant tank struck on the orbiter of the Space Shuttle Columbia, causing disintegration while reentering the atmosphere and killing seven crew members

(National Aeronautics and Space Administration, 2003). In 1997, Delta II Mission 241 was unsuccessful as Delta II rocket motor fulminated 12.5 seconds after lifting off. According to NASA engineers, the occurrence of damage stemmed from cracks due to vibration possibly occurred during transportation of the system (Balageas, Fritzen, & Güemes, 2006).

When magnitude of these systems and the resultant loss of life and property in case of a failure are taken into consideration, it is essential to study possible failure modes and their affects thoroughly in design stage of a rocket system. Service life prediction of propellants is just one aspect of these failures within rocket science, and this thesis is centered upon the indicated issue accounting for chemical ageing.

3.1 Classification of Rockets

A rocket is comprised of several main parts depending on the rocket type. There are various ways to classify rockets such as according to type of energy source, their basic function, type of construction or method of producing thrust (Sutton & Biblarz, 2001). Chemical propulsion, nuclear propulsion, electrical propulsion and solar propulsion can be given as examples considering the methods of producing thrust. Since the most efficient way to produce thrust is chemical combustion, majority of the rockets are driven by chemical propulsion. Chemical rocket propulsion devices can also be categorized depending on state of the propellant.

Solid propellant rocket motors are propelled by burning at a predetermined rate of solid propellant charge called “grain” prefilled inside of the case. Burning of the propellant is initiated by an igniter and continued due to internal cavity in the middle of the case. Resulting hot gas by the way of consumed propellant discharges through nozzle creating thrust. The case is obliged to withstand operation temperatures and pressures. Insulation is crucial in order to protect inside surface of the case (Davenas, 1992). An example of a solid propellant rocket motor can be seen in Figure 3-1.

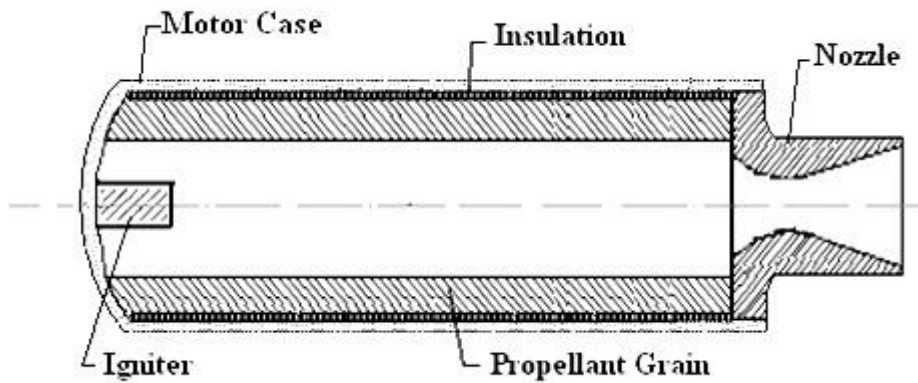


Figure 3-1. Main parts of a solid rocket motor (Açık, 2010).

Liquid propellant rocket engines function by liquid propellant fed from tank into combustion chamber to decompose into hot gas by pressure (Figure 3-2) or by a pump (Figure 3-3), and ejected through nozzle. Liquid propellants can also be divided into two: *monopropellants* are single liquids containing both fuel and oxidizing agents within itself and reacted by a catalyzer, whereas bipropellants consist of a fuel and an oxidizer separately.

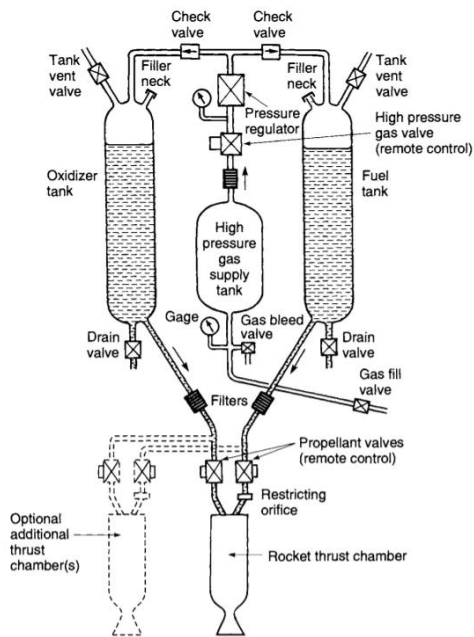


Figure 3-2. Schematic flow diagram of a liquid propellant rocket engine with a gas pressure feed system (Sutton & Biblarz, 2001).

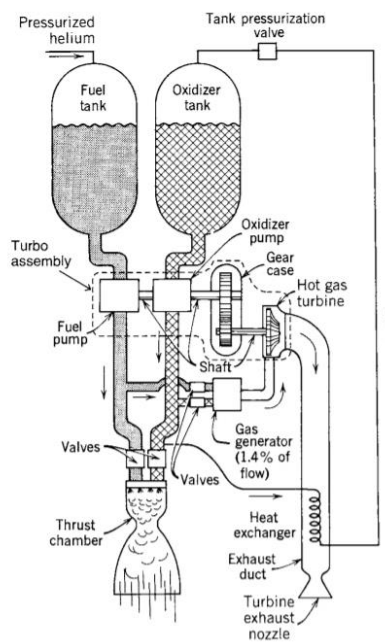


Figure 3-3. Schematic flow diagram of a liquid propellant rocket engine with turbopump feed system (Sutton & Biblarz, 2001).

Gaseous propellant rocket engines are driven by high pressure gas stored in heavy tanks resistant to pressure. Nuclear rockets can be given as an example for this kind.

Hybrid propellant rocket engines use liquid propellant as oxidizer and solid propellant as fuel (Yıldırım, 2007). There are also hybrid engines where liquid propellant is pressurized and hot gas used for pressurization is generated by solid propellant.

Among rocket motor types, solid rocket motors (SRM) are primary preferences especially regarding short and medium range missiles due to their ease of design, manufacture and operation, considerably long life-time storage when compared other fore mentioned rocket engines, robustness and requirements of little maintenance in case needed (Mahjub, Mazlan, Abdullah, & Azam, 2020); (Mason & Roland, 2019). Being the source of propulsion, SRMs are indispensable for solid propellant rocket systems. In a typical medium range missile, a SRM takes up room of %50-60 of total rocket mass (AGARD, 1997). For longer range missiles, SRMs are even much heavier in so far as propellant mass increases in order to provide sufficient thrust. As a consequence of this, propellant formulation and related service life studies should be addressed as SRM design parameters.

CHAPTER 4

EXPERIMENTAL SECTION

Propellants with altering polymer types were prepared in 25 liters of vertical dual blade planetary mixer. All these polymers belong to HTPB class having varied suppliers both from Turkey and abroad. Different polymer types used within the propellants, related denotations and differences between them are as follows:

Table 1. Polymers being used in the structure of studied propellants.

Polymer Type Being Used	Propellant Denotation	Hydroxyl Values (meq/g)	C/P values
Type V	A	0.75	0.74
CH1471	B	0.65	0.91
Type III	C	0.89	0.70
CH1080	D	0.80	0.78
Type I	E	0.52	0.87
Type II	F	0.69	0.80

Hydroxyl value can be defined as the amount of hydroxyl groups inside of a polymer that is available for curing reactions, therefore is a crucial parameter indicating the functionality of a polymer. It is commonly expressed as ratio of moles of hydroxyl groups to number of average molecular weight of the polymer and denoted in *meq/g* (Foli, Esposti, Toselli, Morselli, & Fabbri, 2019). In order to minimize the dissimilarities between curing and ageing mechanisms of propellants, curative to polymer (C/P) ratios were regulated as in Table 1. Since lower hydroxyl value means there are lesser possible sites of hydroxyl groups ready to react with isocyanate groups in order to create linkage through themselves, generally amount of curative added has to be increased to be able to enhance the chance of coinciding hydroxyl groups of the polymer and isocyanate groups of curative with each other. However, this value can be arranged in many cases, especially when scale-up is needed.

4.1 Propellant Preparation

Propellant formulation besides polymer is kept the same having %8-12 of HTPB polymeric binder matrix, %60-70 of trimodal AP as oxidizer, %15-20 of Al as fuel and other ingredients in small portions such as ferric oxide (Fe_2O_3) as burning rate catalyzer, IPDI as curing agent, an aziridinyl type of bonding agent, antioxidants and organic compound DOA as plasticizer. These types of propellants are called “heterogeneous propellants” since solid particles AP, Al, Fe_2O_3 are held inside of a polymeric binder matrix with all the liquid materials of curing agent, bonding agent and plasticizer inside. Propellants were mixed in several steps. Initial step was the mixing of liquid substances, prepolymer with bonding agent, antioxidants and plasticizer at 40-45°C. Solid particles were then poured into the mixer and all the requisites were mixed at 40-45°C before curing agent was added as the final step. Finally, the total blend was mixed for several minutes. During mixing, mixer blades were scraped in some specific time intervals in order to include the leftover propellants adhered on the blade into the reservoir of the mixer.

Propellants were prepared at the end of proximately 4 hours of mixing. Before mixing, ingredients were preconditioned at the mixing temperature in order to ensure proper, homogeneous mixing and to prevent wetting of solid particles. In some of the steps, mixing under vacuum was essential in order to prevent swelling.

4.2 Ageing Specimen Preparation

Propellants were poured into rectangular boxes with aluminum interior using a casting bench. Thereafter, propellant boxes were left to curing in temperature-controlled air circulating drying and ex-proof, a total of two different ovens adjusted to 50°C. Data loggers were placed into these IBK Industriebedarf GmbH Oven and Vötsch Explosion-Proof Heating and Drying Oven VFT 60/90 (see

Figure 4-1) for temperature and humidity check. Data indicated that temperatures of the ovens were at $50\pm 1^{\circ}\text{C}$ with a relative humidity of $5\pm 1\%$. Curing of propellants was monitored via hardness test and it took approximately 7 days for all of the 6 propellants.



Figure 4-1. IBK Industribedarf GmbH Oven and Vötsch Explosion-Proof Heating and Drying Oven VFT 60/90, respectively (IBK Industribedarf GmbH Vacuum Drying Ovens); (Weiss Technik Explosion-Proof Drying oven, VFT with ATEX type examination).

4.3 Propellant Ageing

Thermal ageing of the propellants was carried out in Vötsch Explosion-Proof Heating and Drying Oven VFT 60/90 for 80 and 90°C studies whereas for 60 and 70°C accelerated ageing studies in hot rooms with temperature and humidity control under atmospheric pressure. Data loggers were placed into these rooms and oven and resulting data demonstrated a fluctuation of $\pm 1^{\circ}\text{C}$ and $\pm 5\%$ temperature and relative humidity, respectively.

Ageing process and conditions were chosen according to van't Hoff approach. For chemically driven ageing processes, van't Hoff suggests that for a 10°C of temperature change, speed of a chemical reaction - to wit change in enthalpy of the reaction - changes by a specific factor of F ($\Delta H/R$), varying between 2 to 6 depending on the nature of the reaction. In order to commence the study with an initial guess, heuristic of F being equal to 2.5 for composite and energetic materials was endorsed. By this means, for a 10°C of temperature increase, propellant ages approximately 2.5 times faster.

$$t_E = t_T * \frac{F^{\frac{T_E - T_T}{\Delta T_F}}}{365.25} \quad \text{Equation 12}$$

Where t_E is service time in years at in-use temperature T_E , t_T is accelerated ageing time at elevated ageing temperature T_T , F is the reaction rate change factor with respect to temperature change ΔT_F , 10°C in this case. Since this study was designed with 10°C of temperature changes from 60 to 90°C, ageing periods were generated as in Table 2. The ageing times were rounded up for fractional day counts.

Table 2. Ageing periods and durations of the propellants.

Ageing Temperature (°C)	0 th Period (days)	1 st Period (days)	2 nd Period (days)	3 rd Period (days)	4 th Period (days)	5 th Period (days)
25	0	730	1460	2190	2920	3650
60	0	30	60	90	120	150
70	0	12	24	36	48	60
80	0	5	10	15	20	25
90	0	2	4	6	8	10

First row of Table 2 represents the case of ageing corresponding to 10 years in ambient conditions. To be able to monitor property changes plainly, accelerated ageing durations were divided into five equal intervals after calculating total ageing duration for each temperature by means of van't Hoff. This approach in fact, is similar to Arrhenius approach with an initial activation energy assumption. When total ageing duration is calculated using van't Hoff equation, it basically stands for

the range of 75-82 kJ/mol for test temperatures of 60-90°C. This is a quite conformable guess while activation energy for solid rocket propellants generally lies in between 10-140 kJ/mol (Adel & Liang, 2019).

Evaluation of the specimens' mechanical, chemical and physical performance was attained by taking specimens out from the rectangular boxes in slices through the instrument of guillotine. Slices were aged in specified time intervals according to Table 2 to be afterwards punched to constitute forms of samples for performing aforementioned tests. For some specific ageing time intervals, some propellants were prone to different ageing periods than in Table 2 due to shutdown period of the company. Imposed ageing days are specified in tables from Table 15 to Table 61 and all modeling calculations were performed accordingly.

4.4 Tests

4.4.1 Uniaxial Tensile Tests

Uniaxial tensile test was carried out with dog bone shaped specimens (Figure 4-2) having dimensions according to STANAG 4581 using an Instron 5965 Series Tensile Testing Machine (Figure 4-3) with a video extensometer at a crosshead speed of 50 mm/min and temperature of $23\pm 2^{\circ}\text{C}$ as stated in STANAG 4506. Measurement of strain was held through the instrument of extensometer. Each uniaxial test was conducted with 6 specimens and results were recorded as their mean values and standard deviations (SD) unless presence of outlier results with 95% confidence level. Outliers were automatically disregarded by the instrument if they fall outside of 95% confidence level. These are indicated by empty slots in tables from Table 15 to Table 61. While strain values are given in percent change, stress at break values are given in both MPa and psi units.



Figure 4-2. A photo of dog-bone shaped samples after uniaxial tests were completed.



Figure 4-3. 5900 Series Universal Testing Systems (Intron Testing Systems).

4.4.2 Hardness Tests

Hardness tests were carried out using hand-held analog durometer type A (Figure 4-4) according to ASTM D2240. Durometer is a device measuring the indentation depth of a presser foot assembly, indicating the resistance of the sample to penetration under a constant force. Tests were conducted at $23\pm 2^{\circ}\text{C}$.



Figure 4-4. Hand-held analog durometer type A.

4.4.3 Soluble Fraction Tests

Soluble fraction was determined by extraction procedure using a Foss Soxtec 2055 extractor apparatus (Figure 4-5) and dichloromethane as solvent by following the instructions in STANAG 4581. Samples of shredded propellants (Figure 4-6) were subjected to evaporation to eliminate excess solvent and ultimately, soluble content in Soxtec thimbles is retained.



Figure 4-5. Foss Soxtec 2055 extractor (FOSS Analytical, 2007).



Figure 4-6. A photo of soluble fraction test samples before extraction.

CHAPTER 5

RESULTS AND DISCUSSION

In this study, six different HTPB/AP/Al based propellants were exposed to accelerated ageing for monitoring mechanical and chemical properties of the propellants during the ageing period in order to establish a mathematical model for service life determination using chemical properties. Since service life determination of propellants is being widely conducted via mechanical properties, it was necessary to observe both properties to be able to advocate the physical meaning behind the model.

The methodology followed can be divided into several steps. Propellant preparation and casting was the initial step of this study. Second step involved accelerated ageing process of the propellants at temperatures higher than the ambient temperature: 60, 70, 80 and 90°C. As a third step; mechanical, chemical and physical property change of the propellants were monitored during the course of accelerated ageing test plans. And ultimately, being the aim of this work, strain and soluble fraction values were tuned into mathematical models.

5.1 Mechanical Property Change During Ageing

Mechanical properties of the propellants were monitored during ageing periods starting from the very first cured version t_0 until t_{final} corresponding to 10 years of isothermal ageing at 25°C. When oxidative ageing mechanism is prominent, propellant properties are expected to change in a direction representing the hardening of the polymeric matrix. Hence, during ageing, mechanical properties demonstrate different trends depending on the mode they are representing; while stress values are expected to increase, strain values are expected to decrease as these tendency epitomizes propellant hardening. Change in mechanical property values for all

polymers with altering temperatures is given in Appendix, from Table 15 to Table 62 and shown in figures from Figure 5-1 to Figure 5-8.

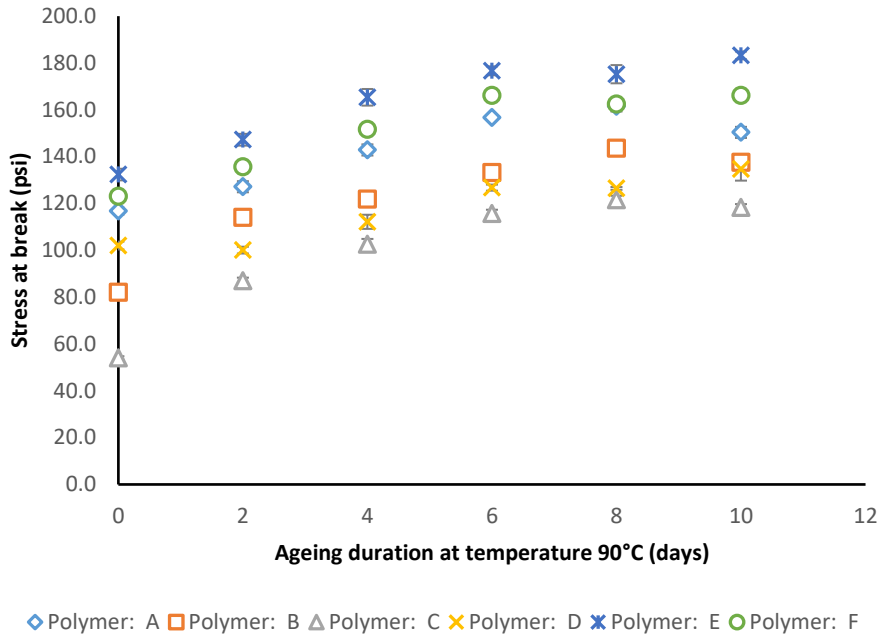


Figure 5-1. Stress at break values of propellants aged at 90°C.

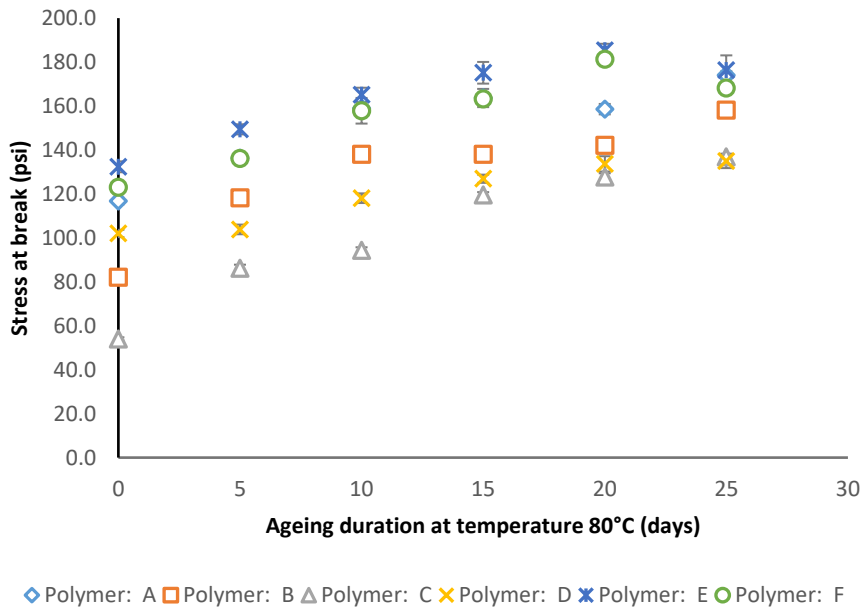


Figure 5-2. Stress at break values of propellants aged at 80°C.

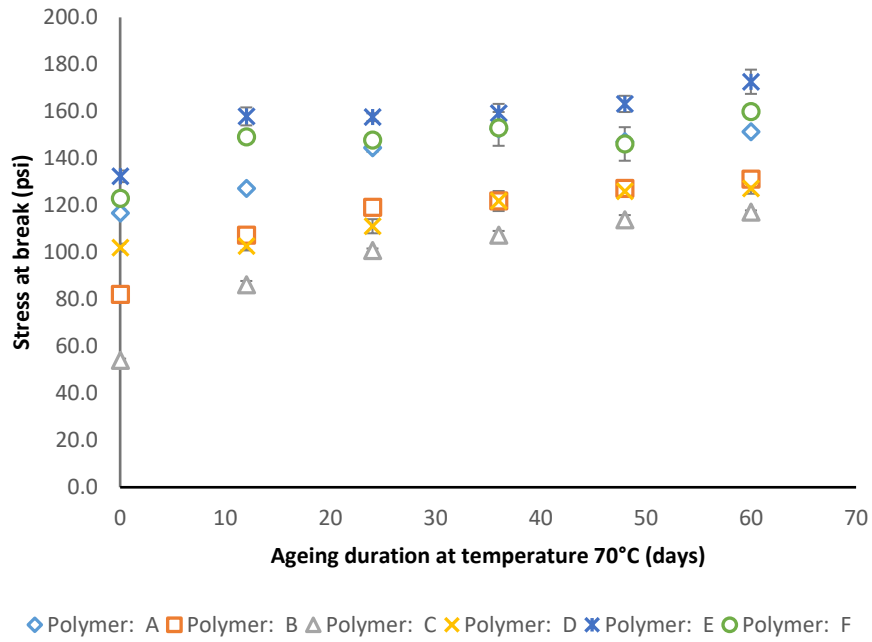


Figure 5-3. Stress at break values of propellants aged at 70°C.

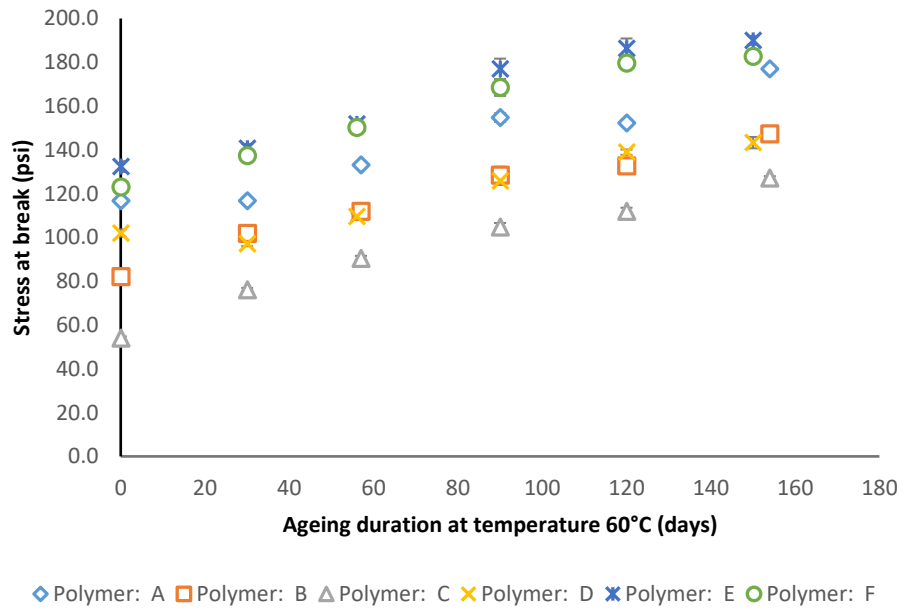


Figure 5-4. Stress at break values of propellants aged at 60°C.

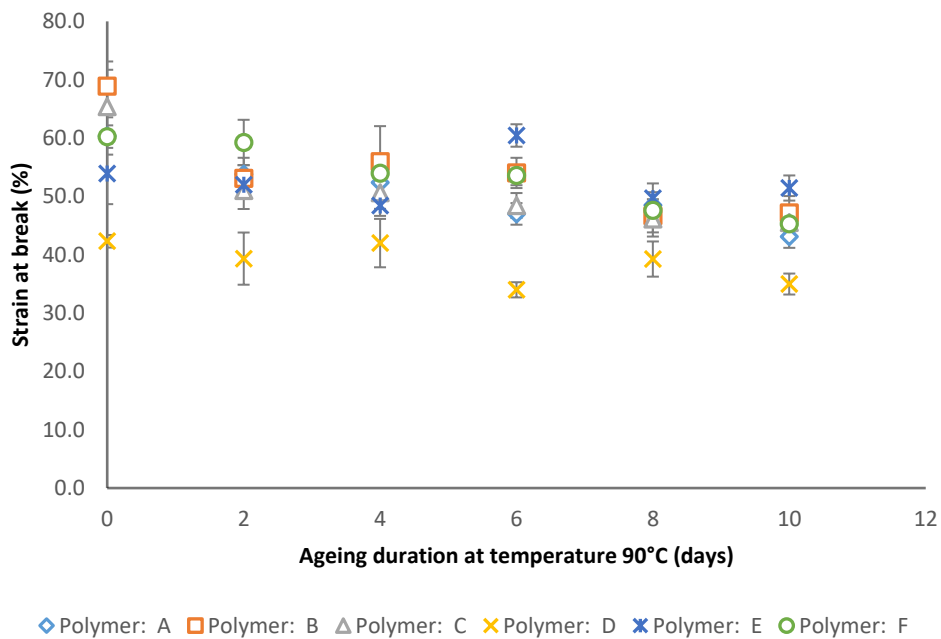


Figure 5-5. Strain at break values of propellants aged at 90°C.

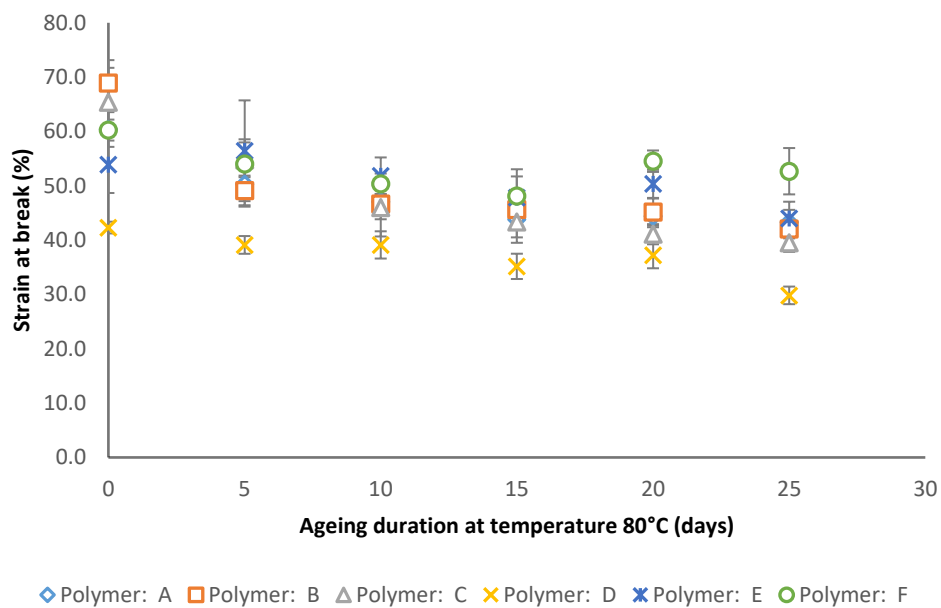


Figure 5-6. Strain at break values of propellants aged at 80°C.

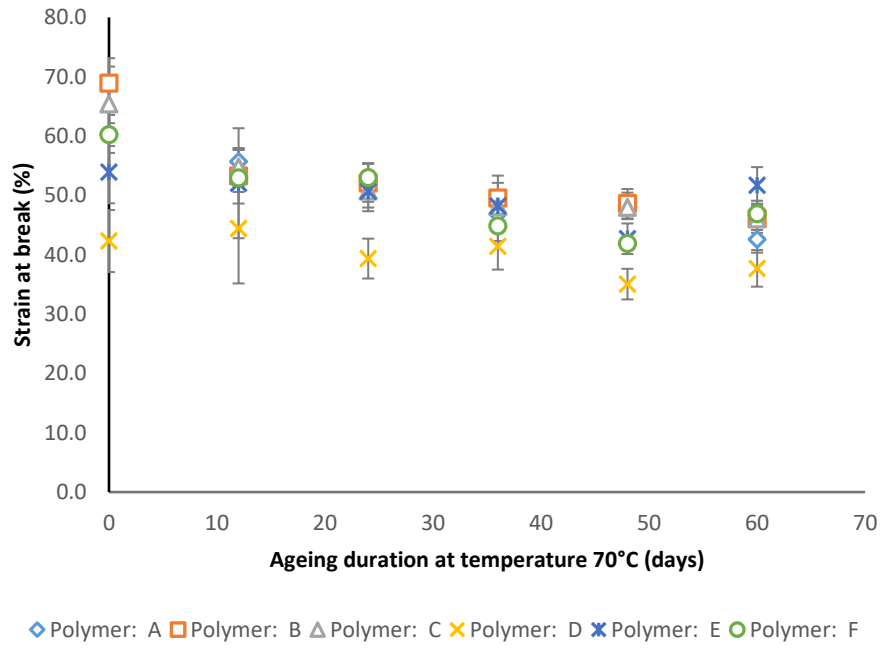


Figure 5-7. Strain at break values of propellants aged at 70°C.

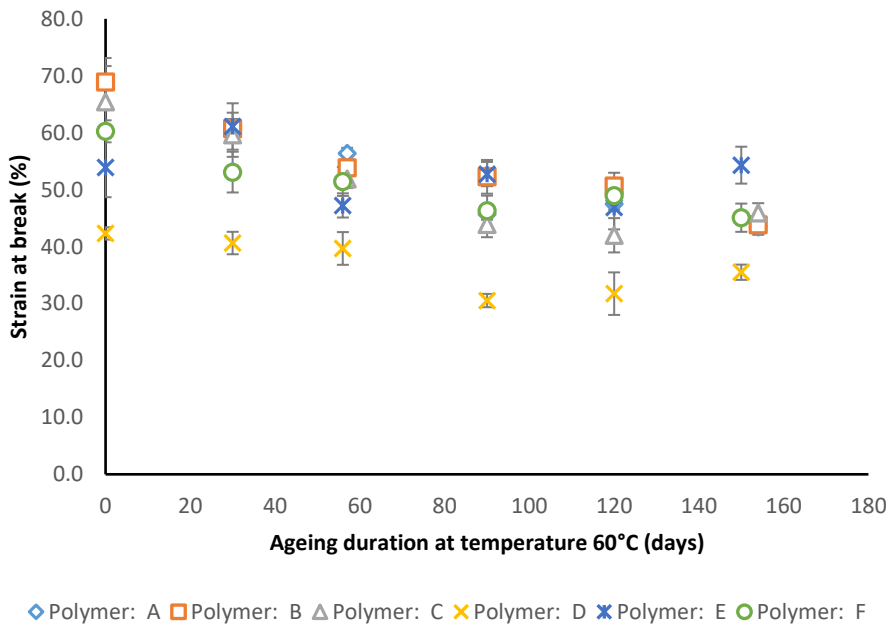


Figure 5-8. Strain at break values of propellants aged at 60°C.

From the figures above, it is distinguishable that there are several test results contrary to expected ageing tendency. This out of scope cases can be explained by AP dewetting due to heterogeneous structure of the solid propellant and hydrolysis reactions due to humidity fluctuations during transportation of samples from heating ovens to laboratories or between laboratories where mechanical and chemical tests are conducted. Although hydrolysis reactions are not entirely understood yet, they are known to be occurring from the attacks of water particles to possible sites of composite propellants: polymer (HTPB) backbone or the interface between binder and filler (Iqbal & Liang, 2006). When moisture content increases within the propellant, while stress and modulus values decreases strain values generally remain stable or show a tendency of increase. This behavior of uniaxial test results is conclusive evidence that humidity content mostly has an effect on binder-filler interaction rather than the binder network (Davis, 2001). This content of moisture inevitably affects chemical test results as humidity easily causing polymer chain scission and inducing undesired side reactions, directly having an impact on soluble fraction values. These results are demonstrated in the following chapters.

In order to make a comparison between selected ageing temperatures and corresponding ageing durations, mechanical property change at different temperatures for a single, arbitrarily chosen propellant type (Propellant A) are given in Figure 5-9 (A) and Figure 5-10 (A) for stress at break and strain at break values, respectively. These values with respect to normalized ageing durations corresponding to ageing at ambient conditions in real life case are given in Figure 5-9 (B) and Figure 5-10 (B), respectively. As can be seen from the figures, it can be deduced that ageing trends for each selected ageing temperature are very similar to each other. This similarity shows that accelerated ageing durations and temperatures obtained through van't Hoff approach is quite conformable.

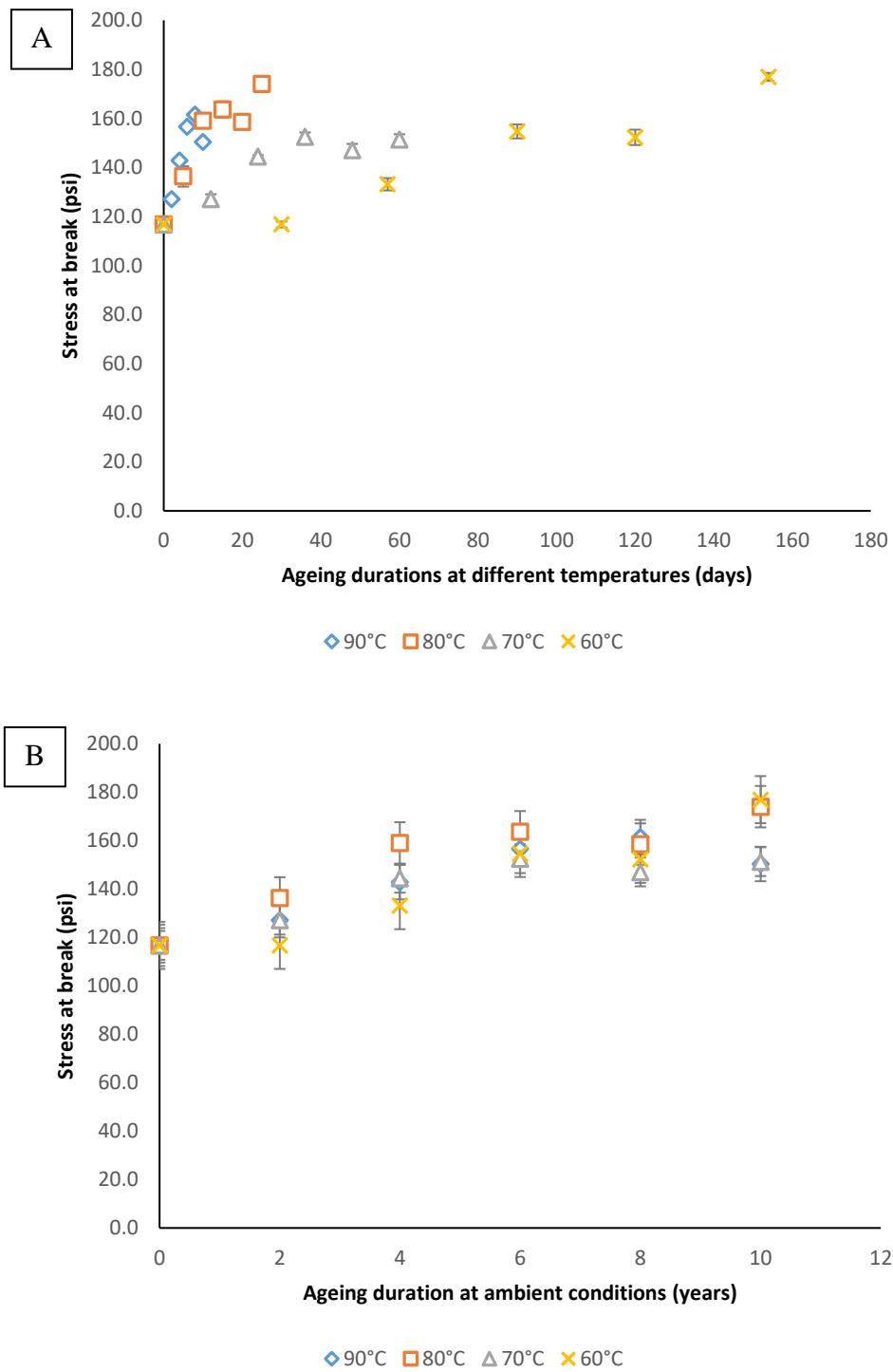


Figure 5-9. Stress at break values for a single propellant type. (A) Stress at break values for Propellant A aged at different temperatures, (B) Stress at break values for Propellant A corresponding real-life ageing duration at ambient conditions.

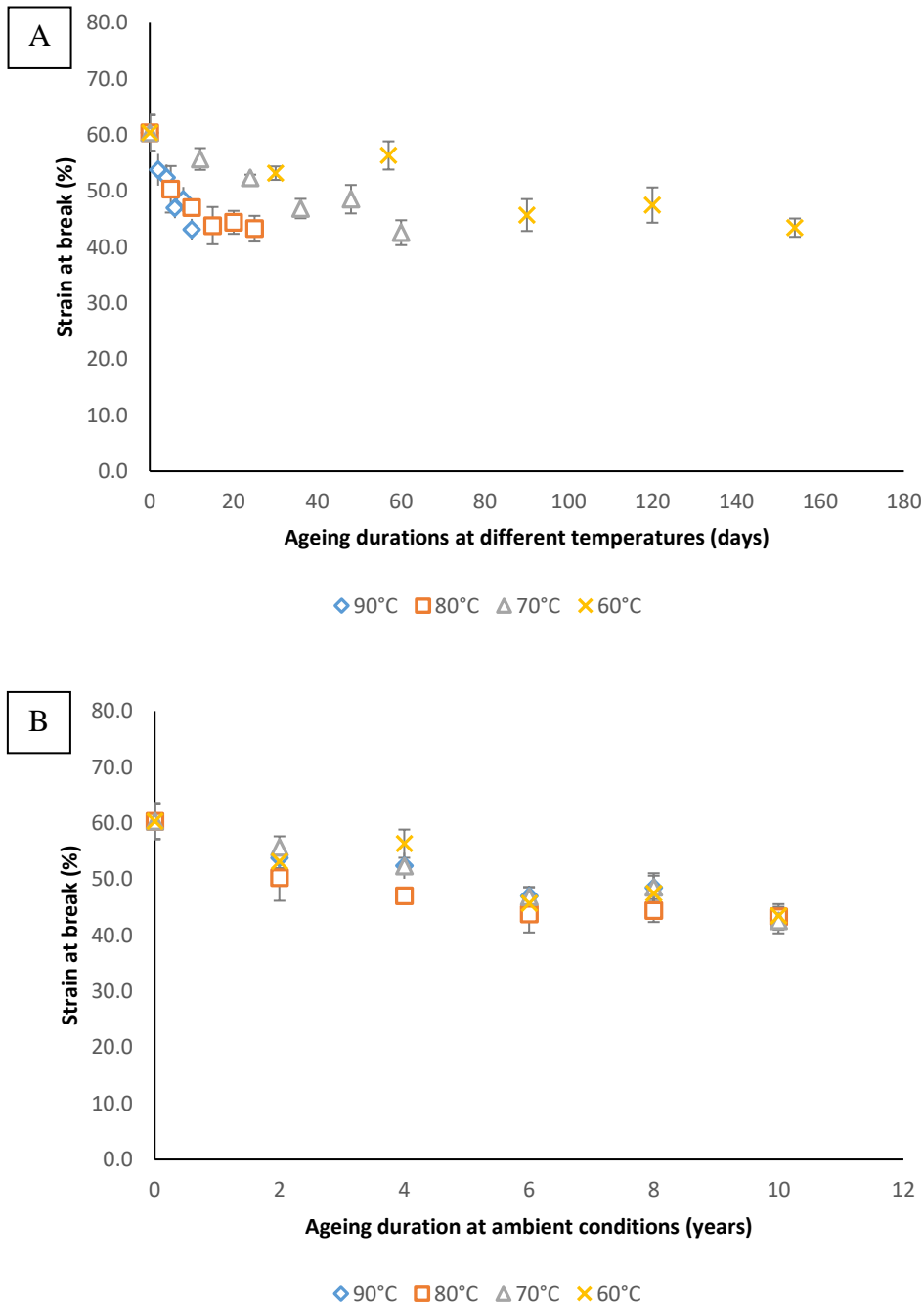


Figure 5-10. Strain at break values for a single propellant type. (A) Strain at break values for Propellant A aged at different temperatures, (B) Strain at break values for Propellant A corresponding real-life ageing duration at ambient conditions.

5.2 Physical Property Change During Ageing

Along with the mechanical properties, hardness values of the propellants were also observed throughout ageing for the cognizance of alterations. On the score of oxidative crosslinking being a process results in hardening, it is also termed as “oxidative hardening” (Davis, 2001). On the grounds that hardness is a demonstration of how far crosslinking make great strides, this value is expected to increase with ageing. Yet, ambient conditions regarding humidity changes give cause for propellant softening (Adel & Liang, 2019). Along with the stress diminution, one can also show regard to hardness parameter as well beneficial to have an insight for property change of propellant.

As also mentioned in Chapter 5.1, fluctuations in hardness test results may arise from the instantaneous humidity level change on test habitat or weather outside since samples are transported from ovens to laboratories when ageing process finishes. Change in hardness values for all polymers with altering temperatures and hardness change at different temperatures for a single propellant type are given in Appendix, Table 65 and Table 66, and shown in figures from Figure 5-11 to Figure 5-14.

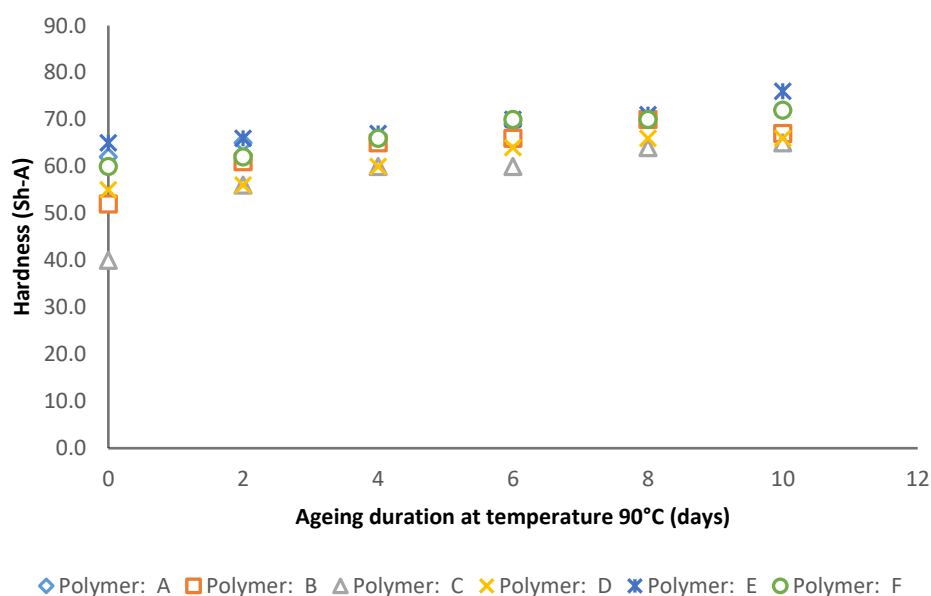


Figure 5-11. Hardness values of propellants aged at 90°C.

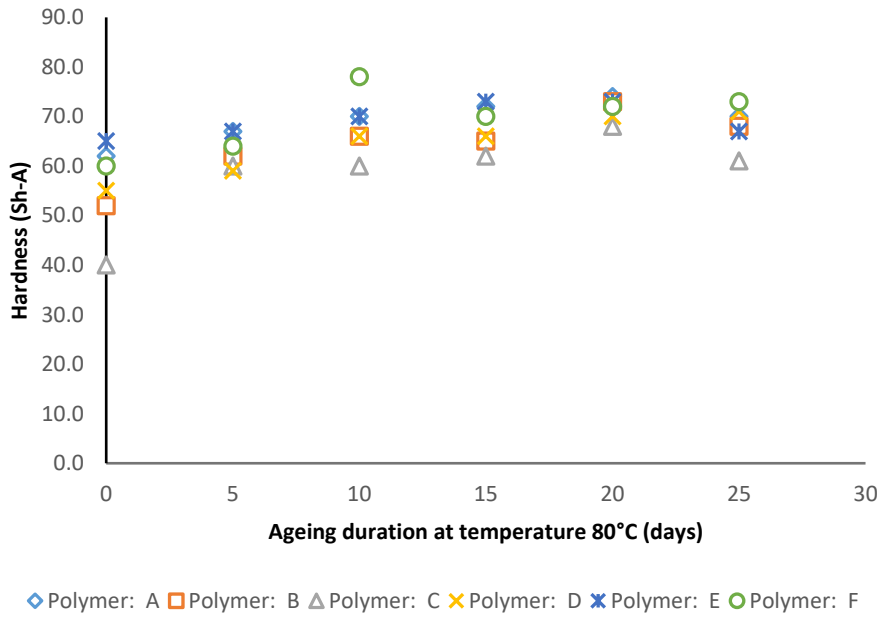


Figure 5-12. Hardness values of propellants aged at 80°C.

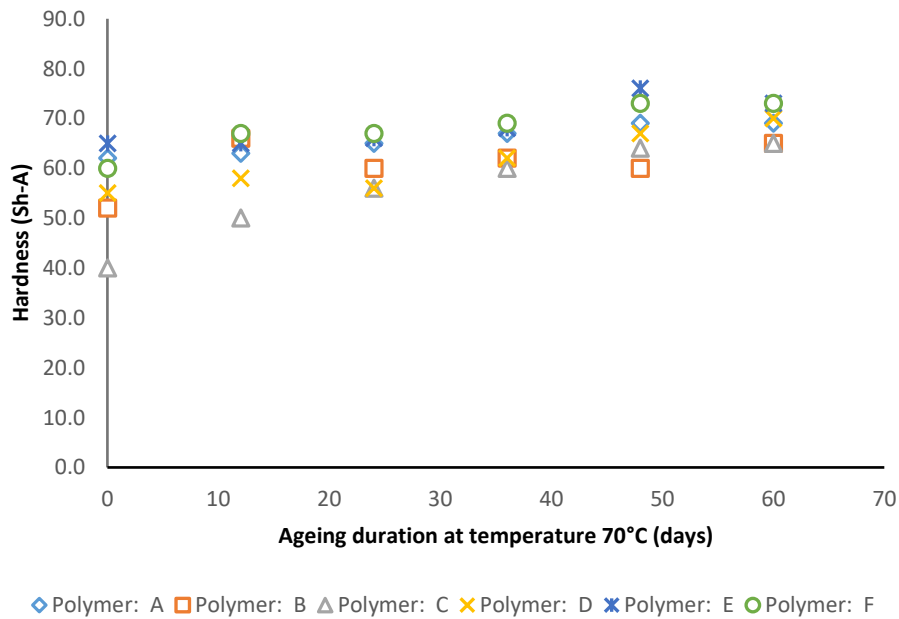


Figure 5-13. Hardness values of propellants aged at 70°C.

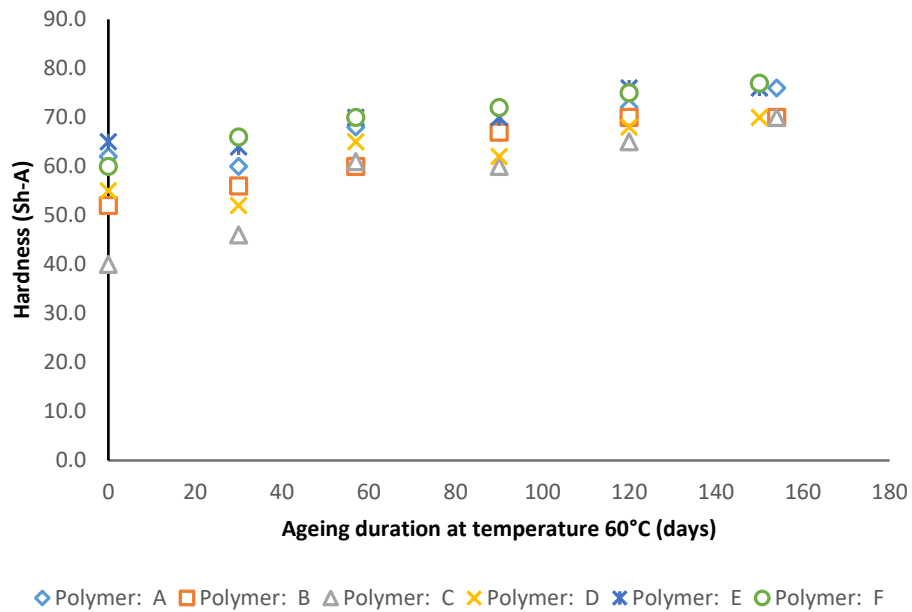


Figure 5-14. Hardness values of propellants aged at 60°C.

In order to make a comparison between selected ageing temperatures and corresponding ageing durations, physical property change at different temperatures for a single, arbitrarily chosen propellant type (Propellant A) is given in Figure 5-15 (A). Hardness values with respect to normalized ageing durations corresponding to ageing at ambient conditions in real life case are given in Figure 5-15 (B). As can be seen from the figures, it can be deduced that ageing trends for each selected ageing temperature are very similar to each other. This similarity shows that accelerated ageing durations and temperatures obtained through van't Hoff approach is quite conformable.

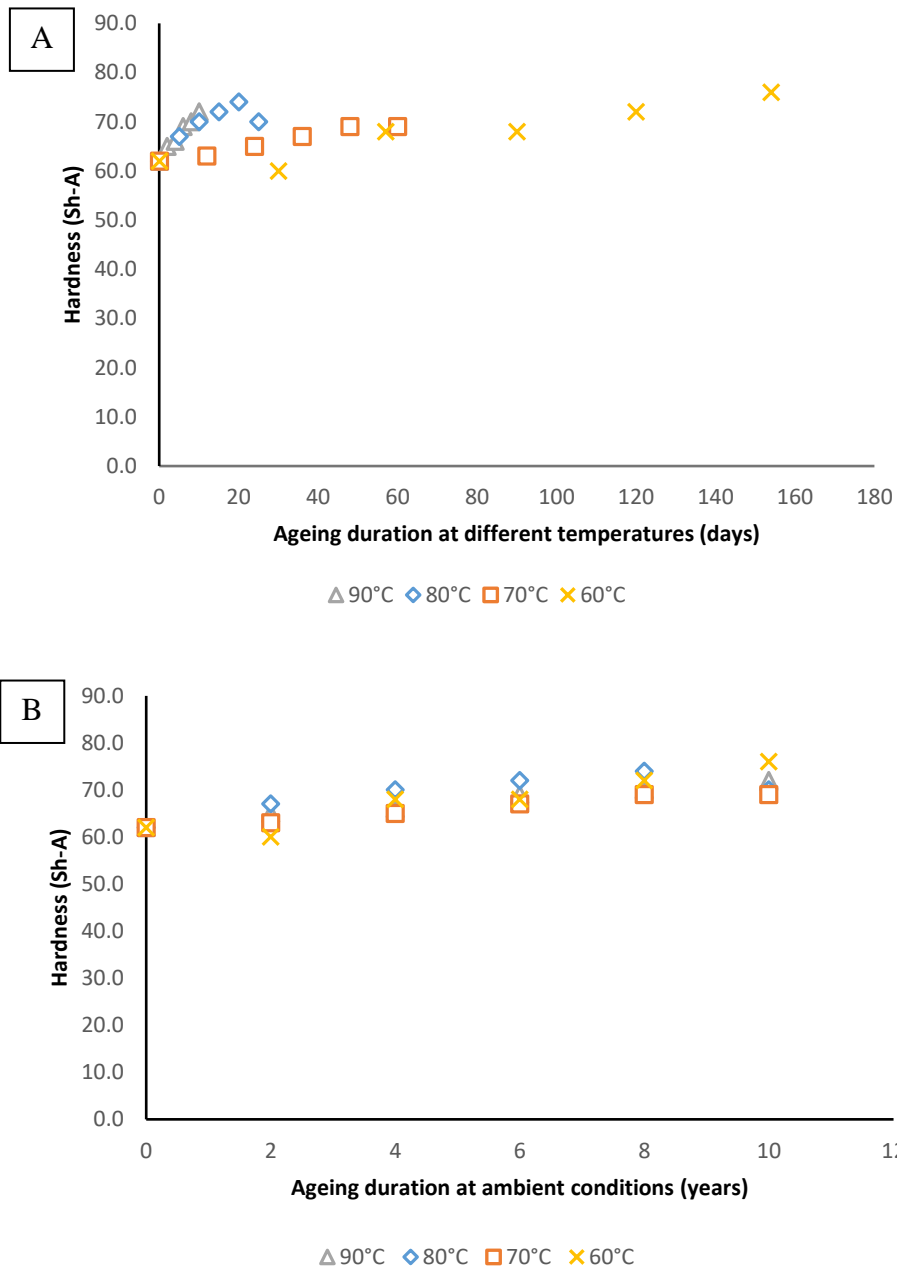


Figure 5-15. Hardness values for a single propellant type. (A) Hardness values for Propellant A aged at different temperatures, (B) Hardness values for Propellant A corresponding real-life ageing duration at ambient conditions.

5.3 Chemical Property Change During Ageing

During ageing periods, chemical properties were tracked in order to construct a mathematical model speaking for the alteration in these properties during service life. All the while of oxidative ageing, mechanical property change can also be traced by observing chemical properties directly. This is a plain method where soluble fraction is a portrayal of the polymeric matrix' portion apart from 3D network. As oxygen molecules attack onto the HTPB's double bond, polymer becomes stiffer. Impact of this phenomenon may be examined via soluble fraction change being detected by extraction method. During extraction, not only the uncrosslinked portion of the propellant is extricated; but also plasticizer, stabilizer and - if present - water molecules owing to humidity exposure may be abstracted from the matrix. Since plasticizer and stabilizer are very low in volume inside of the propellant when compared to polymer network, it would not be incorrect to presume that soluble portion extracted from the matrix is purely polymer that has not been affiliated to 3D network in a moisture-free environment. Withal, this issue should be kept in mind as it exerts an influence over chemical test results. Change in soluble fraction values for all polymers with altering temperatures and soluble fraction change at different temperatures for a single propellant type are given in Appendix, Table 63 and Table 64, and shown in figures from Figure 5-16 to Figure 5-19.

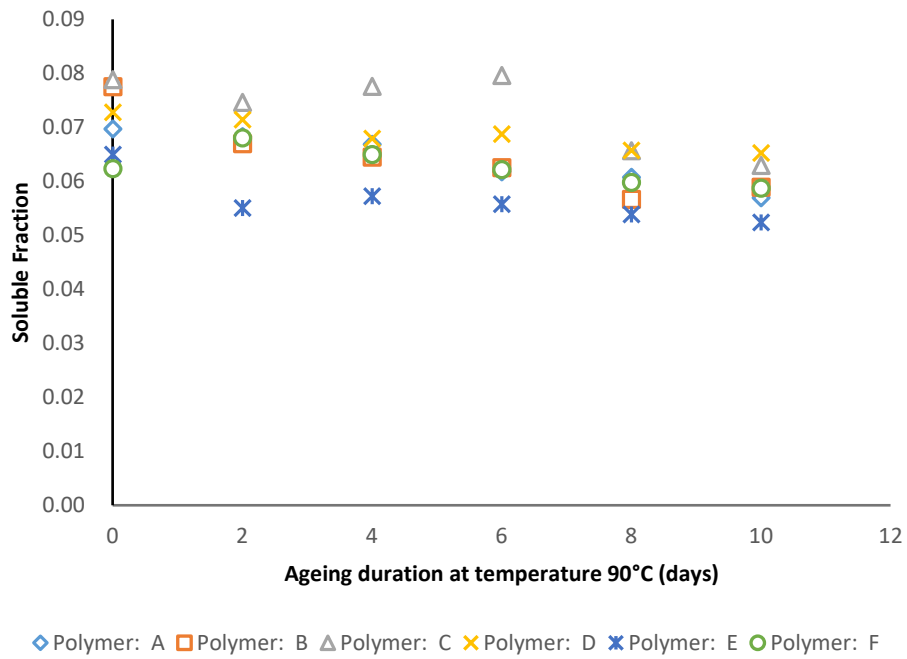


Figure 5-16. Soluble fraction values of propellants aged at 90°C.

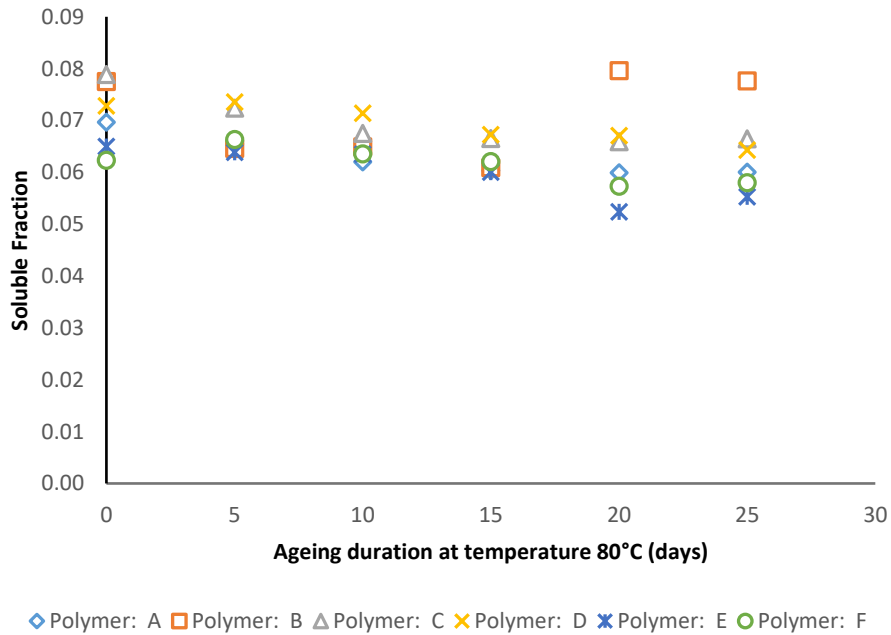


Figure 5-17. Soluble fraction values of propellants aged at 80°C.

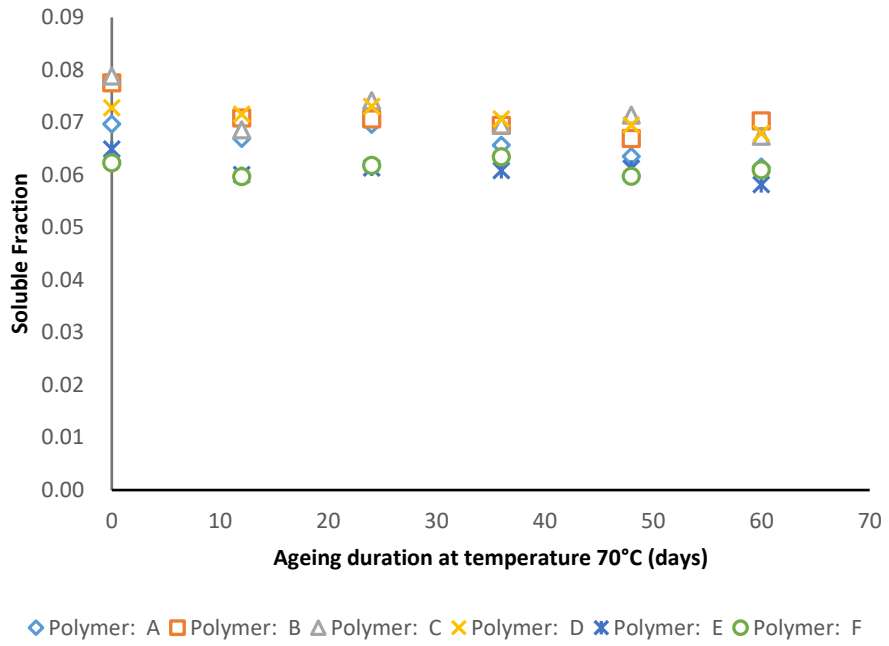


Figure 5-18. Soluble fraction values of propellants aged at 70°C.

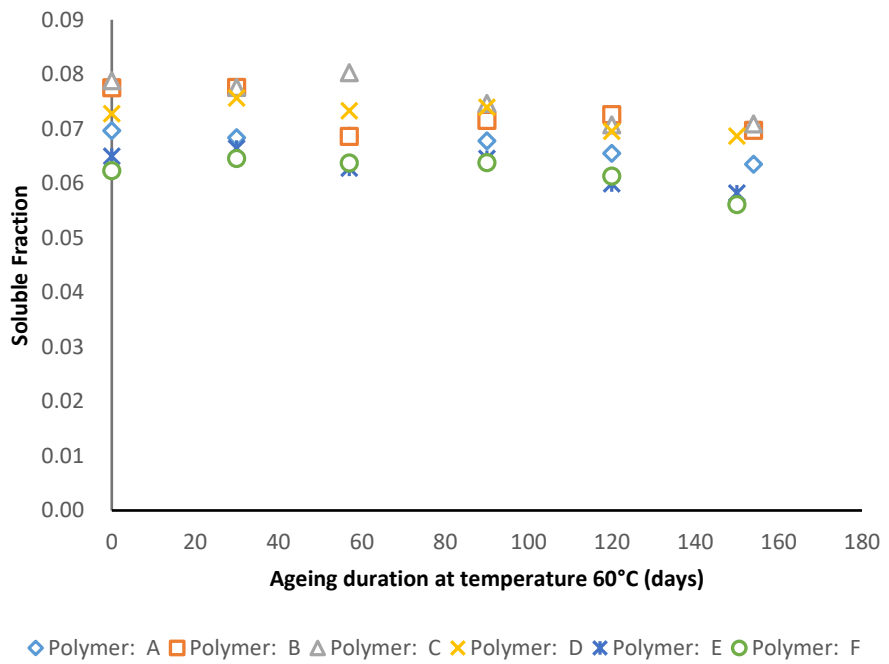


Figure 5-19. Soluble fraction values of propellants aged at 60°C.

In order to make a comparison between selected ageing temperatures and corresponding ageing durations, chemical property change at different temperatures for a single, arbitrarily chosen propellant type (Propellant A) is given in Figure 5-20 (A). Soluble fraction values with respect to normalized ageing durations corresponding to ageing at ambient conditions in real life case are given in Figure 5-20 (B). As can be seen from the figures, it can be deduced that ageing trends for each selected ageing temperature are very similar to each other. This similarity shows that accelerated ageing durations and temperatures obtained through van't Hoff approach is quite conformable.

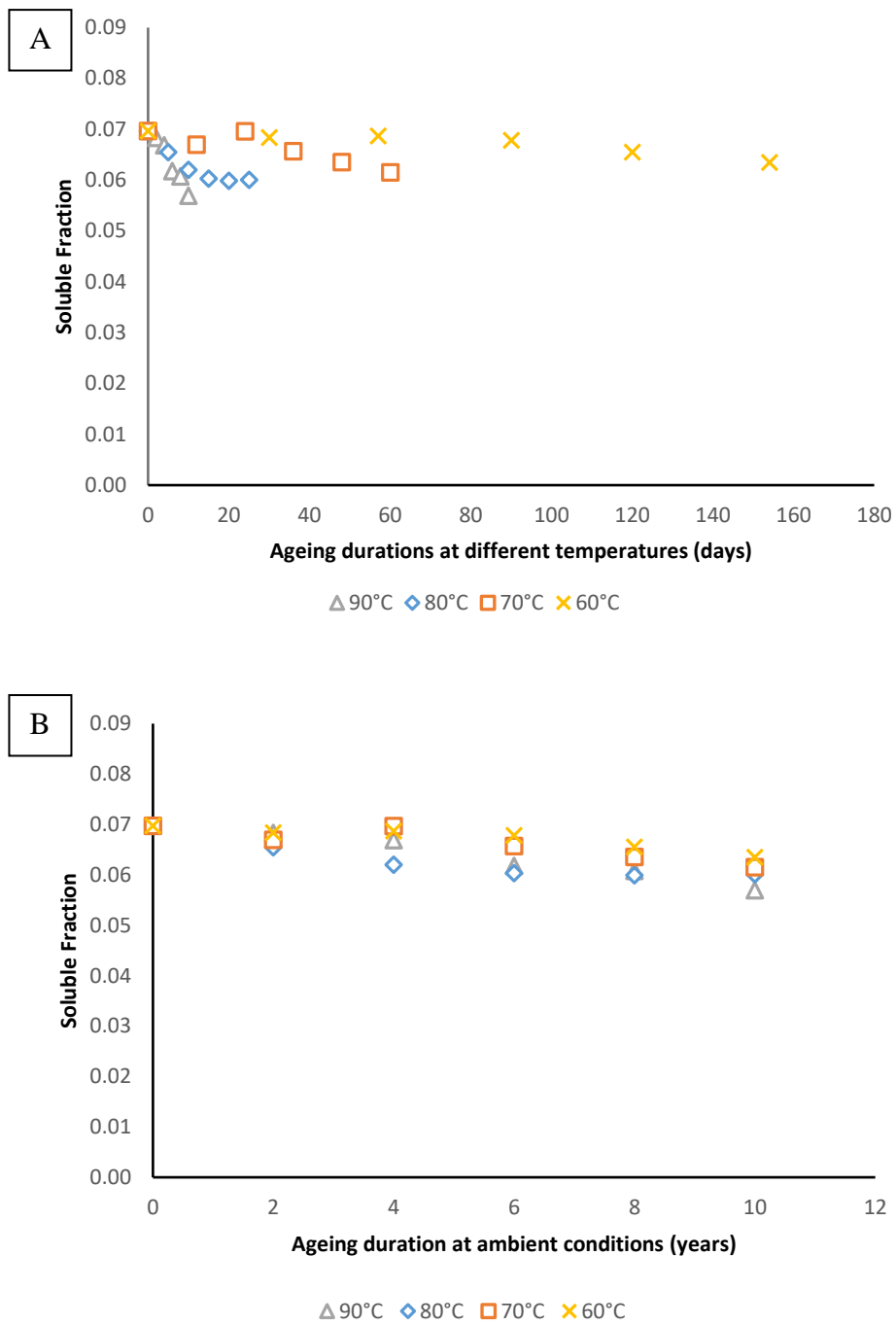


Figure 5-20. Soluble fraction values for a single propellant type. (A) Soluble fraction values for Propellant A aged at different temperatures, (B) Soluble fraction values for Propellant A corresponding real-life ageing duration at ambient conditions.

5.4 Comparison of Models

In order to compare the mathematical expressions, least squares method (LSM) is applied. This method is chosen to be able to find the best fit for a specific model with the data set on hand, by minimizing the sum of residuals between the available data points and the points on the model equation graph. A perfect fit would be indicated by sum of squares being equal to zero. Therefore, the closer to zero the result, the merrier it is.

Here, estimated data is the data as the output of the model with the given time and temperature variables. Assuming a first order rate equation regarding oxidative crosslinking and calculating activation energy in conformity with this approach by use of LSE give rate orders as in Table 3 and Table 4 for strain and soluble fraction values, respectively.

Table 3. First order equation rate parameters for strain values and corresponding sum of squared errors (SSE).

Propellant Type		A	B	C	D	E	F
Strain	k90 (1/days)	-0.0339	-0.0451	-0.0454	-0.0190	-0.0053	-0.0270
	SSE	0.0072	0.0419	0.0439	0.0234	0.0288	0.0039
	k80 (1/days)	-0.0169	-0.0247	-0.0240	-0.0114	-0.0062	-0.0086
	SSE	0.0306	0.1010	0.0287	0.0154	0.0122	0.0352
	k70 (1/days)	-0.0057	-0.0081	-0.0071	-0.0023	-0.0027	-0.0062
	SSE	0.0055	0.0476	0.0256	0.0163	0.0249	0.0266
	k60 (1/days)	-0.0022	-0.0029	-0.0033	-0.0020	-0.0005	-0.0021
	SSE	0.0143	0.0102	0.0361	0.0452	0.0429	0.0147

Table 4. First order equation rate parameters for soluble fraction values and corresponding sum of squared errors (SSE).

Propellant Type		A	B	C	D	E	F
Soluble Fraction	k90 (1/days)	-0.0184	-0.0350	-0.0181	-0.0117	-0.0247	-0.0029
	SSE	0.0072	0.0018	0.0149	0.0193	0.0008	0.0168
	k80 (1/days)	-0.0076	-0.0058	-0.0091	-0.0044	-0.0073	-0.0023
	SSE	0.0306	0.0049	0.1076	0.0102	0.0019	0.0093
	k70 (1/days)	-0.0018	-0.0026	-0.0028	-0.0009	-0.0018	-0.0004
	SSE	0.0055	0.0024	0.0086	0.0143	0.0008	0.0043
	k60 (1/days)	-0.0005	-0.0007	-0.0006	-0.0009	-0.0005	-0.0003
	SSE	0.0143	0.0007	0.0082	0.0039	0.0280	0.0041

Obtained activation energies for the propellants are summarized in Table 5. Attained activation energies falls within the range of expected values for solid rocket propellants (SRPs). These results also show that initial van't Hoff assumption, or assuming an activation energy in between 75-82 kJ/mol, is congruous for planning phase of accelerated ageing studies since resultant activation energies, especially calculated for strain values, are quite similar to the initial guesses.

Table 5. Activation energies obtained by integral method.

Propellant Type	Strain		Soluble Fraction	
	E _A (kJ/mol)	R ²	E _A (kJ/mol)	R ²
A	92.8591	0.9956	122.6564	0.9946
B	93.3413	0.9904	122.7313	0.9711
C	91.3625	0.9869	111.5656	0.9845
D	82.8232	0.9016	90.8221	0.8933
E	79.7504	0.8046	127.7030	0.9972
F	79.5766	0.9599	85.8421	0.9122

These activation energies differ from each other due to different polymer types being preferred. Since polymer is the main part of a propellant especially determining the mechanical properties, obtaining disparate activation energy values is expected.

Among the propellants being studied, average activation energy for strain values is 86.6189 ± 6.6002 kJ/mol.

Although chemical properties of a propellant are also affected hugely by the polymer, they are also closely related to energetic materials and their proportions present in the propellant. These propellants only differ by the polymers as mentioned before; however, molecular interactions associated with polymer molecular weights, cis-trans isomerism and number of vinyl groups all have an effect on the properties of propellants. All these parameters have a combined effect on propellant characteristics, especially on chemical properties. Discrepancies on ageing mechanism occur due to steric hindrance differences in line with polymer structures aforementioned. Although not being understood yet (Hori & Iwama, 1985), oxidative crosslinking is thought to take place on the basis of reactions including several different ingredients: not only polymer but also aziridine groups present in bonding agent, tris-1-(2-methylaziridinyl) phosphine oxide (MAPO) and oxidizer, ammonium perchlorate (AP) (Christiansen, Layton, & Carpenter, 1981). Despite all these substances were added in the same amounts to all propellants being studied, chemical properties are greatly influenced by the dissimilarities among number of vinyl groups, isomerism and molecular weight as these parameters result in different rates of ageing reaction due to distinctive amounts of crosslinking sites present in the polymer (Haddad, et al., 2018). Thus, polymer characterization at t_0 - after completion of curing & before artificial ageing - should be held in order to clarify the property differences thoroughly. As this study is focused more on mathematical modeling of these properties during the course of ageing, detailed analyses such as nuclear magnetic resonance (NMR) spectroscopy, gel permeation chromatography (GPC) and Fourier-transform infrared spectroscopy (FTIR) used for total polymer characterization were disregarded since it would redirect the scope of this study.

It comes as no surprise that activation energies obtained from strain and soluble test results are different from each other due to possible humidity effect on the samples as these specimens being aged and transported in silver foil wrappers are not very sheltered from external factors. In this respect, it is even apprehensible activation

energies belonging chemical properties are higher than that of mechanical properties due to the fact that chemical tests are carried on with diminutive sample dimensions. Being more impressionable to outer factors, response to temperature alterations might be more pronounced. Among the propellants being studied, average activation energy for soluble fraction values is 110.2201 ± 17.8282 kJ/mol. The higher standard deviation for chemical tests stems from the fact that chemical test samples are more prone to external effects than mechanical test samples due to the difference in sample dimensions.

When differential method is applied to data set, outcome is a bit underwhelming. As can be seen in Table 6 and Table 7, activation energies calculated by taking specifically first three periods of ageing process into consideration quite differ from the ones obtained by integral method. Although ageing is held in temperature and humidity controlled ovens, fluctuations through ageing are expected and unavoidably admissible due to reasons explained earlier in this chapter. This is actually the reason why there is not a direct correlation between activation energies obtained using two different methods: For instance, while activation energy obtained following integral method is lower than that of differential method for strain values of Propellant A, the situation is reversed for the same data of propellant B. This method might not offer an explanation regarding total ageing process as it disregards the fact that some changes are momentary.

Table 6. Activation energies calculated for strain values obtained by integral and differential methods* for comparison.

Propellant Type	Strain			
	Integral Method		Differential Method	
	E_A (kJ/mol)	R^2	E_A (kJ/mol)	R^2
A	92.8591	0.9956	115.3734	0.9570
B	93.3413	0.9904	87.5880	0.9721
C	91.3625	0.9869	94.5468	0.9921
D	82.8232	0.9016	26.7719	0.1759
E	79.7504	0.8046	77.4324	0.7601
F	79.5766	0.9599	81.8438	0.9758

* Differential method calculation by taking strain values appertaining to first three periods of ageing into consideration

Table 7. Activation energies calculated for soluble fraction values by integral and differential methods** for comparison.

Propellant Type	Soluble Fraction			
	Integral Method		Differential Method	
	E_A (kJ/mol)	R^2	E_A (kJ/mol)	R^2
A	122.6564	0.9946	167.1530	0.5884
B	122.7313	0.9711	106.3028	0.9728
C	111.5656	0.9845	93.9149	0.5926
D	90.8221	0.8933	174.3695	0.9028
E	127.7030	0.9972	117.4685	0.8469
F	85.8421	0.9122	114.5254	0.8448

** Differential method calculation by taking soluble fraction values appertaining to first three periods of ageing into consideration

When severity factor approach is applied to the data set by the help of nonlinear regression within MATLAB version of 2021b, severity equation parameters and resulting SSE values are acquired as can be seen in Table 8 and Table 9.

Table 8. Severity factor equation parameters for strain values and corresponding SSE.

Propellant Type	Strain			
	β	γ	ω	SSE
A	2.1813E-04	0.6413	10.6562	0.0439
B	2.6270E-03	0.3689	10.2460	0.0753
C	1.2124E-03	0.4769	10.6413	0.0692
D	1.5350E-05	0.9816	12.3534	0.1281
E	7.5393E-06	0.9403	11.7533	0.1331
F	1.4354E-03	0.5198	14.9657	0.0739

Table 9. Severity factor equation parameters for strain values and corresponding SSE.

Propellant Type	Soluble Fraction			
	β	γ	ω	SSE
A	4.4483E-07	1.0219	8.6022	0.0135
B	2.0083E-04	0.0866	1.7748	0.0926
C	5.7341E-06	0.8655	9.3776	0.0573
D	3.1029E-09	1.4474	8.9003	0.0087
E	5.6213E-06	0.6336	6.5609	0.0296
F	6.7395E-11	2.0935	11.5143	0.0296

When same data set is modeled through surface fit by the aid of MATLAB, resulting surface fit equation becomes:

$$P(t) = p00 + p10 * x + p01 * y + p20 * x^2 + p11 * x * y + p02 * y^2 \quad \text{Equation 13}$$

Where P(t) is property at any time (t); p00, p10, p01, p20, p11, p02 are surface fit parameters; x and y ageing temperatures in °C and time in days, respectively. Surface fit parameters obtained for strain values and interrelated SSEs are as in Table 10 and Table 11. Surface fit parameters attained for soluble fraction values and interrelated SSEs are as in

Table 12 and Table 13.

Table 10. Surface fit equation parameters for strain values of propellants A, B and C, and corresponding SSEs.

Propellant Type		A	B	C
Strain	p00	1.9690E-01	-8.1001E-01	-2.9940E-01
	p10	-6.2533E-03	1.9628E-02	3.4921E-03
	p01	-1.9097E-03	-1.6287E-02	-1.0275E-02
	p20	4.4467E-05	-9.8513E-05	1.8867E-05
	p11	4.2338E-05	3.2243E-04	2.5468E-04
	p02	-1.2424E-06	-6.1888E-06	-1.8283E-05
	SSE	1.9690E-01	-8.1001E-01	-2.9940E-01

Table 11. Surface fit equation parameters for strain values of propellants D, E and F, and corresponding SSEs.

Propellant Type		D	E	F
Strain	p00	3.1136E-01	-7.4772E-01	2.5099E-03
	p10	-1.2180E-02	1.8311E-02	5.7867E-01
	p01	-3.5611E-03	-4.7676E-03	1.8370E-04
	p20	1.0511E-04	-1.1172E-04	2.5384E-03
	p11	1.1693E-04	1.1766E-04	6.5639E-02
	p02	-1.2056E-05	-1.1812E-05	-1.9286E-02
	SSE	3.1136E-01	-7.4772E-01	2.5099E-03

Table 12. Surface fit equation parameters for soluble fraction values of propellants A, B and C, and corresponding SSEs.

Propellant Type		A	B	C
Soluble Fraction	p00	4.3166E-03	5.9894E-01	-9.2943E-02
	p10	-4.4393E-04	-1.9659E-02	3.0713E-03
	p01	-1.4410E-02	-1.6018E-03	-2.1235E-02
	p20	8.3044E-06	1.6286E-04	-1.8820E-05
	p11	2.4088E-04	5.1280E-05	3.3303E-04
	p02	1.9731E-06	-6.3397E-06	1.2616E-05
	SSE	4.3166E-03	5.9894E-01	-9.2943E-02

Table 13. Surface fit equation parameters for soluble fraction values of propellants D, E and F, and corresponding SSEs.

Propellant Type		D	E	F
Soluble Fraction	p00	2.6912E-02	2.4172E-06	2.8151E-06
	p10	-3.4621E-03	1.1065E-03	1.2972E-03
	p01	-6.2584E-06	1.1782E-07	1.3442E-07
	p20	4.2886E-05	-3.7187E-07	-1.5215E-05
	p11	1.0439E-05	1.4421E-07	-3.8761E-06
	p02	-7.1843E-09	5.3572E-07	3.4207E-06
	SSE	2.6912E-02	2.4172E-06	2.8151E-06

To be able to compare these models, obtained SSE values of the six propellants are summed up for each model type and summarized in Table 14.

Table 14. Total SSE of the models.

Model Type	Total SSE (Strain)	Total SSE (Soluble Fraction)
Arrhenius Approach with 1 st Order Rate Equation	0.6729	0.2980
Severity Index Approach	0.5234	0.2313
Surface Fit Approach	0.5288	0.3482

As one can easily see from Table 14, total SSE values for models are not very distinct from each other. Hence, it is avowable that all three models are applicable for service life determination of solid rocket propellants, in terms of both mechanical and chemical properties. Even, obtaining lower SSE values while modeling soluble fraction test results is quite promising for switching to perform chemical tests instead of monitoring mechanical properties when tested samples are in small quantities within service life determination and extension missions.

Functionality and usage of Arrhenius approach has been attested by many studies in respect of chemical reaction kinetics for many years. Surface fit approach has also been in high demand in modeling being applied for function approximation (Tong, et al., 2021). Although having a substantial history, severity index approach is a quite new approach for characterization of propellant ageing (Dubois & Perreault, 2002). Therefore, it would be underlined that all models - especially Arrhenius approach and severity kinetics - are adequate enough to be used for propellant ageing in terms of monitoring and modeling chemical properties.

Undoubtedly that, modeling chemical properties through accelerated ageing process is just the opening gambit for this replacement. In the following studies, first of all, selected model should be validated by arranging natural ageing experiments with propellants possessing same formulations. This study would eliminate the possibility of triggering unexpected processes and chemical reactions occurring within the propellant at elevated temperatures that will not be encountered during ordinary ageing in the course of service life. Hence, the resulting model is ought to reflect the ordinary and everyday situation, either. Other than this confirmation, structural analyses should be conducted for specified geometries of rocket motors in order to corroborate the model for real systems besides solely examination of propellant itself. Into the bargain, model should be checked whether its applicability is newsworthy for other type of propellants: propellants having different proportions of the same ingredients or different sizes of solid particles, or propellants consisting different constituents such as liquid burn-rate modifiers, ammonium nitrate (AN) as

oxidizer, oxamide as burn-rate suppressant, hydroxyl-terminated polyether (HTPE) or glycidyl azide polymer (GAP) as prepolymer.

CHAPTER 6

CONCLUSIONS

In this study, chemical properties of HTPB/AP/Al based propellants are monitored during the course of accelerated ageing in order to propound a mathematical model representing service life of energetic polymeric matrixes. Besides chemical properties, mechanical and physical properties were also trailed to be able to offer a more monolithic approach regarding service life determination. This work provides fundamental tidings on modeling of chemical properties in the course of accelerated ageing. By this means, service life determination can be carried through using very small amounts of samples as soluble fraction test requires much less extent of specimen when compared to mechanical tests. Therefore, just in design phase of an HTPB-based solid propellant rocket system, service life prognosis can be made using severity index model through the agency of accelerated ageing. Further, being cognizant of the thermal conditions of the whole rocket system, this model can be applicable even for rockets on the phase of service life extension.

Besides being applicable for propellants, this model is expected to be pertinent to other energetic or non-energetic polymeric materials having defined service lives being used within the body of other industries. Due to these reasons, *one model to rule them all* is most welcome.

To sum up, all three models appear to be pertinent for service life determination in terms of modeling both mechanical and chemical properties. Nonetheless, demonstrating the minimum SSE values besides convenience of fictionalizing ageing experiments and interpreting collected artificial ageing data, severity index approach seems to have the price possession among the models have been studied. Independent of model selection, this study demonstrates the feasibility of chemical property modeling within the context of propellant ageing. Wherefore, modeling of

chemical properties could be a neat solution for reducing operational cost as related test procedure requires much less labor when compared to that of mechanical testing, especially in conditions where sampling should be carried out on a limited scale due to scantiness of rocket motors reserved for service life extension studies. Unquestionably, there is also a trade-off right here since chemical test samples are apt to external effects more than mechanical test samples due to the difference in sample sizes. Nonetheless, conducting nondestructive tests - if possible - or executing tests with minor sample amounts without impairing the integrity of the assembly within the scope of service life determination and extension studies are crucial for such industries, especially where products are costly.

Withal, service life prediction of propellants is just a drop in the ocean when the subject is reliable lifetime of a rocket system as mentioned earlier. Being aware of the importance of a rocket system's service life integrally, it is needed to be said that this is a sophisticated issue deserving to be emphasized and discussed with scrupulous attention to detail.

REFERENCES

- Abatzoglou, N., Chornet, E., Belkacemi, K., & Overend, R. P. (1992, June 26). Phenomenological Kinetics of Complex Systems: The Development of a Generalized Severity Parameter and Its Application to Lignocellulosics Fractionation. *Chemical Engineering Science*, 47(5), pp. 1109-1122.
- Açık, S. (2010). Internal Ballistic Design Optimization of a Solid Rocket Motor. *Graduate School of Natural and Applied Science of Middle East Technical University*.
- Adel, W. M., & Liang, G. (2019). Service Life Prediction of AP/Al/HTPB Solid Rocket Propellant with Consideration of Softening Aging Behavior. *Chinese Journal of Aeronautics*, 32(2), pp. 361-368. doi:10.1016/j.cja.2018.08.003
- AGARD. (1997). *AGARD Advisory Report 350: Structural Assessment of Solid Propellant Grains*. Quebec: Canada Communication Group Inc.
- Balageas, D., Fritzen, C.-P., & Güemes, A. (2006). Introduction to Structural Health Monitoring. In D. Balageas, C.-P. Fritzen, & A. Güemes, *Structural Health Monitoring* (pp. 13-43). ISTE .
- Biggs, G. (2009, August 2-5). Solid Propellant Aging Kinetics. *45th AIAA/ASME/SAE/ASEE Joint Propulsion Conference & Exhibit*. doi:10.2514/6.2009-5423
- Bilis, M. (2016, June 9). *Throwback Thursday: Robert Goddard Is Granted Another Patent for Rocketry*. Retrieved from Boston Magazine: <https://www.bostonmagazine.com/news/2016/06/09/robert-goddard-rocket/>
- Bohn, M. A., & Cerri, S. (2010). Ageing Behaviour of Composite Rocket Propellant Formulations Investigated. *Insensitive Munitions & Energetic Materials Technology Symposium (IMEMTS)*. München: NDIA 2010.

- Boin, A. (2008). Learning from crisis: NASA and the Challenger disaster. In A. Boin, & A. a. McConnell, *Governing after Crisis: The Politics of Investigation, Accountability and Learning* (pp. 232–254). Cambridge: Cambridge University Press.
- Brief History of Rockets*. (n.d.). Retrieved from NASA Website: https://www.grc.nasa.gov/www/k-12/TRC/Rockets/history_of_rockets.html
- Bryce Space and Technology. (2017). *Global Space Industry Dynamics: Research Paper for Australian Government, Department of Industry, Innovation and Science by Bryce Space and Technology, LLC*.
- Bunyan, P., Cunliffe, A., Davis, A., & Kirby, F. (1993). The Degradation and Stabilisation of Solid Rocket Propellants. *Polymer Degradation and Stability*, 40(2), pp. 239-250. doi:[https://doi.org/10.1016/0141-3910\(93\)90211-Z](https://doi.org/10.1016/0141-3910(93)90211-Z)
- Celina, M., Elliott, J. S., Winters, S., Assink, R., & Minier, L. (2006). Correlation of antioxidant depletion and mechanical performance during thermal degradation of an HTPB elastomer. *Polymer Degradation and Stability* 91, s. 1870-1879. doi:10.1016/j.polymdegradstab.2005.11.006
- Cerri, S., Bohn, M. A., Menke, K., & Galfetti, L. (2009). Ageing Behaviour of HTPB Based Rocket Propellant Formulations. *Central European Journal of Energetic Materials*, 6(2), pp. 149-165.
- Chaturvedi, S., & Dave, P. N. (2019, December). Solid propellants: AP/HTPB composite propellants. *Arabian Journal of Chemistry*, s. 2061-2068.
- Christiansen, A., Layton, L. H., & Carpenter, R. L. (1981). HTPB Propellant Aging. *AIAA/SAE/ASME 16th Joint Propulsion Conference*. 3, pp. 211-215. Utah: Journal of Spacecraft and Rockets.

- Clark University Robert H. Goddard Library. (2021, August 31). *Archives and Special Collections: Robert H. Goddard Collection*. Retrieved from Clark University: <https://clarku.libguides.com/archives>
- Clegg, B. (2020, September 29). *A history of rocket science*. Retrieved from Science Focus: <https://www.sciencefocus.com/space/rocket-science-history/>
- Connors, K. A. (1990). *Chemical Kinetics: The Study of Reaction Rates in Solution*. VCH Publishers Inc.
- Cook, W. D., Mehrabi, M., & Edward, G. H. (1999, March). Ageing and yielding in model epoxy thermosets. *Polymer*, 40(5), pp. 1209-1218. doi:10.1016/S0032-3861(98)00343-7
- Corradini, M. G., & Peleg, M. (2006, January). Shelf-life estimation from accelerated storage data. *Trends in Food Science & Technology*, 18(1), 37-47. doi:10.1016/j.tifs.2006.07.011
- Davenas, A. (1992). *Solid Rocket Propulsion Technology*. Oxford / New York / Seoul / Tokyo: Pergamon Press.
- Davis, D. (2001). Use of dilatation in understanding composite propellant aging. In *37th Joint Propulsion Conference and Exhibit*. American Institute of Aeronautics and Astronautics. doi:10.2514/6.2001-3283
- Deng, P., Wang, H., Yang, X., Ren, H., & Jiao, Q. (2020, June 25). Thermal decomposition and combustion performance of high-energy ammonium perchlorate-based molecular perovskite. *Journal of Alloys and Compounds*.
- Dubois, C., & Perreault, F. (2002, July 17). Shelf Life Prediction of Propellants Using a Reaction Severity Index. *Propellants, Explosives, Pyrotechnics*(27), pp. 253-261.
- Farhadian, A. H., Tehrani, M. K., Keshavarz, M. H., Karimi, M., Darbani, S. M., & Rezayi, A. H. (2015, November 20). A Novel Approach for Investigation of Chemical Aging in Composite Propellants Through Laser-Induced

- Breakdown Spectroscopy (LIBS). *Journal of Thermal Analysis and Calorimetry*, 124(1), pp. 279-286. doi:10.1007/s10973-015-5116-9
- Fauld explosion 70th anniversary: New memorial unveiled.* (2014, November 27). Retrieved from BBC News Website: <https://www.bbc.com/news/uk-england-stoke-staffordshire-30218324>
- Foli, G., Esposti, M. D., Toselli, M., Morselli, D., & Fabbri, P. (2019, February 4). Facile method based on ¹⁹F-NMR for the determination of hydroxyl value and molecular weight of hydroxyl terminated polymers. *Analyst (The Royal Society of Chemistry 2019)*(144), 2087–2096. doi:10.1039/c8an02518e
- FOSS Analytical. (2007, September). Soxtec™ 2055Fat Extraction System Data Sheet.
- Garrote, G., Dominguez, H., & Parajo, J. C. (2002, October 17). Interpretation of deacetylation and hemicellulose hydrolysis during hydrothermal treatments on the basis of the severity factor. *Process Biochemistry*(37), pp. 1067–1073.
- Genov, B., Nedelchev, D., Mihovski, M., & Mirchev, Y. (2019). Comprehensive Approach for Service Life Assessment of Solid-Propellant Rocket Motors. *Bulgarian Society for NDT*.
- Haddad, T. S., Moore, L. M., Reams, J. T., Ford, M. D., Marcischak, J. C., Guenther, A. J., . . . Ghiassi, K. B. (2018, October 16). NMR Analysis of Hydroxyl-Terminated Polybutadiene End Groups and Reactivity Differences with Monoisocyanates. *Polymer Chemistry*, pp. 2665-2671. doi:<https://doi.org/10.1002/pola.29250>
- Hardy, V. (2015). *Voices from the Explosion: RAF Fauld, the World's Largest Accidental Blast, 1944*. Dark River.
- Hoffman, D. M., Hawkins, T. W., Lindsay, G. A., Wardle, R. B., & Manser, G. E. (1994). Clean, agile alternative binders, additives and plasticizers for propellant and explosive formulations. *Life Cycle of Energetic Materials*

Meeting in Del Mar, CA. Livermore, CA: Lawrence Livermore National Laboratory.

Hori, K., & Iwama, A. (1985). On the Adhesion between Hydroxyl-Terminated Polybutadiene Fuel-Binder and Ammonium Perchlorate. Performance of Bonding Agents. *Propellants, Explosives, Pyrotechnics*(10), pp. 176-180.

Howell, E. (2018, October 25). *The History of Rockets*. Retrieved from SPACE: <https://www.space.com/29295-rocket-history.html>

IBK Industriebedarf GmbH Vacuum Drying Ovens. (n.d.). Retrieved from IBK Industriebedarf GmbH Web Site: <http://ibk-industriebedarf.com/index.php%3Fpage%3Dprodukte%26id%3D45%26PHPSESSID%3Dd22khruuv96o6db6f2nr34qpm0.4>

Instron Testing Systems. (n.d.). Retrieved from Instron Web Site: <https://www.instron.com/en/products/testing-systems/universal-testing-systems/low-force-universal-testing-systems/5900-series-universal-testing-systems-up-to-50-kn>

Iqbal, M. M., & Liang, W. (2006). Modeling the moisture effects of solid ingredients on composite propellant properties. *Aerospace Science and Technology*, 10(8), 695-699. doi:10.1016/j.ast.2006.07.003

Johlitz, M. (2012, June 28). On the Representation of Ageing Phenomena. *The Journal of Adhesion*, 88(7), pp. 620-648. doi:10.1080/00218464.2012.682905

Jr. Lutz, J. T., & Grossman, R. F. (2001). *Polymer Modifiers and Additives*. New York: Marcel Dekker Inc.

Judge, M. D. (2003). An Investigation of Composite Propellant Accelerated Ageing Mechanisms and Kinetics. *Propellants, Explosives, Pyrotechnics*, 28(3), 114-119.

- Keizers, H., Brouwer, G. R., Weijl, J., & Weterings, F. (2002, September 23-26). Evaluation of Rocket Motor Safelife Based on Condition Monitoring and Ageing Modelling. *NATO UNCLASSIFIED*. Aalborg, Denmark: RTO-MP-091.
- Khan, M. A., Dey, A., Athar, J., & Sikder, A. K. (2014, July 4). Calculation of enthalpies of formation and band gaps of polymeric binders. *Royal Society of Chemistry*, pp. 32840–32846.
- Kohga, M., & Togo, S. (2020). Catalytic Effect of Added Fe₂O₃ Amount on Thermal Decomposition Behaviors and Burning Characteristics of Ammonium Nitrate/Ammonium Perchlorate Propellant. *Combustion Science and Technology*, s. 1668-1681.
- Launius, R. D. (2004). *Frontiers of Space Exploration* (Second ed.). London: Greenwood Press.
- Layton, L. H. (1975). *Chemical Structural Aging Studies on an HTPB Propellant*. United States Air Force. Utah: Thiokol Corporation.
- Lee, S., Ditko, S. (Writers), & Raimi, S. (Director). (2002). *Spider-Man* [Motion Picture].
- Lee, S., Choi, C. H., Hong, I.-K., & Lee, J. W. (2015). Polyurethane curing kinetics for polymer bonded explosives: HTPB/IPDI binder. *Korean J. Chem. Eng.*, 32(8), pp. 1701-1706. doi:10.1007/s11814-014-0366-y
- Lokander, M., & Stenberg, B. (1998). A Novel Method for Determination of the Concentration of Active Antioxidant in Stored HTPB-Based Composite Propellants. *Propellants, Explosives, Pyrotechnics* 23, pp. 272-278. doi:10.1002/(SICI)1521-4087(199811)<272::AID-PREP272>3.0.CO;2-3
- Mahjub, A., Mazlan, N. M., Abdullah, M. Z., & Azam, Q. (2020, January). Design Optimization of Solid Rocket Propulsion: A Survey of Recent

- Advancements. *Journal of Spacecraft and Rockets*, 57(1).
doi:<https://doi.org/10.2514/1.A34594>
- Mason, B., & Roland, C. (2019). Solid Propellants. *Rubber Chemistry and Technology*, 92(1), pp. 1-24.
- McKeen, L. W. (2017). *Permeability Properties of Plastics and Elastomers* (Fourth Edition ed.). Elsevier Inc. doi:<https://doi.org/10.1016/B978-0-323-50859-9.00001-4>
- Military Agency for Standardization. (2006, December 13). STANAG 4581 - Explosives, Assessment of Ageing Characteristics of Composite Propellants Containing an Inert Binder. Brussels, Belgium: North Atlantic Treaty Organisation.
- Muhammad, M.-u.-d., Lu, G.-z., & Ren, K.-l. (2006, February). Technique to Assess Aging of Propellant Grain. *Chinese Journal of Aeronautics*, 19(1).
- Naseem, H., Yerra, J., Murthy, H., & Ramakrishna, P. (2021, May 14). Ageing Studies on AP/HTPB Based Composites Solid Propellants. *Energetic Materials Frontiers*, 2(2), pp. 111-124.
doi:<https://doi.org/10.1016/j.enmf.2021.02.001>
- National Aeronautics and Space Administration. (2003). *Columbia Accident Investigation Board, Volume I*. National Aeronautics and Space Administration. Washington, D.C.: National Aeronautics and Space Administration and the Government Printing Office.
- NC, B. (1993). *Atmospheric Oxidation and Antioxidants* (Vol. 2). (G. Scott, Ed.) Amsterdam, Netherlands: Elsevier.
- Price, E. W., Sigmani, R. K., Sambamurthi, J. K., & Park, C. J. (1982). *Behavior of Aluminum in Solid Propellant Combustion*. Georgia: Georgia Institute of Technology.

- Rocket Fundamentals. (2012). In U. Walter, *Astronautics: The Physics of Space Flight* (pp. 1-23). Wiley-VCH Verlag GmbH & Co. KGaA.
- Shu, W. R., & Ross, L. L. (1982). Cracking Severity Index in Pyrolysis of Petroleum Fractions. *Industrial & Engineering Chemistry Process Design and Development*(21), pp. 371-377.
- Siddiqi, A. (2008, February 12). The Space Race Today. (NOVA, Interviewer) Retrieved from <https://www.pbs.org/wgbh/nova/article/space-race-today/>
- Siddiqi, A. A. (2000). *Challenge to Apollo: The Soviet Union and the Space Race, 1945-1974*. Washington, DC: National Aeronautics and Space Administration (NASA) History Division.
- Simpson, J. A., Weiner, E. S., & Oxford University Press. (1989). The Oxford English Dictionary. Oxford: Clarendon Press.
- Singh, H. (2005). A Scientific Approach for Life Extension of Solid Rocket Propellants/Rocket Motors. *Proceedings 45th Israel Annual Conference on Aerospace Sciences*.
- Stoček, R., Kratina, O., Ghosh, P., Maláč, J., & Mukhopadhyay, R. (2017). Influence of Thermal Ageing Process on the Crack Propagation of Rubber Used for Tire Application. In *Deformation and Fracture Behaviour of Polymer Materials* (Vol. 247, pp. 351-364). Springer International Publishing. doi:10.1007/978-3-319-41879-7_24
- Sutton, G. P., & Biblarz, O. (2001). *Rocket Propulsion Elements*. New York / Chichester / Weinheim / Brisbane / Singapore / Toronto: John Wiley & Sons.
- The History of Spaceflight. (2011). In J. R. Wertz, D. F. Everett, & J. J. Puschell, *Space Mission Engineering: The New SMAD* (pp. 4-10). Microcosm Press.
- Thring, R. W., & Chornet, E. (1993, February). Thermolysis of Glycol Lignin in the Presence of Tetralin. *The Canadian Journal of Chemical Engineering*(71), pp. 107-115.

- Tong, Y., Yu, L., Li, S., Liu, J., Qin, H., & Li, W. (2021, April 27). Polynomial Fitting Algorithm Based on Neural Network. *The ASP Transactions on Pattern Recognition and Intelligent Systems (TPRIS)*, 1(1), pp. 32–39. doi:10.52810/TPRIS.2021.100019
- Villar, L. D., Silva, R. F., Diniz, M. F., Takahashi, M. F., & Rezende, L. C. (2010, 8). The role of antioxidant on propellant binder reactivity during thermal aging. *Journal of Aerospace Technology and Management*, 2(2), pp. 163-168. doi:10.5028/jatm.2010.02027310
- Vorozhtsov, A., Lerner, M., Rodkevich, N., Sokolov, S., Perchatkina, E., & Paravan, C. (2020, November 1). Preparation and Characterization of Al/HTPB Composite for High Energetic Materials. *Nanomaterials*, 10(11). doi:10.3390/nano10112222
- Weiss Technik Explosion-Proof Drying oven, VFT with ATEX type examination. (n.d.). Retrieved from Weiss Technik Web Site: <https://www.weiss-technik.com/en/products/produkte-detail/explosion-proof-drying-oven-vft-with-atex-type-examination>
- Yıldırım, C. (2007). Analysis of Grain Burnback and Internal Flow in Solid Propellant Rocket Motors in 3-Dimensions. *Graduate School of Natural and Applied Science of Middle East Technical University*.
- Yoon, H.-K. (2014, December 5). Application of the Arrhenius Equation in Geotechnical Engineering. *The Journal of Engineering Geology*, 24(4), 575-581. doi:http://dx.doi.org/10.9720/kseg.2014.4.575
- Zibdeh, H. S., & Heller, R. A. (1989, July-August). Rocket Motor Service Life Calculations Based on the First-Passage Method. *Journal of Spacecraft and Rockets*, 26(4), pp. 279-284. doi:https://doi.org/10.2514/3.26067

APPENDICES

A. Mechanical Test Results

Table 15. 90°C Mechanical test results for propellant A.

Accelerated Ageing Temperature (°C)	Accelerated Ageing Duration (days)	Sample	Stress at break (MPa)	Stress at break (psi)	Strain at break (%)
90	0	1	0.8100	117.4805	61.3998
		2	0.7900	114.5798	60.7326
		3	0.8200	118.9309	54.2037
		4	0.8100	117.4805	63.3056
		5	0.8000	116.0302	62.1759
		6	0.8000	116.0302	60.3067
		Mean ± SD	0.8050 ± 0.0105	116.7553 ± 1.5212	60.3540 ± 3.1968
	2	1	0.8700	126.1828	57.1697
		2	0.8600	124.7324	54.2818
		3	0.8600	124.7324	57.0129
		4	0.8800	127.6332	51.3822
		5	0.9000	130.5339	52.1846
		6	0.8900	129.0836	50.6774
		Mean ± SD	0.8767 ± 0.0163	127.1497 ± 2.3685	53.7848 ± 2.8325
	4	1	0.9900	143.5873	50.7445
		2	0.9900	143.5873	53.9098
		3	1.0100	146.4881	49.5409
		4	0.9800	142.1369	54.6733
5		0.9800	142.1369	50.7271	
6		0.9600	139.2362	54.7995	
Mean ± SD		0.9850 ± 0.0164	142.8621 ± 2.3832	52.3992 ± 2.3203	

Table 16. 90°C Mechanical test results for propellant A, cont'd.

Accelerated Ageing Temperature (°C)	Accelerated Ageing Duration (days)	Sample	Stress at break (MPa)	Stress at break (psi)	Strain at break (%)
90	6	1	1.0800	156.6407	47.0265
		2	1.0900	158.0911	46.4118
		3	1.0800	156.6407	49.4090
		4	1.0800	156.6407	46.3090
		5	1.0700	155.1903	44.1985
		6	1.0800	156.6407	48.6298
		Mean ± SD	1.0800 ± 0.0063	156.6407 ± 0.9173	46.9974 ± 1.8511
	8	1	1.1000	159.5415	44.9265
		2	1.1000	159.5415	50.7657
		3	1.1200	162.4422	48.6388
		4	1.1100	160.9918	50.7354
		5	1.1100	160.9918	48.7720
		6	1.1400	165.3430	46.9975
		Mean ± SD	1.1133 ± 0.0151	161.4753 ± 2.1836	48.4727 ± 2.2471
	10	1	1.0400	150.8392	40.5023
		2	1.0600	153.7400	43.7306
		3	1.0200	147.9385	44.9305
		4	1.0300	149.3888	41.1004
5		1.0500	152.2896	43.2663	
6		1.0200	147.9385	45.0959	
Mean ± SD		1.0367 ± 0.0163	150.3557 ± 2.3685	43.1043 ± 1.9238	

Table 17. 80°C Mechanical test results for propellant A.

Accelerated Ageing Temperature (°C)	Accelerated Ageing Duration (days)	Sample	Stress at break (MPa)	Stress at break (psi)	Strain at break (%)
80	0	1	0.8100	117.4805	61.3998
		2	0.7900	114.5798	60.7326
		3	0.8200	118.9309	54.2037
		4	0.8100	117.4805	63.3056
		5	0.8000	116.0302	62.1759
		6	0.8000	116.0302	60.3067
		Mean ± SD	0.8050 ± 0.0105	116.7553 ± 1.5212	60.3540 ± 3.1968
	5	1	0.9600	139.2362	49.6471
		2	0.9400	136.3354	43.4087
		3	0.9600	139.2362	53.5085
		4	0.9300	134.8851	48.2162
		5	0.9100	131.9843	52.3351
		6	0.9400	136.3354	54.7115
		Mean ± SD	0.9400 ± 0.0190	136.3354 ± 2.7519	50.3045 ± 4.1511
	10	1	1.1000	159.5415	47.1682
		2	1.1000	159.5415	46.0578
		3	1.1000	159.5415	45.6799
		4	1.0800	156.6407	47.5342
5		1.1000	159.5415	47.4175	
6		1.1000	159.5415	48.3226	
Mean ± SD		1.0967 ± 0.0082	159.0580 ± 1.1842	47.0300 ± 0.9861	

Table 18. 80°C Mechanical test results for propellant A, cont'd.

Accelerated Ageing Temperature (°C)	Accelerated Ageing Duration (days)	Sample	Stress at break (MPa)	Stress at break (psi)	Strain at break (%)
80	15	1	1.0800	156.6407	38.4377
		2	1.1200	162.4422	48.7312
		3	1.1200	162.4422	44.1722
		4	1.1400	165.3430	42.8576
		5	1.1600	168.2437	44.8694
		6	1.1500	166.7934	43.8814
		Mean ± SD	1.1283 ± 0.0286	163.6509 ± 4.1448	43.8249 ± 3.3240
	20	1	1.0700	155.1903	45.8569
		2	1.1000	159.5415	45.5002
		3	1.1100	160.9918	44.4960
		4	1.0800	156.6407	41.1170
		5	1.0900	158.0911	42.9302
		6	1.1100	160.9918	46.5568
		Mean ± SD	1.0933 ± 0.0163	158.5746 ± 2.3685	44.4095 ± 2.0461
	25	1	1.2000	174.0452	42.3700
		2	1.2200	176.9460	45.1771
		3	1.1900	172.5949	42.7529
		4	1.2000	174.0452	40.1997
5		1.1900	172.5949	45.8798	
6					
Mean ± SD		1.2000 ± 0.0122	174.0452 ± 1.7763	43.2759 ± 2.2887	

Table 19. 70°C Mechanical test results for propellant A.

Accelerated Ageing Temperature (°C)	Accelerated Ageing Duration (days)	Sample	Stress at break (MPa)	Stress at break (psi)	Strain at break (%)
70	0	1	0.8100	117.4805	61.3998
		2	0.7900	114.5798	60.7326
		3	0.8200	118.9309	54.2037
		4	0.8100	117.4805	63.3056
		5	0.8000	116.0302	62.1759
		6	0.8000	116.0302	60.3067
		Mean ± SD	0.8050 ± 0.0105	116.7553 ± 1.5212	60.3540 ± 3.1968
	12	1	0.8900	129.0836	53.1840
		2	0.8800	127.6332	54.8157
		3	0.8800	127.6332	54.4127
		4	0.8700	126.1828	57.8591
		5	0.8700	126.1828	57.9908
		6	0.8700	126.1828	56.0196
		Mean ± SD	0.8767 ± 0.0082	127.1497 ± 1.1842	55.7137 ± 1.9380
	24	1	0.9900	143.5873	51.7875
		2	1.0000	145.0377	52.4434
		3	0.9800	142.1369	51.8589
		4	1.0100	146.4881	52.4411
5		1.0000	145.0377	53.1916	
6					
Mean ± SD		0.9960 ± 0.0114	144.4575 ± 1.6537	52.3445 ± 0.5663	

Table 20. 70°C Mechanical test results for propellant A, cont'd.

Accelerated Ageing Temperature (°C)	Accelerated Ageing Duration (days)	Sample	Stress at break (MPa)	Stress at break (psi)	Strain at break (%)
70	36	1	1.0100	146.4881	47.6589
		2	1.0100	146.4881	48.5882
		3	1.0000	145.0377	48.5890
		4	1.1000	159.5415	44.2391
		5	1.1000	159.5415	46.4112
		6	1.0900	158.0911	45.7142
		Mean ± SD	1.0517 ± 0.0496	152.5313 ± 7.1888	46.8668 ± 1.7319
	48	1	1.0200	147.9385	50.0329
		2	1.0300	149.3888	47.0629
		3	1.0100	146.4881	45.1736
		4	1.0100	146.4881	51.7039
		5	1.0000	145.0377	48.7057
		6			
		Mean ± SD	1.0140 ± 0.0114	147.0682 ± 1.6537	48.5358 ± 2.5387
	60	1	1.0400	150.8392	46.5308
		2	1.0400	150.8392	42.0980
		3	1.0400	150.8392	40.0408
		4	1.0500	152.2896	41.0938
5		1.0400	150.8392	42.6744	
6		1.0500	152.2896	42.9453	
Mean ± SD		1.0433 ± 0.0052	151.3227 ± 0.7490	42.5638 ± 2.2199	

Table 21. 60°C Mechanical test results for propellant A.

Accelerated Ageing Temperature (°C)	Accelerated Ageing Duration (days)	Sample	Stress at break (MPa)	Stress at break (psi)	Strain at break (%)
60	0	1	0.8100	117.4805	61.3998
		2	0.7900	114.5798	60.7326
		3	0.8200	118.9309	54.2037
		4	0.8100	117.4805	63.3056
		5	0.8000	116.0302	62.1759
		6	0.8000	116.0302	60.3067
		Mean ± SD	0.8050 ± 0.0105	116.7553 ± 1.5212	60.3540 ± 3.1968
	30	1	0.7900	114.5798	54.2940
		2	0.8100	117.4805	52.9844
		3	0.8100	117.4805	51.5760
		4	0.8100	117.4805	53.8795
		5			
		6			
		Mean ± SD	0.8050 ± 0.0100	116.7553 ± 1.4504	53.1835 ± 1.2029
	57	1	0.9200	133.4347	59.9511
		2	0.9300	134.8851	57.7177
		3	0.9100	131.9843	54.3412
		4	0.9200	133.4347	53.8653
5		0.9100	131.9843	55.8452	
6					
Mean ± SD		0.9180 ± 0.0084	133.1446 ± 1.2135	56.3441 ± 2.5151	

Table 22. 60°C Mechanical test results for propellant A, cont'd.

Accelerated Ageing Temperature (°C)	Accelerated Ageing Duration (days)	Sample	Stress at break (MPa)	Stress at break (psi)	Strain at break (%)
60	90	1	1.0700	155.1903	41.7522
		2	1.0900	158.0911	44.0482
		3	1.0600	153.7400	47.3784
		4	1.0500	152.2896	49.8276
		5	1.0600	153.7400	46.6906
		6	1.0700	155.1903	44.5711
		Mean ± SD	1.0667 ± 0.0137	154.7069 ± 1.9816	45.7113 ± 2.8433
	120	1	1.0600	153.7400	46.0932
		2	1.0400	150.8392	51.0920
		3	1.0500	152.2896	45.2901
		4			
		5			
		6			
		Mean ± SD	1.0500 ± 0.0100	152.2896 ± 1.4504	47.4918 ± 3.1436
	154	1	1.2100	175.4956	42.1743
		2	1.2300	178.3964	41.3635
		3	1.2100	175.4956	42.5261
		4	1.2200	176.9460	45.0456
5		1.2200	176.9460	45.1020	
6		1.2300	178.3964	44.5432	
Mean ± SD		1.2200 ± 0.0089	176.9460 ± 1.2973	43.4591 ± 1.6312	

Table 23. 90°C Mechanical test results for propellant B.

Accelerated Ageing Temperature (°C)	Accelerated Ageing Duration (days)	Sample	Stress at break (MPa)	Stress at break (psi)	Strain at break (%)
90	0	1	0.5800	84.1219	62.8314
		2	0.5700	82.6715	66.8372
		3	0.5600	81.2211	72.5409
		4	0.5600	81.2211	72.9981
		5	0.5600	81.2211	69.3074
		6			
		Mean ± SD	0.5660 ± 0.0089	82.0913 ± 1.2973	68.9030 ± 4.2220
	2	1	0.7900	114.5798	50.5614
		2	0.7900	114.5798	52.0076
		3	0.7800	113.1294	53.2611
		4	0.7900	114.5798	53.2019
		5	0.7800	113.1294	57.2518
		6	0.7900	114.5798	52.0810
		Mean ± SD	0.7867 ± 0.0052	114.0963 ± 0.7490	53.0608 ± 2.2277
	4	1	0.8400	121.8317	63.7016
		2	0.8300	120.3813	56.3982
		3	0.8400	121.8317	61.5638
		4	0.8500	123.2820	55.2479
5		0.8300	120.3813	47.4530	
6		0.8500	123.2820	51.2126	
Mean ± SD		0.8400 ± 0.0089	121.8317 ± 1.2973	55.9295 ± 6.1145	

Table 24. 90°C Mechanical test results for propellant B, cont'd.

Accelerated Ageing Temperature (°C)	Accelerated Ageing Duration (days)	Sample	Stress at break (MPa)	Stress at break (psi)	Strain at break (%)
90	6	1	0.9300	134.8851	52.0675
		2	0.9300	134.8851	51.3403
		3	0.9400	136.3354	51.9406
		4	0.9000	130.5339	57.6558
		5	0.9100	131.9843	55.9422
		6	0.9000	130.5339	55.1895
		Mean ± SD	0.9183 ± 0.0172	133.1930 ± 2.4981	54.0226 ± 2.5922
	8	1	0.9900	143.5873	48.4805
		2	0.9800	142.1369	50.1152
		3	1.0000	145.0377	44.4598
		4	1.0000	145.0377	43.1797
		5	0.9800	142.1369	47.1332
		6			
		Mean ± SD	0.9900 ± 0.0100	143.5873 ± 1.4504	46.6737 ± 2.8473
	10	1	0.9300	134.8851	50.4397
		2	0.9200	133.4347	49.3040
		3	0.9500	137.7858	49.1638
		4	0.9500	137.7858	43.1064
5		0.9700	140.6866	45.9531	
6		0.9700	140.6866	44.8577	
Mean ± SD		0.9483 ± 0.0204	137.5441 ± 2.9606	47.1374 ± 2.9173	

Table 25. 80°C Mechanical test results for propellant B.

Accelerated Ageing Temperature (°C)	Accelerated Ageing Duration (days)	Sample	Stress at break (MPa)	Stress at break (psi)	Strain at break (%)
80	0	1	0.5800	84.1219	62.8314
		2	0.5700	82.6715	66.8372
		3	0.5600	81.2211	72.5409
		4	0.5600	81.2211	72.9981
		5	0.5600	81.2211	69.3074
		6			
		Mean ± SD	0.5660 ± 0.0089	82.0913 ± 1.2973	68.9030 ± 4.2220
	5	1	0.7900	114.5798	51.6983
		2	0.8100	117.4805	45.3745
		3	0.8300	120.3813	50.3807
		4	0.8300	120.3813	49.1115
		5			
		6			
		Mean ± SD	0.8150 ± 0.0191	118.2057 ± 2.7773	49.1412 ± 2.7242
	10	1	0.9500	137.7858	48.2131
		2	0.9600	139.2362	46.0061
		3	0.9400	136.3354	44.2697
		4	0.9600	139.2362	47.6648
5		0.9500	137.7858	50.6683	
6		0.9500	137.7858	42.9815	
Mean ± SD		0.9517 ± 0.0075	138.0275 ± 1.0918	46.6339 ± 2.7985	

Table 26. 80°C Mechanical test results for propellant B, cont'd.

Accelerated Ageing Temperature (°C)	Accelerated Ageing Duration (days)	Sample	Stress at break (MPa)	Stress at break (psi)	Strain at break (%)
80	15	1	0.9300	134.8851	50.1497
		2	0.9400	136.3354	46.5721
		3	0.9500	137.7858	46.1708
		4	0.9800	142.1369	43.1523
		5	0.9700	140.6866	41.3031
		6	0.9400	136.3354	46.5399
		Mean ± SD	0.9517 ± 0.0194	138.0275 ± 2.8149	45.6480 ± 3.0755
	20	1	0.9900	143.5873	45.4061
		2	0.9700	140.6866	41.9205
		3	1.0000	145.0377	43.0400
		4	0.9700	140.6866	48.8606
		5	0.9700	140.6866	46.7007
		6	0.9800	142.1369	45.0276
		Mean ± SD	0.9800 ± 0.0126	142.1369 ± 1.8346	45.1592 ± 2.4954
	25	1	1.1000	159.5415	42.5267
		2	1.1100	160.9918	41.3445
		3	1.0800	156.6407	44.4308
		4	1.0800	156.6407	39.4775
5		1.0800	156.6407	41.2800	
6		1.0900	158.0911	43.2505	
Mean ± SD		1.0900 ± 0.0126	158.0911 ± 1.8346	42.0517 ± 1.7347	

Table 27. 70°C Mechanical test results for propellant B.

Accelerated Ageing Temperature (°C)	Accelerated Ageing Duration (days)	Sample	Stress at break (MPa)	Stress at break (psi)	Strain at break (%)
70	0	1	0.5800	84.1219	62.8314
		2	0.5700	82.6715	66.8372
		3	0.5600	81.2211	72.5409
		4	0.5600	81.2211	72.9981
		5	0.5600	81.2211	69.3074
		6			
		Mean ± SD	0.5660 ± 0.0089	82.0913 ± 1.2973	68.9030 ± 4.2220
	12	1	0.7400	107.3279	49.2335
		2	0.7200	104.4271	59.1029
		3	0.7300	105.8775	51.4171
		4	0.7500	108.7783	57.2699
		5	0.7600	110.2287	49.2624
		6			
		Mean ± SD	0.7400 ± 0.0158	107.3279 ± 2.2932	53.2571 ± 4.6317
	24	1	0.8300	120.3813	50.1060
		2	0.8400	121.8317	50.5374
		3	0.8200	118.9309	53.0583
		4	0.8100	117.4805	54.5926
5		0.8100	117.4805	56.4992	
6		0.8200	118.9309	47.8581	
Mean ± SD		0.8217 ± 0.0117	119.1726 ± 1.6956	52.1086 ± 3.1905	

Table 28. 70°C Mechanical test results for propellant B, cont'd.

Accelerated Ageing Temperature (°C)	Accelerated Ageing Duration (days)	Sample	Stress at break (MPa)	Stress at break (psi)	Strain at break (%)
70	36	1	0.8200	118.9309	53.7910
		2	0.8100	117.4805	48.9957
		3	0.8600	124.7324	44.6858
		4	0.8700	126.1828	50.6854
		5			
		6			
		Mean ± SD	0.8400 ± 0.0294	121.8317 ± 4.2698	49.5395 ± 3.7966
	48	1	0.8700	126.1828	50.3908
		2	0.8600	124.7324	46.7264
		3	0.9000	130.5339	48.7666
		4			
		5			
		6			
		Mean ± SD	0.8767 ± 0.0208	127.1497 ± 3.0192	48.6279 ± 1.8362
	60	1	0.8900	129.0836	44.3279
		2	0.9200	133.4347	47.4426
		3	0.9100	131.9843	48.1376
		4	0.8900	129.0836	43.8160
5		0.9100	131.9843	46.7402	
6					
Mean ± SD		0.9040 ± 0.0134	131.1141 ± 1.9459	46.0929 ± 1.9184	

Table 29. 60°C Mechanical test results for propellant B.

Accelerated Ageing Temperature (°C)	Accelerated Ageing Duration (days)	Sample	Stress at break (MPa)	Stress at break (psi)	Strain at break (%)
60	0	1	0.5800	84.1219	62.8314
		2	0.5700	82.6715	66.8372
		3	0.5600	81.2211	72.5409
		4	0.5600	81.2211	72.9981
		5	0.5600	81.2211	69.3074
		6			
		Mean ± SD	0.5660 ± 0.0089	82.0913 ± 1.2973	68.9030 ± 4.2220
	30	1	0.7000	101.5264	62.0551
		2	0.7000	101.5264	60.1295
		3	0.7100	102.9768	62.1875
		4	0.7000	101.5264	61.1273
		5	0.7000	101.5264	58.1163
		6			
		Mean ± SD	0.7020 ± 0.0045	101.8165 ± 0.6486	60.7231 ± 1.6756
	57	1	0.8000	116.0302	51.0153
		2	0.7800	113.1294	54.9027
		3	0.7800	113.1294	53.2856
		4	0.7400	107.3279	51.7561
5		0.7600	110.2287	56.7171	
6		0.7700	111.6790	55.3227	
Mean ± SD		0.7717 ± 0.0204	111.9208 ± 2.9606	53.8332 ± 2.2016	

Table 30. 60°C Mechanical test results for propellant B, cont'd.

Accelerated Ageing Temperature (°C)	Accelerated Ageing Duration (days)	Sample	Stress at break (MPa)	Stress at break (psi)	Strain at break (%)
60	90	1	0.8900	129.0836	51.6812
		2	0.9100	131.9843	50.4123
		3	0.9100	131.9843	55.1178
		4	0.8500	123.2820	48.6243
		5	0.8700	126.1828	55.4197
		6			
		Mean ± SD	0.8860 ± 0.0261	128.5034 ± 3.7821	52.2510 ± 2.9630
	120	1	0.9100	131.9843	47.8266
		2	0.9200	133.4347	48.4844
		3	0.9300	134.8851	51.1375
		4	0.9200	133.4347	52.9098
		5	0.9000	130.5339	53.5418
		6	0.9100	131.9843	49.9840
		Mean ± SD	0.9150 ± 0.0105	132.7095 ± 1.5212	50.6474 ± 2.3157
	154	1	1.0300	149.3888	45.6147
		2	1.0300	149.3888	42.0022
		3	1.0200	147.9385	45.4002
		4	1.0000	145.0377	44.0551
5		1.0000	145.0377	42.0305	
6					
Mean ± SD		1.0160 ± 0.0152	147.3583 ± 2.1996	43.8205 ± 1.7521	

Table 31. 90°C Mechanical test results for propellant C.

Accelerated Ageing Temperature (°C)	Accelerated Ageing Duration (days)	Sample	Stress at break (MPa)	Stress at break (psi)	Strain at break (%)
90	0	1	0.3700	53.6639	68.8555
		2	0.3700	53.6639	72.3291
		3	0.3800	55.1143	58.5705
		4	0.3700	53.6639	61.8521
		5			
		6			
		Mean ± SD	0.3725 ± 0.0050	54.0265 ± 0.7252	65.4018 ± 6.3030
	2	1	0.5900	85.5722	50.4289
		2	0.6000	87.0226	45.0636
		3	0.5900	85.5722	52.6706
		4	0.6100	88.4730	52.7510
		5	0.6100	88.4730	51.1513
		6	0.6000	87.0226	53.8597
		Mean ± SD	0.6000 ± 0.0089	87.0226 ± 1.2973	50.9875 ± 3.1503
	4	1	0.7000	101.5264	53.0962
		2	0.7200	104.4271	48.8697
		3	0.7300	105.8775	49.5257
		4	0.7100	102.9768	49.5828
5		0.6900	100.0760	47.7365	
6		0.6900	100.0760	54.8395	
Mean ± SD		0.7067 ± 0.0163	102.4933 ± 2.3685	50.6084 ± 2.7418	

Table 32. 90°C Mechanical test results for propellant C, cont'd.

Accelerated Ageing Temperature (°C)	Accelerated Ageing Duration (days)	Sample	Stress at break (MPa)	Stress at break (psi)	Strain at break (%)
90	6	1	0.8100	117.4805	47.9176
		2	0.8100	117.4805	46.0002
		3	0.7900	114.5798	47.7930
		4	0.7900	114.5798	48.6106
		5	0.7900	114.5798	51.8508
		6			
		Mean ± SD	0.7980 ± 0.0110	115.7401 ± 1.5888	48.4345 ± 2.1393
	8	1	0.8200	118.9309	48.0159
		2	0.8400	121.8317	45.3979
		3	0.8500	123.2820	42.0151
		4	0.8500	123.2820	43.3453
		5	0.8400	121.8317	49.3383
		6	0.8300	120.3813	48.5286
		Mean ± SD	0.8383 ± 0.0117	121.5899 ± 1.6956	46.1068 ± 2.9941
	10	1	0.8200	118.9309	47.1621
		2	0.8100	117.4805	45.7312
		3	0.8300	120.3813	47.2141
		4	0.8100	117.4805	40.1517
5		0.8000	116.0302	48.2346	
6		0.8200	118.9309	44.4631	
Mean ± SD		0.8150 ± 0.0105	118.2057 ± 1.5212	45.4928 ± 2.9295	

Table 33. 80°C Mechanical test results for propellant C.

Accelerated Ageing Temperature (°C)	Accelerated Ageing Duration (days)	Sample	Stress at break (MPa)	Stress at break (psi)	Strain at break (%)
80	0	1	0.3700	53.6639	68.8555
		2	0.3700	53.6639	72.3291
		3	0.3800	55.1143	58.5705
		4	0.3700	53.6639	61.8521
		5			
		6			
		Mean ± SD	0.3725 ± 0.0050	54.0265 ± 0.7252	65.4018 ± 6.3030
	5	1	0.5800	84.1219	57.0474
		2	0.5900	85.5722	57.5582
		3	0.5900	85.5722	56.6392
		4	0.6100	88.4730	51.9318
		5	0.6000	87.0226	50.7139
		6			
		Mean ± SD	0.5940 ± 0.0114	86.1524 ± 1.6537	54.7781 ± 3.2000
	10	1	0.6500	94.2745	51.1002
		2	0.6600	95.7249	46.5091
		3	0.6400	92.8241	40.4378
		4			
5					
6					
Mean ± SD		0.6500 ± 0.0100	94.2745 ± 1.4504	46.0157 ± 5.3483	

Table 34. 80°C Mechanical test results for propellant C, cont'd.

Accelerated Ageing Temperature (°C)	Accelerated Ageing Duration (days)	Sample	Stress at break (MPa)	Stress at break (psi)	Strain at break (%)
80	15	1	0.8100	117.4805	39.4724
		2	0.8300	120.3813	39.3213
		3	0.8200	118.9309	45.4709
		4	0.8300	120.3813	44.3743
		5	0.8300	120.3813	48.0471
		6			
		Mean ± SD	0.8240 ± 0.0089	119.5111 ± 1.2973	43.3372 ± 3.8365
	20	1	0.8800	127.6332	39.1775
		2	0.8700	126.1828	39.6507
		3	0.9000	130.5339	41.2696
		4	0.8800	127.6332	43.8953
		5	0.8700	126.1828	41.4209
		6			
		Mean ± SD	0.8800 ± 0.0122	127.6332 ± 1.7763	41.0828 ± 1.8534
	25	1	0.9300	134.8851	37.5939
		2	0.9600	139.2362	40.7407
		3	0.9400	136.3354	38.1555
		4	0.9400	136.3354	38.2382
5		0.9500	137.7858	41.1737	
6		0.9400	136.3354	41.0778	
Mean ± SD		0.9433 ± 0.0103	136.8189 ± 1.4979	39.4967 ± 1.6651	

Table 35. 70°C Mechanical test results for propellant C.

Accelerated Ageing Temperature (°C)	Accelerated Ageing Duration (days)	Sample	Stress at break (MPa)	Stress at break (psi)	Strain at break (%)
70	0	1	0.3700	53.6639	68.8555
		2	0.3700	53.6639	72.3291
		3	0.3800	55.1143	58.5705
		4	0.3700	53.6639	61.8521
		5			
		6			
		Mean ± SD	0.3725 ± 0.0050	54.0265 ± 0.7252	65.4018 ± 6.3030
	12	1	0.5800	84.1219	57.0474
		2	0.5900	85.5722	57.5582
		3	0.5900	85.5722	56.6392
		4	0.6100	88.4730	51.9318
		5	0.6000	87.0226	50.7139
		6			
		Mean ± SD	0.5940 ± 0.0114	86.1524 ± 1.6537	54.7781 ± 3.2000
	24	1	0.7000	101.5264	48.1482
		2	0.6900	100.0760	54.2596
		3	0.6900	100.0760	48.9328
		4	0.7000	101.5264	51.5251
5					
6					
Mean ± SD		0.6950 ± 0.0058	100.8012 ± 0.8374	50.7164 ± 2.7680	

Table 36. 70°C Mechanical test results for propellant C, cont'd.

Accelerated Ageing Temperature (°C)	Accelerated Ageing Duration (days)	Sample	Stress at break (MPa)	Stress at break (psi)	Strain at break (%)
70	36	1	0.7300	105.8775	51.0323
		2	0.7300	105.8775	44.1278
		3	0.7400	107.3279	50.0862
		4	0.7400	107.3279	47.0307
		5	0.7600	110.2287	48.5885
		6			
		Mean ± SD	0.7400 ± 0.0122	107.3279 ± 1.7763	48.1731 ± 2.7238
	48	1	0.8100	117.4805	46.9024
		2	0.7900	114.5798	48.3738
		3	0.7800	113.1294	46.1184
		4	0.7800	113.1294	51.3532
		5	0.7700	111.6790	46.9314
		6	0.7800	113.1294	48.1545
		Mean ± SD	0.7850 ± 0.0138	113.8546 ± 1.992	47.9723 ± 1.8596
	60	1	0.8100	117.4805	48.6987
		2	0.8000	116.0302	46.5044
		3	0.8100	117.4805	43.0167
		4	0.8100	117.4805	45.8732
5					
6					
Mean ± SD		0.8075 ± 0.0050	117.1179 ± 0.7252	46.0232 ± 2.3417	

Table 37. 60°C Mechanical test results for propellant C.

Accelerated Ageing Temperature (°C)	Accelerated Ageing Duration (days)	Sample	Stress at break (MPa)	Stress at break (psi)	Strain at break (%)
60	0	1	0.3700	53.6639	68.8555
		2	0.3700	53.6639	72.3291
		3	0.3800	55.1143	58.5705
		4	0.3700	53.6639	61.8521
		5			
		6			
		Mean ± SD	0.3725 ± 0.0050	54.0265 ± 0.7252	65.4018 ± 6.3030
	30	1	0.5300	76.8700	58.9021
		2	0.5200	75.4196	58.4159
		3	0.5200	75.4196	57.7987
		4	0.5300	76.8700	63.4851
		5	0.5300	76.8700	54.3660
		6	0.5200	75.4196	64.8557
		Mean ± SD	0.5250 ± 0.0055	76.1448 ± 0.7944	59.6372 ± 3.8791
	57	1	0.6300	91.3738	51.1271
		2	0.6300	91.3738	52.2462
		3	0.6100	88.4730	54.1848
		4	0.6200	89.9234	52.6753
5		0.6300	91.3738	49.5410	
6		0.6200	89.9234	51.3422	
Mean ± SD		0.6233 ± 0.0082	90.4068 ± 1.1842	51.8528 ± 1.5749	

Table 38. 60°C Mechanical test results for propellant C, cont'd.

Accelerated Ageing Temperature (°C)	Accelerated Ageing Duration (days)	Sample	Stress at break (MPa)	Stress at break (psi)	Strain at break (%)
60	90	1	0.7100	102.9768	44.7475
		2	0.7400	107.3279	46.6941
		3	0.7200	104.4271	41.6197
		4	0.7200	104.4271	42.5928
		5			
		6			
		Mean ± SD	0.7225 ± 0.0126	104.7897 ± 1.8250	43.9135 ± 2.2681
	120	1	0.7900	114.5798	45.8862
		2	0.7700	111.6790	41.6884
		3	0.7600	110.2287	41.5606
		4	0.7700	111.6790	43.1874
		5	0.7700	111.6790	37.5937
		6			
		Mean ± SD	0.7720 ± 0.0110	111.9691 ± 1.5888	41.9833 ± 3.0090
	154	1	0.8800	127.6332	47.7923
		2	0.8700	126.1828	45.4701
		3	0.8800	127.6332	44.3922
		4			
5					
6					
Mean ± SD		0.8767 ± 0.0058	127.1497 ± 0.8374	45.8848 ± 1.7376	

Table 39. 90°C Mechanical test results for propellant D.

Accelerated Ageing Temperature (°C)	Accelerated Ageing Duration (days)	Sample	Stress at break (MPa)	Stress at break (psi)	Strain at break (%)
90	0	1	0.7100	102.9768	43.3726
		2	0.7100	102.9768	42.3309
		3	0.6900	100.0760	41.2161
		4			
		5			
		6			
		Mean ± SD	0.7033 ± 0.0115	102.0098 ± 1.6748	42.3066 ± 1.0785
	2	1	0.6900	100.0760	35.8689
		2	0.7000	101.5264	44.3831
		3	0.6800	98.6256	37.7525
		4			
		5			
		6			
		Mean ± SD	0.6900 ± 0.0100	100.0760 ± 1.4504	39.3348 ± 4.4722
	4	1	0.7500	108.7783	37.2064
		2	0.7800	113.1294	44.3374
		3	0.7900	114.5798	44.4374
		4			
5					
6					
Mean ± SD		0.7733 ± 0.0208	112.1625 ± 3.0192	41.9937 ± 4.1462	

Table 40. 90°C Mechanical test results for propellant D, cont'd.

Accelerated Ageing Temperature (°C)	Accelerated Ageing Duration (days)	Sample	Stress at break (MPa)	Stress at break (psi)	Strain at break (%)
90	6	1	0.8800	127.6332	33.8207
		2	0.8700	126.1828	32.0650
		3	0.8800	127.6332	34.0856
		4	0.8600	124.7324	35.7135
		5	0.8800	127.6332	34.2332
		6			
		Mean ± SD	0.8740 ± 0.0089	126.7629 ± 1.2973	33.9836 ± 1.3012
	8	1	0.8700	126.1828	35.9609
		2	0.8700	126.1828	40.4111
		3	0.8700	126.1828	35.3714
		4	0.8800	127.6332	40.1707
		5	0.8700	126.1828	43.2677
		6	0.8700	126.1828	40.3609
		Mean ± SD	0.8717 ± 0.0041	126.4245 ± 0.5921	39.2571 ± 3.0144
	10	1	0.9200	133.4347	32.5213
		2	0.9200	133.4347	37.8936
		3	0.9800	142.1369	35.3749
		4	0.9500	137.7858	34.2479
5		0.9200	133.4347	35.5780	
6		0.8800	127.6332	34.2396	
Mean ± SD		0.9283 ± 0.0337	134.6433 ± 4.8899	34.9759 ± 1.7962	

Table 41. 80°C Mechanical test results for propellant D.

Accelerated Ageing Temperature (°C)	Accelerated Ageing Duration (days)	Sample	Stress at break (MPa)	Stress at break (psi)	Strain at break (%)
80	0	1	0.7100	102.9768	43.3726
		2	0.7100	102.9768	42.3309
		3	0.6900	100.0760	41.2161
		4			
		5			
		6			
		Mean ± SD	0.7033 ± 0.0115	102.0098 ± 1.6748	42.3066 ± 1.0785
	5	1	0.7200	104.4271	41.6949
		2	0.7000	101.5264	37.7199
		3	0.7300	105.8775	40.8752
		4	0.7000	101.5264	39.6364
		5	0.7300	105.8775	35.6370
		6			
		Mean ± SD	0.7160 ± 0.0152	103.8470 ± 2.1996	39.1127 ± 2.4530
	10	1	0.8200	118.9309	41.9380
		2	0.8200	118.9309	41.8113
		3	0.7900	114.5798	39.7471
		4	0.8300	120.3813	37.9931
5		0.8100	117.4805	34.0710	
6					
Mean ± SD		0.8140 ± 0.0152	118.0607 ± 0.0152	39.1121 ± 3.2535	

Table 42. 80°C Mechanical test results for propellant D, cont'd.

Accelerated Ageing Temperature (°C)	Accelerated Ageing Duration (days)	Sample	Stress at break (MPa)	Stress at break (psi)	Strain at break (%)
80	15	1	0.8700	126.1828	33.7232
		2	0.8600	124.7324	33.3134
		3	0.8900	129.0836	36.9681
		4	0.8800	127.6332	36.6633
		5			
		6			
		Mean ± SD	0.8750 ± 0.0129	126.9080 ± 1.8724	35.1670 ± 1.9151
	20	1	0.9100	131.9843	39.9748
		2	0.9100	131.9843	36.7444
		3	0.8900	129.0836	39.4430
		4	0.9300	134.8851	31.0899
		5	0.9300	134.8851	39.2178
		6	0.9600	139.2362	36.9402
		Mean ± SD	0.9217 ± 0.0240	133.6764 ± 3.4829	37.2350 ± 3.2986
	25	1	0.9400	136.3354	28.8527
		2	0.9000	130.5339	27.7192
		3	0.9300	134.8851	29.2052
		4	0.9500	137.7858	33.5212
5					
6					
Mean ± SD		0.9300 ± 0.0216	134.8851 ± 3.1332	29.8246 ± 2.5447	

Table 43. 70°C Mechanical test results for propellant D.

Accelerated Ageing Temperature (°C)	Accelerated Ageing Duration (days)	Sample	Stress at break (MPa)	Stress at break (psi)	Strain at break (%)
70	0	1	0.7100	102.9768	43.3726
		2	0.7100	102.9768	42.3309
		3	0.6900	100.0760	41.2161
		4			
		5			
		6			
		Mean ± SD	0.7033 ± 0.0115	102.0098 ± 1.6748	42.3066 ± 1.0785
	12	1	0.6900	100.0760	47.1023
		2	0.7000	101.5264	44.4976
		3	0.7100	102.9768	42.9974
		4	0.7200	104.4271	43.2138
		5	0.7200	104.4271	44.3294
		6			
		Mean ± SD	0.7080 ± 0.0130	102.6867 ± 1.8911	44.4281 ± 1.6346
	24	1	0.7900	114.5798	40.3126
		2	0.7800	113.1294	37.3169
		3	0.7400	107.3279	42.9640
		4	0.7500	108.7783	36.7125
5		0.7700	111.6790	39.4526	
6					
Mean ± SD		0.7660 ± 0.0207	111.0989 ± 3.0076	39.3517 ± 2.5044	

Table 44. 70°C Mechanical test results for propellant D, cont'd.

Accelerated Ageing Temperature (°C)	Accelerated Ageing Duration (days)	Sample	Stress at break (MPa)	Stress at break (psi)	Strain at break (%)
70	36	1	0.8600	124.7324	41.8798
		2	0.8400	121.8317	41.3488
		3	0.8200	118.9309	37.0088
		4	0.8600	124.7324	42.4520
		5	0.8300	120.3813	43.8974
		6	0.8300	120.3813	41.8741
		Mean ± SD	0.8400 ± 0.0167	121.8317 ± 2.4269	41.4102 ± 2.3274
	48	1	0.8600	124.7324	31.7389
		2	0.8800	127.6332	33.6632
		3	0.8700	126.1828	36.3150
		4	0.8700	126.1828	37.2565
		5	0.8700	126.1828	33.5127
		6	0.8600	124.7324	37.7984
		Mean ± SD	0.8683 ± 0.0075	125.9411 ± 1.0918	35.0474 ± 2.4196
	60	1	0.8800	127.6332	38.8947
		2	0.8600	124.7324	35.8546
		3	0.8900	129.0836	38.3490
		4			
5					
6					
Mean ± SD		0.8767 ± 0.0153	127.1497 ± 2.2155	37.6994 ± 1.6208	

Table 45. 60°C Mechanical test results for propellant D.

Accelerated Ageing Temperature (°C)	Accelerated Ageing Duration (days)	Sample	Stress at break (MPa)	Stress at break (psi)	Strain at break (%)
60	0	1	0.7100	102.9768	43.3726
		2	0.7100	102.9768	42.3309
		3	0.6900	100.0760	41.2161
		4			
		5			
		6			
		Mean ± SD	0.7033 ± 0.0115	102.0098 ± 1.6748	42.3066 ± 1.0785
	30	1	0.6600	95.7249	43.3459
		2	0.6800	98.6256	39.9854
		3	0.6700	97.1753	38.6591
		4	0.6700	97.1753	40.4984
		5			
		6			
		Mean ± SD	0.6700 ± 0.0082	97.1753 ± 1.1842	40.6222 ± 1.9743
	57	1	0.7500	108.7783	39.3182
		2	0.7500	108.7783	35.8005
		3	0.7600	110.2287	36.8393
		4	0.7400	107.3279	42.0886
5		0.7700	111.6790	41.0789	
6		0.7600	110.2287	42.8841	
Mean ± SD		0.7550 ± 0.0105	109.5035 ± 1.5212	39.6683 ± 2.8732	

Table 46. 60°C Mechanical test results for propellant D, cont'd.

Accelerated Ageing Temperature (°C)	Accelerated Ageing Duration (days)	Sample	Stress at break (MPa)	Stress at break (psi)	Strain at break (%)
60	90	1	0.8700	126.1828	31.0533
		2	0.8800	127.6332	31.8042
		3	0.8500	123.2820	29.1030
		4	0.8700	126.1828	30.1135
		5			
		6			
		Mean ± SD	0.8675 ± 0.0126	125.8202 ± 1.8250	30.5185 ± 1.1700
	120	1	0.9500	137.7858	32.1986
		2	0.9600	139.2362	32.8278
		3	0.9700	140.6866	37.0618
		4	0.9600	139.2362	27.2110
		5	0.9500	137.7858	29.3601
		6			
		Mean ± SD	0.9580 ± 0.0084	138.9461 ± 1.2135	31.7319 ± 3.7380
	150	1	1.0000	145.0377	34.0776
		2	0.9600	139.2362	34.7125
		3	1.0000	145.0377	36.3247
		4	0.9800	142.1369	34.9585
5		1.0000	145.0377	37.3866	
6					
Mean ± SD		0.9880 ± 0.0179	143.2972 ± 2.5945	35.4920 ± 1.3394	

Table 47. 90°C Mechanical test results for propellant E.

Accelerated Ageing Temperature (°C)	Accelerated Ageing Duration (days)	Sample	Stress at break (MPa)	Stress at break (psi)	Strain at break (%)
90	0	1	0.9100	131.9843	52.6265
		2	0.8900	129.0836	47.2009
		3	0.9200	133.4347	56.5050
		4	0.9300	134.8851	59.2506
		5			
		6			
		Mean ± SD	0.9125 ± 0.0171	132.3469 ± 2.4770	53.8958 ± 5.2254
	2	1	1.0200	147.9385	53.9559
		2	1.0200	147.9385	49.6779
		3	0.9900	143.5873	51.6815
		4	1.0300	149.3888	52.5639
		5			
		6			
		Mean ± SD	1.0150 ± 0.0173	147.2133 ± 2.5121	51.9698 ± 1.7920
	4	1	1.1100	160.9918	47.3323
		2	1.1400	165.3430	46.6815
		3	1.1400	165.3430	49.0882
		4	1.1700	169.6941	50.5872
5					
6					
Mean ± SD		1.1400 ± 0.0245	165.3430 ± 3.5527	48.4223 ± 1.7653	

Table 48. 90°C Mechanical test results for propellant E, cont'd.

Accelerated Ageing Temperature (°C)	Accelerated Ageing Duration (days)	Sample	Stress at break (MPa)	Stress at break (psi)	Strain at break (%)
90	6	1	1.2200	176.9460	61.7688
		2	1.2100	175.4956	58.0699
		3	1.2400	179.8467	61.0372
		4	1.2100	175.4956	62.5368
		5	1.2100	175.4956	58.7928
		6			
		Mean ± SD	1.2180 ± 0.0130	176.6559 ± 1.8911	60.4411 ± 1.9268
	8	1	1.1800	171.1445	51.3057
		2	1.2200	176.9460	49.5158
		3	1.2200	176.9460	47.8934
		4	1.1800	171.1445	53.0291
		5	1.2400	179.8467	46.8128
		6			
		Mean ± SD	1.2080 ± 0.0268	175.2055 ± 3.8918	49.7113 ± 2.5147
	10	1	1.2500	181.2971	53.3090
		2	1.2700	184.1979	49.0790
		3	1.2700	184.1979	51.9139
		4			
5					
6					
Mean ± SD		1.2633 ± 0.0115	183.2310 ± 1.6748	51.4339 ± 2.1555	

Table 49. 80°C Mechanical test results for propellant E.

Accelerated Ageing Temperature (°C)	Accelerated Ageing Duration (days)	Sample	Stress at break (MPa)	Stress at break (psi)	Strain at break (%)
80	0	1	0.9100	131.9843	52.6265
		2	0.8900	129.0836	47.2009
		3	0.9200	133.4347	56.5050
		4	0.9300	134.8851	59.2506
		5			
		6			
		Mean ± SD	0.9125 ± 0.0171	132.3469 ± 2.4770	53.8958 ± 5.2254
	5	1	1.0500	152.2896	56.8571
		2	1.0200	147.9385	53.0951
		3	1.0400	150.8392	57.3824
		4	1.0100	146.4881	58.6650
		5	1.0300	149.3888	56.2212
		6			
		Mean ± SD	1.0300 ± 0.0158	149.3888 ± 2.2932	56.4442 ± 2.0766
	10	1	1.1300	163.8926	53.6670
		2	1.1600	168.2437	50.8715
		3	1.1000	159.5415	47.0670
		4	1.1400	165.3430	53.9624
5		1.1600	168.2437	51.0065	
6		1.1400	165.3430	54.5544	
Mean ± SD		1.1383 ± 0.0223	165.1012 ± 3.2323	51.8548 ± 2.8151	

Table 50. 80°C Mechanical test results for propellant E, cont'd.

Accelerated Ageing Temperature (°C)	Accelerated Ageing Duration (days)	Sample	Stress at break (MPa)	Stress at break (psi)	Strain at break (%)
80	15	1	1.1800	171.1445	50.3100
		2	1.2200	176.9460	44.6298
		3	1.1800	171.1445	46.3993
		4	1.2500	181.2971	49.8492
		5			
		6			
		Mean ± SD	1.2075 ± 0.0340	175.1330 ± 4.9363	47.7971 ± 2.7393
	20	1	1.2800	185.6483	55.3863
		2	1.3100	189.9994	49.1998
		3	1.2600	182.7475	50.1252
		4	1.2800	185.6483	48.4540
		5	1.2600	182.7475	48.5810
		6			
		Mean ± SD	1.2780 ± 0.0205	185.3582 ± 2.9724	50.3493 ± 2.8923
	25	1	1.2000	174.0452	42.0620
		2	1.2600	182.7475	43.5942
		3	1.2100	175.4956	43.7305
		4	1.2600	182.7475	49.2803
5		1.1500	166.7934	41.2434	
6					
Mean ± SD		1.2160 ± 0.0462	176.3658 ± 6.6938	43.9821 ± 3.1413	

Table 51. 70°C Mechanical test results for propellant E.

Accelerated Ageing Temperature (°C)	Accelerated Ageing Duration (days)	Sample	Stress at break (MPa)	Stress at break (psi)	Strain at break (%)
70	0	1	0.9100	131.9843	52.6265
		2	0.8900	129.0836	47.2009
		3	0.9200	133.4347	56.5050
		4	0.9300	134.8851	59.2506
		5			
		6			
		Mean ± SD	0.9125 ± 0.0171	132.3469 ± 2.4770	53.8958 ± 5.2254
	12	1	1.0700	155.1903	45.8306
		2	1.0600	153.7400	41.8478
		3	1.0700	155.1903	45.0582
		4	1.1000	159.5415	62.8327
		5	1.1000	159.5415	62.9484
		6	1.1300	163.8926	53.7719
		Mean ± SD	1.0883 ± 0.0264	157.8494 ± 3.8282	52.0483 ± 9.2699
	24	1	1.1000	159.5415	54.2835
		2	1.0800	156.6407	46.4371
		3	1.0700	155.1903	48.2869
		4	1.0900	158.0911	50.8886
5		1.0900	158.0911	53.5843	
6					
Mean ± SD		1.0860 ± 0.0114	157.5109 ± 1.6537	50.6961 ± 3.3612	

Table 52. 70°C Mechanical test results for propellant E, cont'd.

Accelerated Ageing Temperature (°C)	Accelerated Ageing Duration (days)	Sample	Stress at break (MPa)	Stress at break (psi)	Strain at break (%)
70	36	1	1.1300	163.8926	45.2478
		2	1.0700	155.1903	51.4230
		3	1.1100	160.9918	51.7180
		4	1.0800	156.6407	44.3764
		5			
		6			
		Mean ± SD	1.0975 ± 0.0275	159.1789 ± 3.9940	48.1913 ± 3.9200
	48	1	1.1000	159.5415	41.9054
		2	1.1400	165.3430	44.6650
		3	1.1100	160.9918	39.3807
		4	1.1500	166.7934	44.8151
		5			
		6			
		Mean ± SD	1.1250 ± 0.0238	163.1674 ± 3.4526	42.6915 ± 2.5809
	60	1	1.2100	175.4956	53.1309
		2	1.2200	176.9460	54.4717
		3	1.1400	165.3430	47.3702
		4	1.1900	172.5949	51.7558
5					
6					
Mean ± SD		1.1900 ± 0.0356	172.5949 ± 5.1619	51.6821 ± 3.0811	

Table 53. 60°C Mechanical test results for propellant E.

Accelerated Ageing Temperature (°C)	Accelerated Ageing Duration (days)	Sample	Stress at break (MPa)	Stress at break (psi)	Strain at break (%)
60	0	1	0.9100	131.9843	52.6265
		2	0.8900	129.0836	47.2009
		3	0.9200	133.4347	56.5050
		4	0.9300	134.8851	59.2506
		5			
		6			
		Mean ± SD	0.9125 ± 0.0171	132.3469 ± 2.4770	53.8958 ± 5.2254
	30	1	0.9900	143.5873	55.9089
		2	0.9600	139.2362	62.8530
		3	0.9700	140.6866	65.4501
		4	0.9600	139.2362	60.1653
		5			
		6			
		Mean ± SD	0.9700 ± 0.0141	140.6866 ± 2.0511	61.0943 ± 4.0751
	57	1	1.0400	150.8392	46.4171
		2	1.0600	153.7400	49.6353
		3	1.0400	150.8392	45.6264
		4			
5					
6					
Mean ± SD		1.0467 ± 0.0115	151.8061 ± 1.6748	47.2263 ± 2.1234	

Table 54. 60°C Mechanical test results for propellant E, cont'd.

Accelerated Ageing Temperature (°C)	Accelerated Ageing Duration (days)	Sample	Stress at break (MPa)	Stress at break (psi)	Strain at break (%)
60	90	1	1.1800	171.1445	55.5230
		2	1.2200	176.9460	52.9474
		3	1.2200	176.9460	52.0368
		4	1.2600	182.7475	50.4234
		5			
		6			
		Mean ± SD	1.2200 ± 0.0327	176.9460 ± 4.7369	52.7326 ± 2.1330
	120	1	1.2700	184.1979	43.3771
		2	1.3200	191.4498	43.8204
		3	1.3000	188.5490	49.2579
		4	1.2500	181.2971	51.0420
		5			
		6			
		Mean ± SD	1.2850 ± 0.0311	186.3734 ± 4.5094	46.8744 ± 3.8561
	150	1	1.3000	188.5490	57.6657
		2	1.3100	189.9994	55.3239
		3	1.3300	192.9001	49.9252
		4	1.3000	188.5490	54.2748
5					
6					
Mean ± SD		1.3100 ± 0.0141	189.9994 ± 2.0511	54.2974 ± 3.2412	

Table 55. 90°C Mechanical test results for propellant F.

Accelerated Ageing Temperature (°C)	Accelerated Ageing Duration (days)	Sample	Stress at break (MPa)	Stress at break (psi)	Strain at break (%)
90	0	1	0.8500	123.2820	56.9684
		2	0.8500	123.2820	61.1969
		3	0.8500	123.2820	61.5235
		4	0.8500	123.2820	60.0320
		5	0.8400	121.8317	61.5051
		6			
		Mean ± SD	0.8480 ± 0.0045	122.9920 ± 0.6486	60.2452 ± 1.9307
	2	1	0.9300	134.8851	63.0560
		2	0.9300	134.8851	61.2062
		3	0.9400	136.3354	63.3048
		4	0.9300	134.8851	54.6021
		5	0.9400	136.3354	55.0053
		6	0.9400	136.3354	58.3405
		Mean ± SD	0.9350 ± 0.0055	135.6102 ± 0.7944	59.2525 ± 3.8782
	4	1	1.0400	150.8392	55.2137
		2	1.0400	150.8392	52.6721
		3	1.0600	153.7400	52.4037
		4	1.0400	150.8392	53.2137
5		1.0400	150.8392	56.6944	
6		1.0500	152.2896	53.7443	
Mean ± SD		1.0450 ± 0.0084	151.5644 ± 1.2135	53.9903 ± 1.6570	

Table 56. 90°C Mechanical test results for propellant F, cont'd.

Accelerated Ageing Temperature (°C)	Accelerated Ageing Duration (days)	Sample	Stress at break (MPa)	Stress at break (psi)	Strain at break (%)
90	6	1	1.1500	166.7934	54.2773
		2	1.1400	165.3430	55.6409
		3	1.1300	163.8926	52.0597
		4	1.1600	168.2437	52.3874
		5			
		6			
		Mean ± SD	1.1450 ± 0.0129	166.0682 ± 1.8724	53.5913 ± 1.6800
	8	1	1.1100	160.9918	47.9479
		2	1.1200	162.4422	49.4789
		3	1.1300	163.8926	45.8551
		4	1.1200	162.4422	48.7986
		5	1.1200	162.4422	45.9435
		6	1.1200	162.4422	47.5937
		Mean ± SD	1.1200 ± 0.0063	162.4422 ± 0.9173	47.6029 ± 1.4749
	10	1	1.1400	165.3430	42.3016
		2	1.1500	166.7934	46.2903
		3	1.1600	168.2437	46.4309
		4	1.1500	166.7934	45.5155
5		1.1400	165.3430	44.9497	
6		1.1300	163.8926	46.2850	
Mean ± SD		1.1450 ± 0.0105	166.0682 ± 1.5212	45.2955 ± 1.5741	

Table 57. 80°C Mechanical test results for propellant F.

Accelerated Ageing Temperature (°C)	Accelerated Ageing Duration (days)	Sample	Stress at break (MPa)	Stress at break (psi)	Strain at break (%)
80	0	1	0.8500	123.2820	56.9684
		2	0.8500	123.2820	61.1969
		3	0.8500	123.2820	61.5235
		4	0.8500	123.2820	60.0320
		5	0.8400	121.8317	61.5051
		6			
		Mean ± SD	0.8480 ± 0.0045	122.9920 ± 0.6486	60.2452 ± 1.9307
	5	1	0.9400	136.3354	55.1911
		2	0.9300	134.8851	45.8179
		3	0.9300	134.8851	54.2745
		4	0.9400	136.3354	52.9826
		5	0.9400	136.3354	59.2746
		6	0.9500	137.7858	56.4737
		Mean ± SD	0.9383 ± 0.0075	136.0937 ± 1.0918	54.0024 ± 4.5479
	10	1	1.0700	155.1903	48.7415
		2	1.0500	152.2896	51.5424
		3	1.0400	150.8392	52.5424
		4	1.1300	163.8926	50.8620
5		1.1300	163.8926	47.3649	
6		1.1100	160.9918	50.9493	
Mean ± SD		1.0883 ± 0.0402	157.8494 ± 5.8316	50.3337 ± 1.9155	

Table 58. 80°C Mechanical test results for propellant F, cont'd.

Accelerated Ageing Temperature (°C)	Accelerated Ageing Duration (days)	Sample	Stress at break (MPa)	Stress at break (psi)	Strain at break (%)
80	15	1	1.1400	165.3430	40.8630
		2	1.1200	162.4422	50.9844
		3	1.1100	160.9918	51.0308
		4	1.1300	163.8926	49.6976
		5			
		6			
		Mean ± SD	1.1250 ± 0.0129	163.1674 ± 1.8724	48.1440 ± 4.8931
	20	1	1.2400	179.8467	53.0230
		2	1.2600	182.7475	52.9948
		3	1.2400	179.8467	55.7559
		4	1.2700	184.1979	57.3996
		5	1.2400	179.8467	53.4326
		6			
		Mean ± SD	1.2500 ± 0.0141	181.2971 ± 2.0511	54.5212 ± 1.9729
	25	1	1.1500	166.7934	52.0576
		2	1.1700	169.6941	59.2209
		3	1.1600	168.2437	52.9595
		4	1.1600	168.2437	51.4248
5		1.1700	169.6941	54.3083	
6		1.1500	166.7934	46.0930	
Mean ± SD		1.1600 ± 0.0089	168.2437 ± 1.2973	52.6774 ± 4.2630	

Table 59. 70°C Mechanical test results for propellant F.

Accelerated Ageing Temperature (°C)	Accelerated Ageing Duration (days)	Sample	Stress at break (MPa)	Stress at break (psi)	Strain at break (%)
70	0	1	0.8500	123.2820	56.9684
		2	0.8500	123.2820	61.1969
		3	0.8500	123.2820	61.5235
		4	0.8500	123.2820	60.0320
		5	0.8400	121.8317	61.5051
		6			
		Mean ± SD	0.8480 ± 0.0045	122.9920 ± 0.6486	60.2452 ± 1.9307
	12	1	1.0300	149.3888	51.3243
		2	1.0300	149.3888	53.5945
		3	1.0400	150.8392	54.9561
		4	1.0200	147.9385	49.0345
		5	1.0200	147.9385	53.5101
		6	1.0300	149.3888	55.4122
		Mean ± SD	1.0283 ± 0.0075	149.1471 ± 1.0918	52.9720 ± 2.3995
	24	1	1.0000	145.0377	52.8662
		2	1.0300	149.3888	53.2209
		3	1.0200	147.9385	50.2801
		4	1.0200	147.9385	55.5621
5		1.0200	147.9385	55.8430	
6		1.0200	147.9385	50.1535	
Mean ± SD		1.0183 ± 0.0098	147.6967 ± 1.4260	52.9876 ± 2.4582	

Table 60. 70°C Mechanical test results for propellant F, cont'd.

Accelerated Ageing Temperature (°C)	Accelerated Ageing Duration (days)	Sample	Stress at break (MPa)	Stress at break (psi)	Strain at break (%)
70	36	1	1.0500	152.2896	43.2177
		2	1.0500	152.2896	41.4349
		3	1.0400	150.8392	47.9172
		4	1.0600	153.7400	46.1871
		5	1.0700	155.1903	45.6009
		6			
		Mean ± SD	1.0540 ± 0.0114	152.8697 ± 1.6537	44.8715 ± 2.5537
	48	1	0.9700	140.6866	42.0040
		2	0.9600	139.2362	41.4566
		3	1.0500	152.2896	42.0562
		4	1.0500	152.2896	42.0635
		5			
		6			
		Mean ± SD	1.0075 ± 0.0492	146.1255 ± 7.1423	41.8951 ± 0.2935
	60	1	1.0900	158.0911	48.5879
		2	1.0900	158.0911	48.4618
		3	1.1100	160.9918	43.8541
		4	1.1200	162.4422	46.6705
5					
6					
Mean ± SD		1.1025 ± 0.0150	159.9041 ± 2.1756	46.8936 ± 2.2074	

Table 61. 60°C Mechanical test results for propellant F.

Accelerated Ageing Temperature (°C)	Accelerated Ageing Duration (days)	Sample	Stress at break (MPa)	Stress at break (psi)	Strain at break (%)
60	0	1	0.8500	123.2820	56.9684
		2	0.8500	123.2820	61.1969
		3	0.8500	123.2820	61.5235
		4	0.8500	123.2820	60.0320
		5	0.8400	121.8317	61.5051
		6			
		Mean ± SD	0.8480 ± 0.0045	122.9920 ± 0.6486	60.2452 ± 1.9307
	30	1	0.9600	139.2362	54.2643
		2	0.9400	136.3354	47.1564
		3	0.9200	133.4347	58.2670
		4	0.9600	139.2362	52.6460
		5	0.9600	139.2362	52.6134
		6	0.9400	136.3354	53.5236
		Mean ± SD	0.9467 ± 0.0163	137.3024 ± 2.3685	53.0784 ± 3.5777
	57	1	1.0400	150.8392	49.2262
		2	1.0200	147.9385	53.2395
		3	1.0400	150.8392	48.2093
		4	1.0400	150.8392	52.6598
5		1.0400	150.8392	53.8294	
6					
Mean ± SD		1.0360 ± 0.0089	150.2591 ± 1.2973	51.4328 ± 2.5384	

Table 62. 60°C Mechanical test results for propellant F, cont'd.

Accelerated Ageing Temperature (°C)	Accelerated Ageing Duration (days)	Sample	Stress at break (MPa)	Stress at break (psi)	Strain at break (%)
60	90	1	1.1700	169.6941	43.8139
		2	1.2000	174.0452	45.6398
		3	1.1800	171.1445	43.1693
		4	1.1400	165.3430	48.2365
		5	1.1500	166.7934	46.5900
		6	1.1300	163.8926	50.2246
		Mean ± SD	1.1617 ± 0.0264	168.4855 ± 3.8282	46.2790 ± 2.6703
	120	1	1.2600	182.7475	47.1727
		2	1.2400	179.8467	49.4236
		3	1.2300	178.3964	49.2433
		4	1.2400	179.8467	48.4908
		5	1.2200	176.9460	50.4603
		6			
		Mean ± SD	1.2380 ± 0.0148	179.5567 ± 2.1513	48.9581 ± 1.2207
	150	1	1.2600	182.7475	45.2022
		2	1.2600	182.7475	49.4370
		3	1.2700	184.1979	42.4747
		4	1.2600	182.7475	43.8149
5		1.2600	182.7475	46.0071	
6		1.2500	181.2971	43.4835	
Mean ± SD		1.2600 ± 0.0063	182.7475 ± 0.9173	45.0699 ± 2.4817	

B. Chemical Test Results

Table 63. Chemical test results of propellants A, B and C, respectively.

Polymer		A	B	C
Accelerated Ageing Temperature (°C)	Accelerated Ageing Duration (days)	Soluble Fraction	Soluble Fraction	Soluble Fraction
90	0	0.0697	0.0775	0.0788
	2	0.0683	0.0669	0.0746
	4	0.0668	0.0645	0.0776
	6	0.0618	0.0625	0.0796
	8	0.0607	0.0566	0.0657
	10	0.0569	0.0589	0.0630
80	0	0.0697	0.0775	0.0788
	5	0.0655	0.0646	0.0724
	10	0.0620	0.0649	0.0675
	15	0.0603	0.0609	0.0665
	20	0.0599	0.0796	0.0659
	25	0.0600	0.0776	0.0664
70	0	0.0697	0.0775	0.0788
	12	0.0669	0.0708	0.0686
	24	0.0696	0.0707	0.0741
	36	0.0657	0.0695	0.0695
	48	0.0635	0.0670	0.0714
	60	0.0615	0.0703	0.0674
60	0	0.0697	0.0775	0.0788
	30	0.0683	0.0776	0.0776
	57	0.0687	0.0686	0.0803
	90	0.0678	0.0715	0.0746
	120	0.0655	0.0726	0.0707
	154	0.0635	0.0697	0.0709

Table 64. Chemical test results of propellants D, E and F, respectively.

Polymer		D	E	F
Accelerated Ageing Temperature (°C)	Accelerated Ageing Duration (days)	Soluble Fraction	Soluble Fraction	Soluble Fraction
90	0	0.0728	0.0649	0.0623
	2	0.0714	0.0551	0.0681
	4	0.0679	0.0573	0.0650
	6	0.0687	0.0558	0.0622
	8	0.0657	0.0539	0.0598
	10	0.0653	0.0524	0.0588
80	0	0.0728	0.0649	0.0623
	5	0.0736	0.0638	0.0663
	10	0.0714	0.0635	0.0635
	15	0.0673	0.0601	0.0621
	20	0.0670	0.0523	0.0573
	25	0.0643	0.0553	0.0580
70	0	0.0728	0.0649	0.0623
	12	0.0715	0.0601	0.0597
	24	0.0731	0.0613	0.0618
	36	0.0706	0.0608	0.0635
	48	0.0695	0.0612	0.0597
	60	0.0679	0.0582	0.0610
60	0	0.0728	0.0649	0.0623
	30	0.0757	0.0664	0.0646
	57	0.0733	0.0628	0.0638
	90	0.0739	0.0646	0.0638
	120	0.0695	0.0599	0.0613
	150	0.0687	0.0582	0.0561

C. Physical Test Results

Table 65. Physical test results of propellants A, B and C, respectively.

Polymer		A	B	C
Accelerated Ageing Temperature (°C)	Accelerated Ageing Duration (days)	Hardness (Sh-A)	Hardness (Sh-A)	Hardness (Sh-A)
90	0	62.0000	52.0000	40.0000
	2	65.0000	61.0000	56.0000
	4	66.0000	65.0000	60.0000
	6	69.0000	66.0000	60.0000
	8	70.0000	70.0000	64.0000
	10	72.0000	67.0000	65.0000
80	0	62.0000	52.0000	40.0000
	5	67.0000	62.0000	60.0000
	10	70.0000	66.0000	60.0000
	15	72.0000	65.0000	62.0000
	20	74.0000	73.0000	68.0000
	25	70.0000	68.0000	61.0000
70	0	62.0000	52.0000	40.0000
	12	63.0000	66.0000	50.0000
	24	65.0000	60.0000	56.0000
	36	67.0000	62.0000	60.0000
	48	69.0000	60.0000	64.0000
	60	69.0000	65.0000	65.0000
60	0	62.0000	52.0000	40.0000
	30	60.0000	56.0000	46.0000
	57	68.0000	60.0000	61.0000
	90	68.0000	67.0000	60.0000
	120	72.0000	70.0000	65.0000
	154	76.0000	70.0000	70.0000

Table 66. Physical test results of propellants D, E and F, respectively.

Polymer		D	E	F
Accelerated Ageing Temperature (°C)	Accelerated Ageing Duration (days)	Hardness (Sh-A)	Hardness (Sh-A)	Hardness (Sh-A)
90	0	55.0000	65.0000	60.0000
	2	56.0000	66.0000	62.0000
	4	60.0000	67.0000	66.0000
	6	64.0000	70.0000	70.0000
	8	66.0000	71.0000	70.0000
	10	66.0000	76.0000	72.0000
80	0	55.0000	65.0000	60.0000
	5	59.0000	67.0000	64.0000
	10	66.0000	70.0000	78.0000
	15	66.0000	73.0000	70.0000
	20	70.0000	73.0000	72.0000
	25	71.0000	67.0000	73.0000
70	0	55.0000	65.0000	60.0000
	12	58.0000	65.0000	67.0000
	24	56.0000	66.0000	67.0000
	36	62.0000	68.0000	69.0000
	48	67.0000	76.0000	73.0000
	60	70.0000	73.0000	73.0000
60	0	55.0000	65.0000	60.0000
	30	52.0000	64.0000	66.0000
	57	65.0000	70.0000	70.0000
	90	62.0000	70.0000	72.0000
	120	68.0000	76.0000	75.0000
	150	70.0000	76.0000	77.0000

D. Calculation of Activation Energy

Activation energies of the six propellants were calculated by two different methods in terms of strain and soluble fraction properties. As crosslink density is a parameter driven from soluble fraction and in order to create a model from a direct usage of chemical test results soluble fraction alteration is taken notice for modeling studies.

Integral Method (Assuming First Order Rate)

This method starts with the assumption that the first order rate equation describes data set on hand very well. Hence, for four accelerated ageing temperatures, reaction rates were evaluated. Calculation of reaction rates was carried through by minimizing least sum of squares of errors between measured values of properties, and estimated values of them attained using first order rate equation (see Equation 5).

An example regarding this calculation is as follows:

Table 67. Strain at break values of Propellant A aged at 90°C.

Accelerated Ageing Temperature (°C)	Accelerated Ageing Duration Corresponding to Accelerated Ageing Temperature (days)	Strain at break (%)
90	0	60.3540
	2	53.7848
	4	52.3992
	6	46.9974
	8	48.4727
	10	43.1043

Each estimated property value was obtained by first order rate equation:

$$P(t) = \exp [\ln(P_0) + k * t] \quad \text{Equation 14}$$

Table 68. Evaluating reaction rate by altering sum of normalized error.

T	k	Measured t (days)	Measured Value of P (%)	Estimated Value of P (%)	Normalized Error
90	-0.0340	0	60.3540	60.3540	0.0000E+00
		2	53.7848	56.3886	2.3438E-03
		4	52.3992	52.6837	2.9492E-05
		6	46.9974	49.2223	2.2411E-03
		8	48.4727	45.9882	2.6270E-03
		10	43.1043	42.9667	1.0193E-05
SUM					7.2515E-03

For each period regarding accelerated ageing temperature normalized error between measured (experimental) values and values estimated via first order rate equation was calculated and their sum indicated sum of squares of normalized errors. Least sum of squares was obtained by altering reaction rate, k using *data solver* add-on in Excel. Least sum of squares approach is preferred in order to make comparison between methods in a simpler way.

This method is called as integral method since reaction rate is attained by covering all accelerated ageing periods and taking all corresponding property change values into consideration.

Differential Method (Instantaneous Activation Energy)

Differential method is applied to data set in order to obtain true (instantaneous) activation energy for more specific time intervals such as first two or three ageing periods rather than taking whole time period into account. While integral method represents a cumulative result of the change upon accelerated ageing, this method takes the initial physical process into account.

In this method, instead of assuming a first order reaction, direct calculation of activation energy is employed.

An example regarding this calculation is as follows:

Table 69. Strain at break values of Propellant A.

Accelerated Ageing Temperature (°C)	Accelerated Ageing Duration Corresponding to Accelerated Ageing Temperature (days)	Strain at break (%)
90	0	60.3540
	2	53.7848
	4	52.3992
	6	46.9974
	8	48.4727
	10	43.1043
80	0	60.3540
	5	50.3045
	10	47.0300
	15	43.8249
	20	44.4095
	25	43.2759
70	0	60.3540
	12	55.7137
	24	52.3445
	36	46.8668
	48	48.5358
	60	42.5638
60	0	60.3540
	30	53.1835
	57	56.3441
	90	45.7113
	120	47.4918
	154	43.4591

Taking first three periods of ageing into consideration as indicated in Table 69 with blue rectangles, instantaneous activation energy is calculated without assuming any reaction rate order.

Table 70. Change in strain at break values for the first three ageing periods of Propellant A.

Ageing Temperature (°C)	1/T	Ageing Duration (days)	Strain (%)	Change in strain, ΔS	$\ln(\Delta S)$
90	2.7537E-03	0	60.3540	0.0000	0.8095
		2	53.7848	-3.2846	
		4	52.3992	-1.9887	
80	2.8317E-03	0	60.3540	0.0000	0.3835
		5	50.3045	-2.0099	
		10	47.0300	-1.3324	
70	2.9142E-03	0	60.3540	0.0000	-1.0668
		12	55.7137	-0.3867	
		24	52.3445	-0.3337	
60	3.0017E-03	0	60.3540	0.0000	-2.2359
		30	53.1835	-0.2390	
		57	56.3441	-0.0703	

When natural logarithm of change in strain ($\ln(\Delta S)$) versus reciprocal of temperature ($1/T$) is transmitted into a graph, slope of the graph indicates $-E_a/R$:

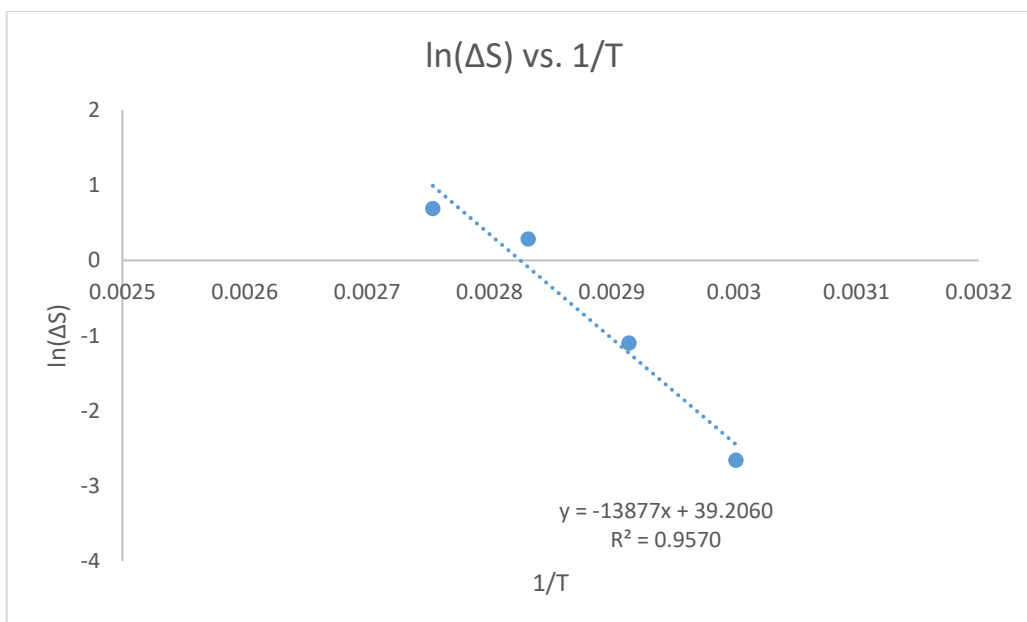


Figure 6-1. $\ln(\Delta S)$ versus $1/T$.

Hence, activation energy is obtained as 115.3734 kJ/mol.

E. Severity Index Approach

Since severity index approach requires non-differential equation solution, MATLAB R2021b comes in handy. This method starts with assuming reasonable initial values for β , γ and ω parameters representing dimensionless reaction rate constant, correction factor for equation to be applicable for high conversion levels and characteristic parameter altering for each propellant, respectively. This calculation is held using “fminsearch” algorithm under Optimization toolbox contained within MATLAB (see Appendix G). This algorithm is preferred in order to minimize least sum of squares after obtaining equation parameters and integrating alpha values, standing for conversion of strain and soluble fraction, into severity index equation (see Equation 9). An example as per the calculation of mechanical property test results belonging Propellant A put in an appearance in Appendix G and resultant MATLAB output is as follows:

Table 71. Calculation of $-\ln(1-a)$ named as *alfa* for strain values of Propellant A.

Ageing Temperature (°C)	Ageing Duration (days)	Strain (%)	Conversion, a	Alfa Value, $-\ln(1-a)$
90	0	60.3540	0.0000	0.0000
	2	53.7848	0.1088	0.1152
	4	52.3992	0.1318	0.1413
	6	46.9974	0.2213	0.2501
	8	48.4727	0.1969	0.2192
	10	43.1043	0.2858	0.3366
80	0	60.3540	0.0000	0.0000
	5	50.3045	0.1665	0.1821
	10	47.0300	0.2208	0.2494
	15	43.8249	0.2739	0.3200
	20	44.4095	0.2642	0.3068
	25	43.2759	0.2830	0.3326
70	0	60.3540	0.0000	0.0000
	12	55.7137	0.0769	0.0800
	24	52.3445	0.1327	0.1424
	36	46.8668	0.2235	0.2529
	48	48.5358	0.1958	0.2179
	60	42.5638	0.2948	0.3492
60	0	60.3540	0.0000	0.0000
	30	53.1835	0.1188	0.1265
	57	56.3441	0.0664	0.0688
	90	45.7113	0.2426	0.2779
	120	47.4918	0.2131	0.2397
	154	43.4591	0.2799	0.3284

In Table 71, “alfa” nominated values stands for “ $-\ln(1-a)$ ” in Equation 9 where a represents conversion of strain values from the initial value called as t_0 . Having known the left hand side of Equation 9, right hand side can be evaluated via nonlinear regression after the determination of severity index, R. As can be clearly discerned in Equation 8, R can be known by assuming characteristic parameter, ω in the first place as time inputs are already specified in the planning phase of the experiments, T_r is the accelerated ageing test temperature, again determined straight off the bat and T_b is the temperature where no degradation occurs, taken as 0°C as chemical degradation slows under room temperature and other failure mechanisms due to

mechanical loads while digressing from the stress-free temperature begin to dominate.

After integrating accelerated ageing temperatures, periods and alfa values into MATLAB, code gives outputs as β , γ and ω values along with the least sum of squares as follows:

```
Command Window

B =

    0.000218154970786
    0.641335689517406
    10.656258650534934

SSE =

    0.043853054147948

fx >>
```

Figure 6-2. Iteration result of β , γ and ω values for strain values of Propellant A.

And the resultant graphs subsequent to running of the code are:

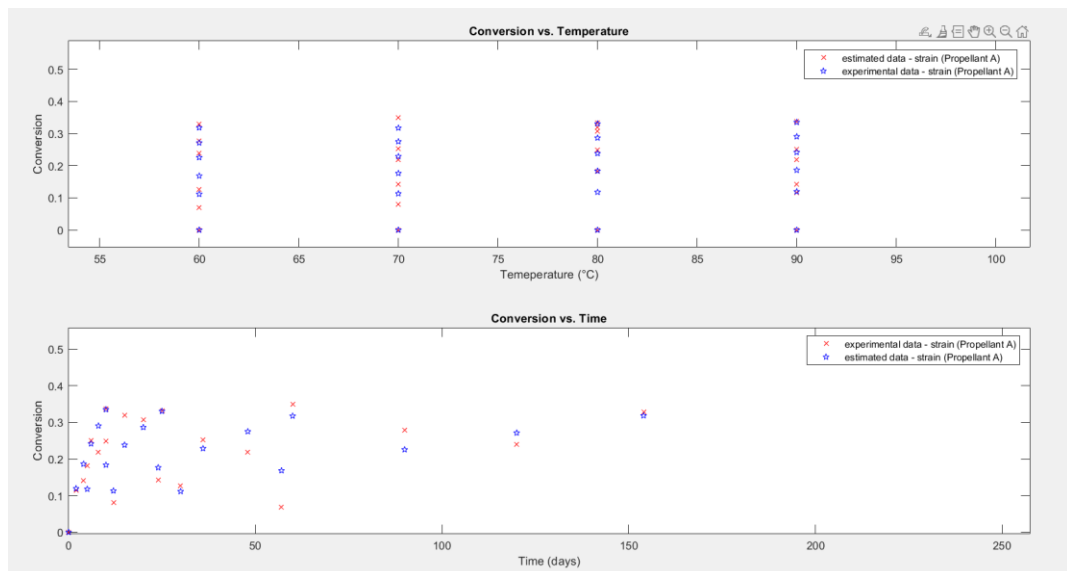


Figure 6-3. MATLAB output regarding conversion versus time and temperature (Propellant A).

F. Surface Fit Approach

Being temperature and time two variables affecting service life of a polymeric system and thus creating input for mathematical model while change in properties of the system can be esteemed as output, representing accelerated ageing data in terms of polymeric surface equation strikes as a good idea. In order to perform modeling, “surffit” algorithm under Curve Fitting toolbox contained within MATLAB (see Appendix H) is used. This algorithm creates a linear model represented by a polynomial formula with fitted coefficients within 95% confidence levels.

Order of the polynomial formula is decided by the user depending on the preferences on how well the data are desired to be fitted. In this study, 2nd order polynomial in both time and temperature variables is chosen as 1st order polynomial would give a low precision model while 3rd order becomes unwieldy.

In this approach, the code is fed with conversion values instead of direct implementation of property values. An example as per the calculation of mechanical property test results belonging Propellant A put in an appearance in Appendix H and resultant MATLAB output is as follows:

Table 72. Conversion results for strain values of Propellant A.

Ageing Temperature (°C)	Ageing Duration (days)	Strain (%)	Conversion, a
90	0	60.3540	0.0000
	2	53.7848	0.1088
	4	52.3992	0.1318
	6	46.9974	0.2213
	8	48.4727	0.1969
	10	43.1043	0.2858
80	0	60.3540	0.0000
	5	50.3045	0.1665
	10	47.0300	0.2208
	15	43.8249	0.2739
	20	44.4095	0.2642
70	0	60.3540	0.0000
	12	55.7137	0.0769
	24	52.3445	0.1327
	36	46.8668	0.2235
	48	48.5358	0.1958
	60	42.5638	0.2948
60	0	60.3540	0.0000
	30	53.1835	0.1188
	57	56.3441	0.0664
	90	45.7113	0.2426
	120	47.4918	0.2131
	154	43.4591	0.2799

An example in accordance with the calculation put in an appearance in Appendix H is as follows:

```

Command Window

Linear model Poly22:
surffit(x,y) = p00 + p10*x + p01*y + p20*x^2 + p11*x*y + p02*y^2
Coefficients (with 95% confidence bounds):
p00 = 0.1617 (-1.914, 2.237)
p10 = -0.006665 (-0.06083, 0.0475)
p01 = -0.01848 (-0.03509, -0.001864)
p20 = 6.728e-05 (-0.0002798, 0.0004143)
p11 = 0.0003417 (0.0001051, 0.0005783)
p02 = -1.597e-06 (-2.179e-05, 1.86e-05)

ans =

Columns 1 through 5

0.161657376747417 -0.006665388029151 -0.018475035216782 0.000067284136795 0.000341675877193

Column 6

-0.000001596676163

```

Figure 6-4. Surface fit equation and resulting coefficients for strain values of Propellant A.

In Figure 6-4, orange box indicates the formula of conversion in terms of x and y, ageing temperature and time, respectively.

Plot of the code gives:

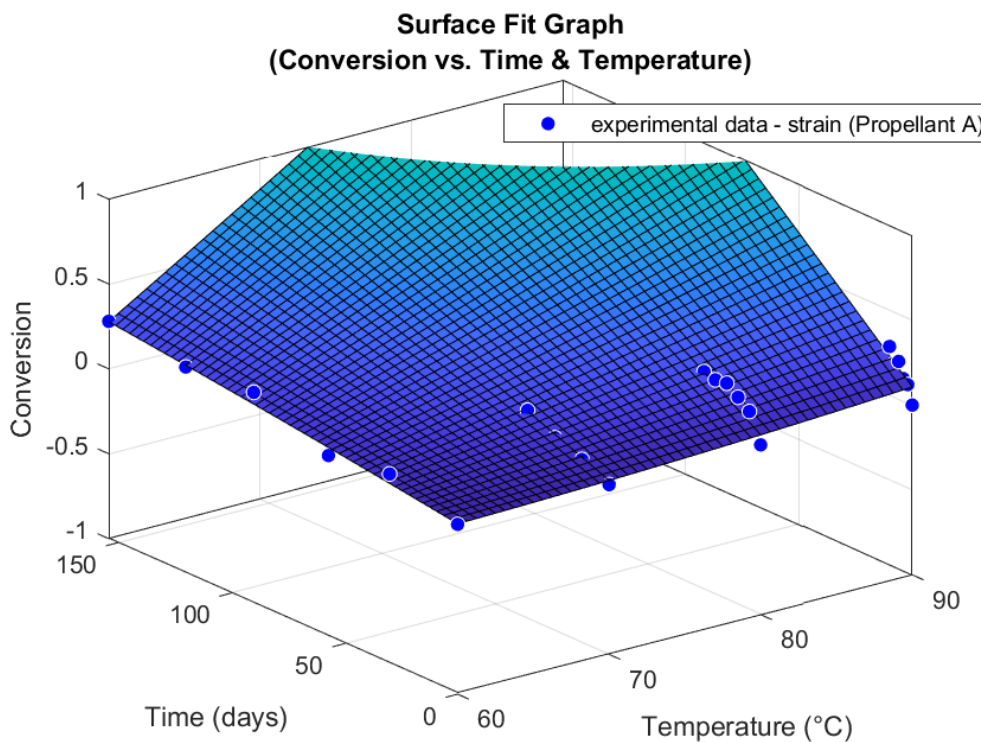


Figure 6-5. Surface fit graph for strain values of Propellant A.

G. Severity Index Calculation – MATLAB Code Example

```

clc
clear all

Tr = [90    90    90    90    90    90    80    80    80    80    80
      80    70    70    70    70    70    70 60 60    60    60    60
      60];
t = [0 2    4    6    8    10    0    5    10    15    20    25
     0 12   24   36   48   60    0   30   57   90
     120 154];
alfa = [0.0000    0.1152 0.1413 0.2501 0.2192 0.3366 0.0000 0.1821 0.2494
        0.3200 0.3068 0.3326 0.0000 0.0800 0.1424 0.2529 0.2179 0.3492 0.0000
        0.1265 0.0688 0.2779 0.2397 0.3284];
format long

Trt = [Tr(:) t(:)]; % Create Single
Variable
% b(1)=beta, b(2)=gamma, b(3)=omega
alfa_fit = @(b,Trt) b(1)/b(2)*[exp(log(Trt(:,2))+Trt(:,1)./b(3))).^b(2);

SSECF = @(b) sum((alfa(:) - alfa_fit(b,Trt)).^2); % Sum-Squared-
Error Function
B0 = [0.002; 1; 10]; % Initial
Parameter Estimates
[B, SSE] = fminsearch(SSECF, B0) % Estimated
Parameters

figure(1);
subplot(2,1,1);
plot(Tr, alfa,'xr', Tr, alfa_fit(B,Trt),'bp');
% grid
subplot(2,1,2);
plot(t, alfa,'xr', t, alfa_fit(B,Trt),'bp');
% grid

```

H. Fitting a Polynomial Surface – MATLAB Code Example

```
clc
close all
clear all

%% Linear Surface Fitting

% Getting transpose of the matrices due to nature of *surffit*

Tr = [90    90    90    90    90    90    80    80    80    80    80
      80    70    70    70    70    70    70 60 60    60    60
      60];
X=Tr';
t = [0 2    4    6    8    10    0    5    10    15    20    25
     0    12   24   36   48   60    0    30   57   90
     120  154];
Y=t';
conversion = [0.0000    -0.0920    -0.0424    0.0020 0.0407 0.0571
              0.0000 -0.0638    -0.0192    0.0042 0.0803 0.0695 0.0000 0.0420
              0.0083 -0.0183    0.0415 0.0216 0.0000 -0.0362    -0.0232    -
0.0241 0.0163 0.0994];
Z=conversion';

%% Surface fitting of the inputs

surffit=fit([X,Y],Z,'poly22') % polyij meaning creating a polynomial
function that is i'th order in x & j'th order in y
plot(surffit,[X,Y],Z); % plotting alfa as a function of temperature and
time, respectively
zlim([-1 1]); % putting limits to alfa as it goes to 1 maximum

x=X; % in order to make the formula easier to express
y=Y; % in order to make the formula easier to express

A=formula(surffit); % surface fit of the polynomial fit

format long

coeffnames(surffit); % Get all the coefficient names
coeffvalues(surffit) % Get all the coefficient values

%% Finding sum of squares between "Z" (transpose of conversion) and
"result_surfacefit values"

Trt = [X(:) Y(:)];
% Create Single Variable
result_surfacefit = @(p,Trt) p(1) + p(2)*Trt(:,1) + p(3)*Trt(:,2) +
p(4)*Trt(:,1).^2 + p(5)*Trt(:,1).*Trt(:,2) + p(6)*Trt(:,2).^2;
% p(1)=p00, p(2)=p10, p(3)=p01, p(4)=p20, p(5)=p11, p(6)=p02

SSECF = @(p) sum((Z(:) - result_surfacefit(p,Trt)).^2);
% Sum-Squared-Error Function
```

```
p0 = [0.2; -0.005; -0.001; 0.00008; 0.0003; -0.000001]; % Initial  
Parameter Estimates % Initial Parameter  
Estimates  
[p, SSE] = fminsearch(SSECF,p0)  
% Estimated Parameter
```